CHALMERS
UNIVERSITY OF TECHNOLOGY

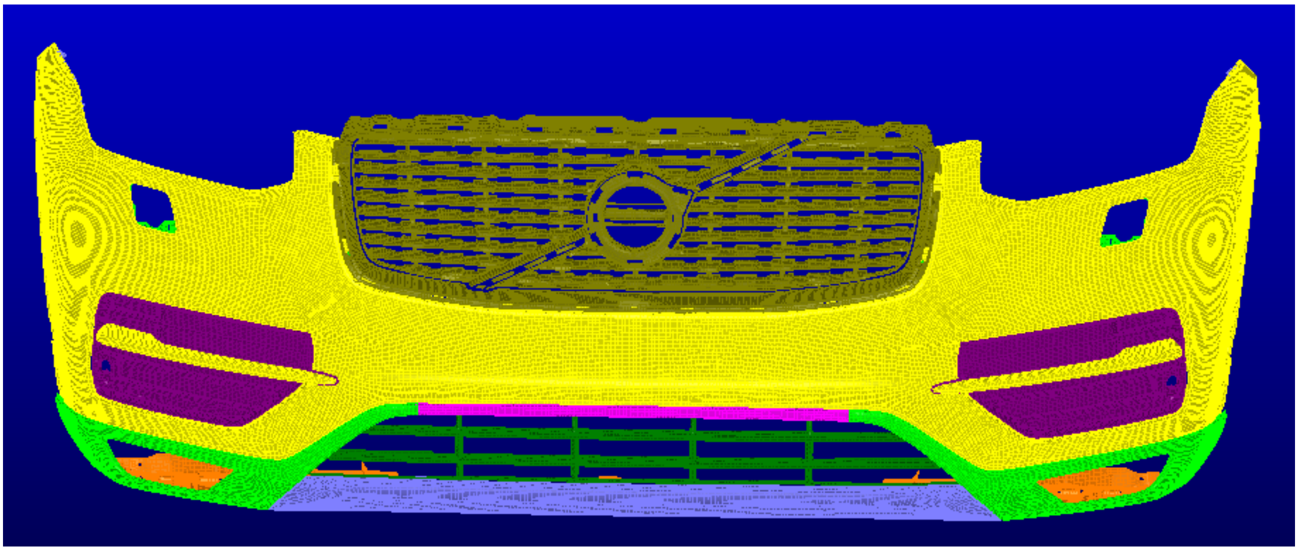

Evaluation of operators’ influence on geometrical defects during manual assembly

Master’s thesis in Production Engineering

Angelica Kjellgren

Department of Product and Production Development
CHALMERS UNIVERSITY OF TECHNOLOGY
Gothenburg, Sweden 2016

Evaluation of operators’ influence on geometrical defects during manual assembly

Master’s Thesis in Production Engineering

ANGELICA KJELLGREN

Department of Product and Production Development

CHALMERS UNIVERSITY OF TECHNOLOGY

Gothenburg, Sweden, 2016

Evaluation of operators’ influence on geometrical defects during manual assembly
ANGELICA KJELLGREN

© ANGELICA KJELLGREN, 2016

Department of Product and Production Development

Chalmers University of Technology

SE-412 96 Gothenburg

Sweden

Telephone: + 46 (0)31-772 1000

Cover:

A picture of a virtual model in RD&T that shows the front bumper

Gothenburg, Sweden 2016

Acknowledgements

This master thesis was performed at the department Robust Design and Tolerancing at Volvo Car Corporation and at the department of Product and Production Development at Chalmers University of Technology during the spring of 2016.

I would like to thank all the people that has been involved in this master thesis and that has helped me in the process of working on this project. I would especially like to thank my supervisor Dag Johansson at Volvo Car Corporation for his expertise, constant support and guidance through the course of this project. I would also like to give thanks to my examiner Lars Lindkvist at Chalmers University of Technology for all his help and support during this project. I would also like to thank all the people that have provided information and helped me during the course of this master thesis including all the people that have attended interviews, all the members at the department Robust Design and Tolerancing, members from Manufacturing Engineering and many more from Volvo Car Corporation.

Gothenburg, May 2016

Angelica Kjellgren

Abstract

The department Robust Design and Tolerancing at Volvo Car Corporation does not consider operators' contribution to variation with regards to different manual assembly sequences for a part in their current working procedure. The purpose of this master thesis was therefore to see if it is possible to find an optimal manual assembly sequence with regards to operators' contribution to variation.

A physical study of the front door was performed in which deviations was measured from the manual assembly of three different components in order to establish if operators do contribute to variation during manual assembly. A virtual study of the front bumper was performed in which a virtual model was created where the front bumper was assembled to the car body. Virtual simulations were executed for two different manual assembly sequences of how the front bumper was mounted to the car body. Deviations was thereby measured in several measurement points on the front bumper for the two manual assembly sequences in order to establish if it is possible to find an optimal assembly sequence with regards to operators' contribution to variation.

The physical study of the front door resulted in obtained deviations for all three components from the manual assembly. The main conclusion from the physical study was therefore that operators do contribute to variation during manual assembly and that the degree of contributing variation differs between assemblers. The virtual study of the front bumper resulted in one optimal manual assembly sequence since it had smaller deviations in the majority of the measurement points in comparison to the other manual assembly sequence. The main conclusion from the virtual study was therefore that it is possible to find an optimal manual assembly sequence with regards to operators' contribution to variation.

Keywords: *Assembly sequence, operator, deviation, force, simulation, physical, virtual, front door, front bumper*

Abbreviations

CAT - Computer Aided Tolerancing

CMM - Coordinate Measuring Machine

FEM - Finite Element Method

FEA - Finite Element Analysis

GRS – Glass Run Seal

OWS – Outer Waist Seal

VCC – Volvo Car Corporation

RD&T – Robust Design and Tolerancing

Table of contents

1 Introduction 1

- 1.1 Background 1
- 1.2 Purpose 1
- 1.3 Research questions 1
- 1.4 Outline of the project 2
- 1.5 Delimitations 2

2 Theoretical Framework 3

- 2.1 Variation 3
- 2.2 Geometrical variation 4
- 2.3 Geometry assurance process 6
- 2.4 Positioning systems 6
- 2.5 The Finite Element Method (FEM) 8
- 2.6 The software Robust Design and Tolerancing (RD&T) 8
  - 2.6.1 Statistical variation simulation 8
  - 2.6.2 Contact modeling 9
  - 2.6.3 Welding sequence 9
- 2.7 Manual assemblies' impact on quality 9
- 2.8 Assembly in relation to force 11
- 2.9 Coordinate Measuring Machine (CMM) 11

3 Method 13

- 3.1 Physical study of the front door 13
  - 3.1.1 Assembly of GRS, OWS and capping 14
  - 3.1.2 Positioning of the left front door 21
  - 3.1.3 Measurement procedure 22
  - 3.1.4 Force measurement procedure 25
- 3.2 Virtual study of the front bumper 26
  - 3.2.1 Assembly sequence for the front bumper 26
  - 3.2.2 Building of virtual model in RD&T 30
  - 3.2.3 Measurements of virtual model in RD&T 34
  - 3.2.4 Measuring of the force on front bumper in RD&T 35
  - 3.2.5 Welding sequences 36
  - 3.2.6 Simulations 37

4 Results 39

- 4.1 Results from physical study of the front door 39

4.1.1 Measurements of deviations and forces 39
4.2 Results from virtual study of the front bumper 40
4.2.1 Measurements of deviations 40
4.2.2 Measurements of forces 52
5 Discussions 61
5.1 Physical study of the front door 61
5.1.1 Contributing factors to obtained deviations from physical study of the front door 61
5.2 Virtual study of the front bumper 62
5.2.1 Optimal assembly sequence in relation to obtained deviations from virtual study of the front bumper 62
5.2.3 Comparison between simulation results and measured data from production 64
5.2.4 Optimal assembly sequence in relation to obtained forces from virtual study of the front bumper 64
6 Conclusions 67
6.1 Physical study of the front door 67
6.2 Virtual study of the front bumper 67
7 References 69
7.1 Articles 69
7.2 Books 70
7.3 Lecture from Chalmers University of Technology 70
7.4 Web-pages 70
7.5 Documents from VCC 71
7.6 Software manual 72
7.7 Interviews 72
8 Appendices 73
8.1 Appendix A: Parts included in the front bumper 73
8.2 Appendix B: Parts included in the car body 74
8.3 Appendix C: Data included in the elastic modulus 76
8.4 Appendix D: Data used in the simulations 77
8.5 Appendix E: Measured deviations from the physical study 78
8.6 Appendix F: Measured forces from the physical study 79
8.7 Appendix G: Results from the physical study 80
8.8 Appendix H: Measurements of deviations from simulation 1 84
8.9 Appendix I: Measurements of deviations from simulation 2 85
8.10 Appendix J: Measurements of forces from simulation 1 86
8.11 Appendix K: Measurements of forces from simulation 2 87

1 Introduction

This chapter contains information about the background for this project, the purpose, research questions, outline of the project and delimitations.

1.1 Background

There is a constant progressive development within the automotive industry to create a car that will be state of the art. It is therefore vital for Volvo Car Corporation (VCC) to stay ahead of its competitors by working with geometry assurance in order to develop product concepts with a robust design. A robust design is insensitive to variation and can therefore better fulfill functional, esthetical and assembly requirements (Söderberg and Lindkvist, 1999).

The department Robust Design and Tolerancing at VCC works with geometry assurance in order to develop cars that are robust and thereby insensitive to geometrical variation. The department uses the software Robust Design and Tolerancing (RD&T) to analyze the geometric stability, sensitivity and variation for the products (Lindau *et.al.*, 2012). The software RD&T can be used to analyze the geometric behavior of components within an assembly process in order to create a product concept that is robust (RD&T_Technology, 2016) (Lindau *et.al.*, 2016). The department Robust Design and Tolerancing does not in their current working procedure, consider operators' contribution to variation with regards to different manual assembly sequences for a part. It would therefore be beneficial for the department if investigations could be made to see if it is possible to consider operators' contribution to variation with regards to different manual assembly sequences, so that the optimal assembly sequence can be selected and thereby create a more robust design concept.

1.2 Purpose

The purpose of this project will be to perform a physical study of a front door and a virtual study of a front bumper. The physical study of the front door will be performed to identify and quantify if and how operators can contribute to variation during manual assembly. The virtual study of the front bumper will be performed to investigate if it is possible to find an optimal manual assembly sequence with regards to operators' contribution to variation.

1.3 Research questions

The research questions for this project are:

- Do the operators contribute to variation during manual assembly?
- Is it possible to identify and quantify how operators can contribute to variation during manual assembly?
- Is it possible to find the optimal manual assembly sequence with regards to operators' contribution to variation in RD&T?

1.4 Outline of the project

This project will be performed in three main steps physical study of the front door, virtual study of the front bumper and analyzing the results from respective study, see figure 1. The first step will be to prepare and perform the physical study of the front door. Preparations for the physical study will be to ensure that all the equipment is in place. Execution of the physical study will be to manually assemble three components on a left front door for one car model in which measurements of deviations will be taken. The applied force during the manual assembly will also be measured. Step two will be to prepare and perform the virtual study of the front bumper. Preparations for the virtual study will include assembly of a virtual model of the front bumper for one car model and to create one virtual model for each assembly sequence. Execution of the virtual study will be to run simulations for two virtual models that each represents one assembly sequence and to obtain measurements of deviations and forces. The third step in the project will be to analyze the results from respective study with regards to obtained deviations and forces.

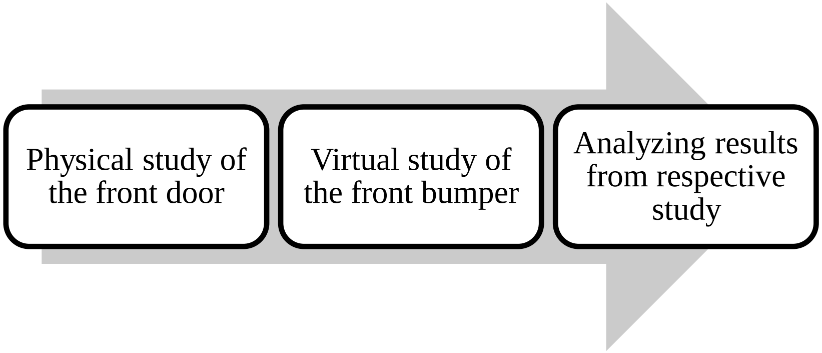
Physical study of the front door
Virtual study of the front bumper
Analyzing results from respective study

Figure 1. Outline of the project

1.5 Delimitations

Delimitations for the physical study will be that only three components on one car model will be analyzed and the ergonomic factors during manual assembly of these components will not be considered. A delimitation for the virtual study will be that the front bumper will not be assembled to all the car body components in the virtual model due to time restrictions and the size of the model. Another delimitation for the virtual study is that the front lamps will not be included in the virtual model.

2 Theoretical Framework

The theoretical framework includes information about the areas variation, geometrical variation, the geometry assurance process, positioning systems, the finite element method, the software Robust Design and Tolerancing, manual assemblies' impact on quality, assembly in relation to force and the coordinate measuring machine.

2.1 Variation

Variation in how objects and situations differ exists everywhere and can therefore come from many different sources (Bergman and Klefsjö, 2010). One source where variation is always present is in the manufacturing processes, which indicate that these processes often deviate from the nominal value (Söderberg and Lindkvist, 1999). The range of variation for an amount of data is defined as the difference between the biggest and smallest value (VCS 5060,6, 2015). Tolerances are used to control the allowed variation of a geometrical feature in order to assure an optimal design, assembly or function (Söderberg and Lindkvist, 1999). A tolerance has an upper tolerance limit and a lower tolerance limit that specifies the area of acceptance (VCS 5060,6, 2015). Tight tolerance limits causes higher manufacturing costs and should be used on the parts of the design that is sensitive for variation. Wide tolerance limits results in lower manufacturing costs and should be used for less sensitive areas of the design in which variation does not impact important output features (Söderberg and Lindkvist, 1999)

There is a target value that is positioned in the middle of the tolerance area between the lower specification limit (LSL) and the upper specification limit (USL), see figure 2 (VCS 5060,6, 2015).

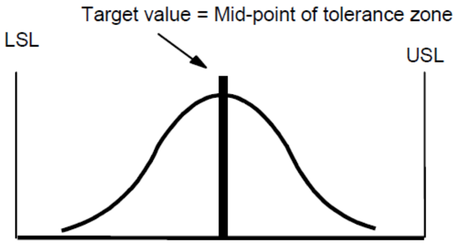

Figure 2. Target value (VCS 5060,6, 2015)

The mean value differs from the target value in situations where the target value is not obtained. Figure 3 shows an example of when the target value is not obtained since the mean value ($\overline{x}$) differs from the midpoint (M) within the tolerance area (VCS 5060,6, 2015).

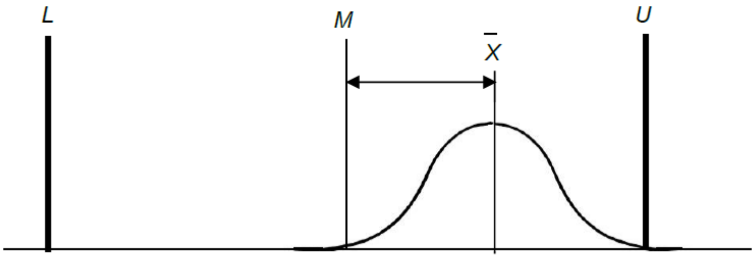

Figure 3. Mean value differs from the target value (VCS 5060,6, 2015)

Standard deviation can be defined as a measure of how a set of observations are distributed in relation to the mean of the observations. If the observations are spread out far from the mean it will result in a high standard deviation and if the observations are close to the mean it will result in a low standard deviation (Mathportal, 2016). The standard deviation gives the size of the spread of a normal distribution (VCS 5060,6, 2015). If a set of observations follows a normal distribution then 99,7% of the observations will lie within the area of three standard deviations ($\pm 3\ sigma$), see figure 4 (Stat yale education, 2016).

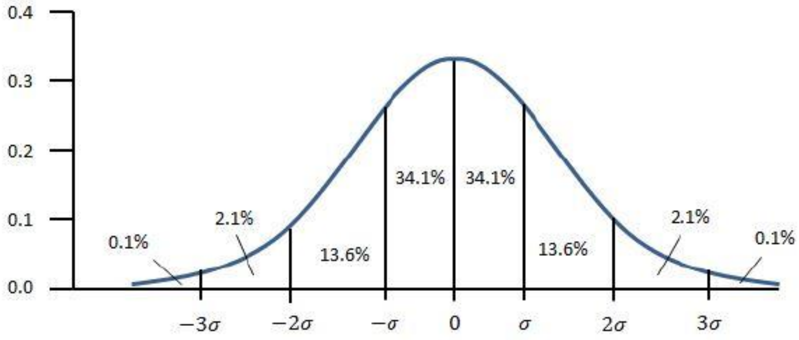

Figure 4. Normal distribution

2.2 Geometrical variation

Geometrical variation is present in production and assembly processes, which can cause products to not meet functional, esthetical or assembly requirements (Söderberg *et.al.*, 2006) (Rosenqvist *et.al.*, 2013). Three factors that causes geometrical variation are the design concept, component variation and assembly variation, see figure 5 (Lindkvist, 2016). Component variation occurs when there are differences between individuals of the same item and is a result of the manufacturing process in which the machine precision and the process variation are contributing factors (Lindkvist, 2016) (Bergman and Klefsjö, 2010). Assembly variation can induce from every individual part in an assembly and how the mating surfaces between parts are located during assembly (Cai *et.al.*, 2015). Assembly variation is a result of the assembly process in which the assembly precision and process variation are contributing factors (Lindkvist, 2016).

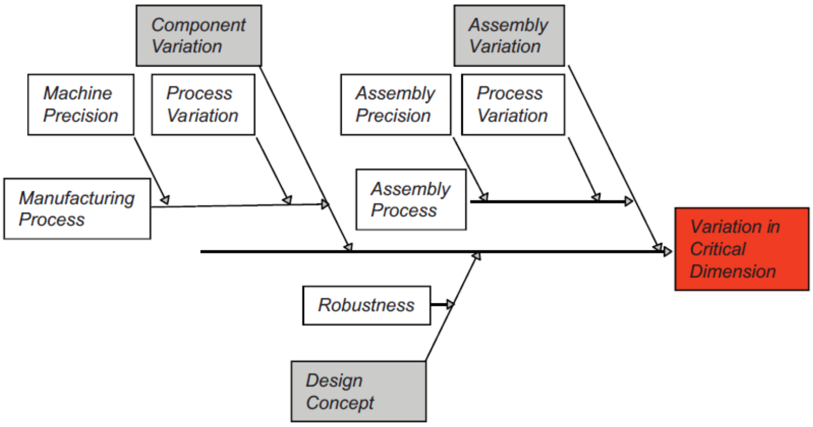
Component Variation
Assembly Variation
Machine Precision
Process Variation
Assembly Precision
Process Variation
Manufacturing Process
Assembly Process
Variation in Critical Dimension
Robustness
Design Concept

Figure 5. Contributors to geometrical variation (Söderberg, 1998)

The design concept can also contribute to geometrical variation as a result of its level of robustness (Lindkvist, 2016). A robust design is insensitive to variation and can therefore better fulfill functional, esthetical and assembly requirements (Söderberg and Lindkvist, 1999). A smaller output variation than input variation results in a robust design, see figure 6 (Lindkvist, 2016).

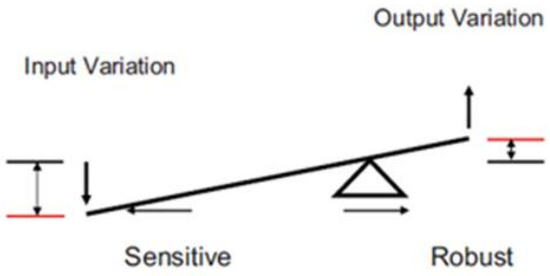

Figure 6. Smaller output variation than input variation leads to an insensitive design (Lindkvist, 2016)

If there is a higher output variation than input variation then it is referred to as a sensitive design, see figure 7 (Lindkvist, 2016).

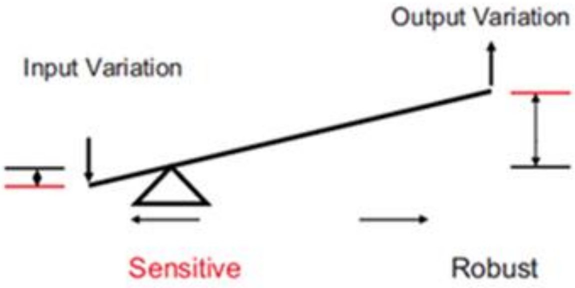

Figure 7. Higher output variation than input variation leads to a sensitive design (Lindkvist, 2016)

Geometrical variation can cause bad visible relations between two parts in the form of split-lines, which results in poor quality from an esthetical perspective (Forslund *et.al.*, 2011). A split-line can result in gap and flush between two parts (Söderberg *et.al.*, 2006). Gap is the distance between two parts and flush is the distance between two parts in normal direction, see figure 8.

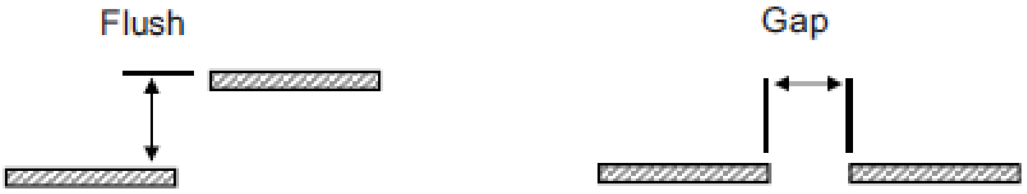

Figure 8. Flush and gap (Lindkvist, 2016).

2.3 Geometry assurance process

Geometry assurance is a vital aspect in the process of developing and manufacturing a product. Quality issues that are caused by geometrical variation are sometimes detected during pre-production or when a product is already being manufactured. Solving these quality issues this late in the product realization process can require large costs and the geometry assurance process it therefore applied to avoid this. The geometry assurance process consists of the concept phase, the verification and pre-production phase and the production phase, see figure 9. The concept phase includes the development of the product and manufacturing concept. The product concepts are in this phase virtually evaluated with regards to optimization against manufacturing variation, optimization of robustness and creation of product tolerances. The verification and pre-production phase is about physically evaluating the product and manufacturing system. If errors are located, corrections are made to the product and the manufacturing system in order to get everything ready for production. The production phase is where the products are being manufactured and the virtual model is in this phase used to control production and to discover potential errors (Söderberg *et.al.,* 2006).

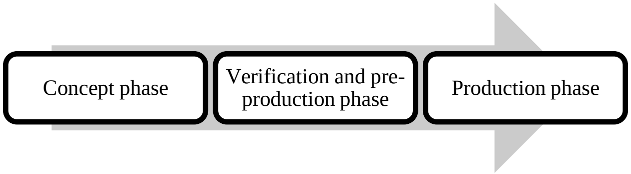

Figure 9. The three phases in the geometry assurance process

2.4 Positioning systems

A positioning system locates and locks different items and assemblies virtually in space (Wärmefjord *et.al.,* 2013). The stability of a system determines how variation increases and spreads through the system and a positioning system is used to control this stability (Söderberg and Lindkvist, 1999). The 3-2-1 positioning system uses six master locating points to locate a rigid part and these reference points are positioned as 3-2-1 in three coordinate planes that are perpendicular to each other, see figure 10 (VCS 5026,4, 2013). Three of the master locating points (A1, A2 and A3) that are positioned in one of the coordinate planes locks three degrees of freedom, two of the master locating points (B1 and B2) locks two degrees of freedom and the last master locating point (C1) that are positioned in the third coordinate plane locks one degree of freedom (Söderberg *et.al.,* 2007). The master location points should generally be distributed as much as possible over the component so that the robustness can be optimized (Söderberg *et.al.,* 2006).

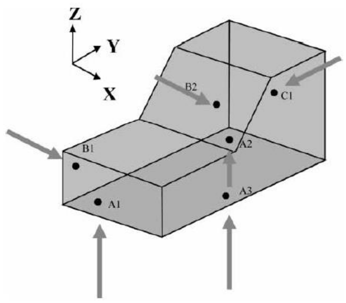

Figure 10. 3-2-1 locating scheme (Söderberg et.al., 2007)

6-directions are a positioning system in which the directions of the six master locating points are non-perpendicular to each other, see figure 11. The reference points (D1-D6) that are positioned in the figure defines the locating directions (Söderberg *et.al.*, 2007).

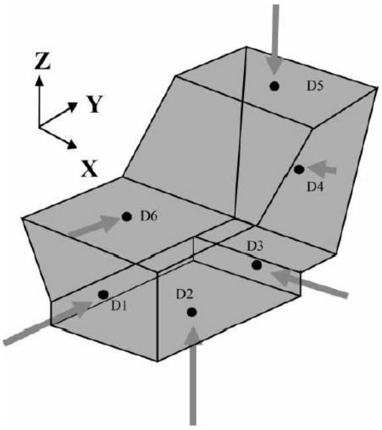

Figure 11. 6-directions locating scheme (Söderberg et.al., 2007)

The 3-2-1 system and the 6-directions system are referred to as constrained locator schemes and are often used for rigid parts where six reference points locks six degrees of freedom (Lindau *et.al.*, 2012) (Wärmefjord *et.al.*, 2013). For non-rigid components it can be necessary to use support location points in addition to the six master location points, which is then referred to as an over-constrained locating scheme (VCS 5026,4, 2013) (Söderberg *et.al.*, 2006). Adding support locating points will enable the non-rigid component to bend and flex (Söderberg *et.al.*, 2006).

Each component has generally its own master location points which are referred to as the master location system of the component (VCS 5026,4, 2013). A components master location system can also be called the P-frame, which represents the positioning system for the component. A component`s local P-frame can be used to position the component to a mating target P-frame that belongs to another component or subassembly, see figure 12 (Söderberg and Lindkvist, 1999).

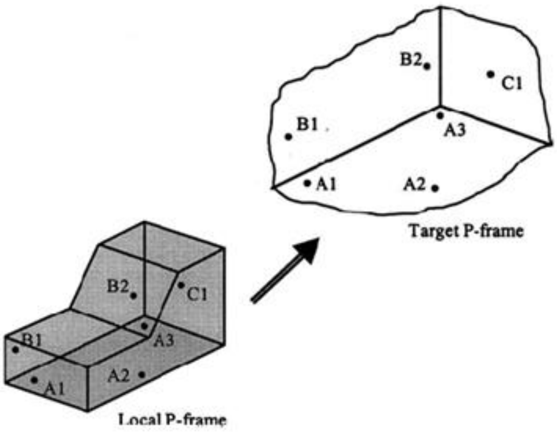

Figure 12. Local P-frame (Söderberg and Lindkvist, 1999)

2.5 The Finite Element Method (FEM)

The Finite Element Method (FEM) is a numerical method that approximately solves differential equations with many unknown variables. These differential equations represent a physical issue that can be visualized in the form of a region that can be one-, two- or three dimensional. This region is divided into finite elements, where each element represents a small area. All of these elements that the region consists of are referred to as a finite element mesh. An approximation is performed on each finite element, which determines how the variable changes within each element and an assumption is made that the variable is known at specific points within each element. These specific points can be found at the boundary of each finite element and they are referred to as nodal points. After an approximation has been performed on each finite element, all the elements in the region are joined together by certain rules which enables one to find an approximated solution for the behavior of the entire meshed model (Ottosen and Petersson, 1992). One type of a meshed model is a mid-surface mesh in which the mid-planes are created from a solid geometry in order to obtain a mid-surface geometry that will then be meshed, which can be referred to as a mid-surface mesh (MSC Apex, 2016).

2.6 The software Robust Design and Tolerancing (RD&T)

It is today essential to use virtual software to consider geometrical variation in early phases of the product development process since it will require less physical tests, improve the product quality and enable for a better production (Söderberg *et.al.,* 2012) (Forslund *et.al.,* 2011) (Lindau *et.al.,* 2016). The software Robust Design and Tolerancing (RD&T) is used to simulate assemblies in order to analyze the geometric stability, sensitivity and variation for different products (Lindau *et.al.,* 2012). RD&T uses statistical variation simulation to predict and visualize deviations during assembly already in the concept stage of the product development process. RD&T is applied throughout the entire geometry assurance process, which then includes the concept phase, the verification and pre-production phase and the production phase. (RD&T_Technology, 2016). The software RD&T can be used to analyze the geometric behavior of components within an assembly process in order to create a product concept that is robust against assembly variation and to foresee the variation in the products critical features (RD&T_Technology, 2016) (Lindau *et.al.,* 2016). Some of the functions that are included in the software RD&T are statistical variation simulation for rigid and non-rigid (compliant) models, weld sequences and contact modeling (Lindau *et.al.,* 2012).

2.6.1 Statistical variation simulation

Statistical variation simulation is a function in RD&T that is used to predict variation and offsets in critical features of assemblies and subassemblies (Wärmefjord *et.al.,* 2013). Statistical variation simulation is based on the Monte Carlo (MC) method. The Monte Carlo method is based on several iterations where numbers are randomly applied to all input parameters and calculates distributions for the output parameters. This is achieved by using an assembly model in RD&T and simulating using the Monte Carlo method can for example result in predictions of the mean value (Söderberg *et.al.,* 2006). The Monte Carlo method can be used for rigid analysis in which components cannot be over-constrained by the locating scheme (Söderberg *et.al.,* 2008). The Monte Carlo method in combination with Finite

Element Analysis (FEA) can be used to perform variation simulations in RD&T for non-rigid (compliant) components. This sort of variation simulation can be used to analyze how non-rigid components, assemblies or subassemblies, like for example plastic parts, behave after assembly. In variation simulation of non-rigid components, over-constrained positioning systems can be applied to enable the components to deform and bend during assembly (Söderberg *et.al.,* 2006).

The geometrical variation of non-rigid components, assemblies and subassemblies are influenced by several aspects that should be considered in the variation simulation in order to achieve as accurate results as possible. One aspect is that data about the elasticity module and Poisson's ratio should be included for all the meshed models in the variation simulation (Söderberg *et.al.,* 2012). The elasticity module indicates how a component deforms in relation to its elastic properties and it can be defined as a measure of stiffness (The Engineering Toolbox, 2016). Poisson's ratio is the relation between the contraction strain and the extension strain (The Engineering Toolbox, 2016). Other aspects that are important to consider is the assembly sequence and contact modeling (Söderberg *et.al.,* 2012).

2.6.2 Contact modeling

Contact modeling is used to prevent mating surfaces from intersecting with one another during the simulation. This creates contact forces that help to deform the components during assembly and it affects the shape of the subassembly after springback. A contact point can be positioned as a node-pair between two adjacent mating surfaces where one node on each of the two surfaces is selected (Lindau *et.al.,* 2016).

2.6.3 Welding sequence

Weld points is a function in RD&T that can be used to join different components. Weld points can assemble non-rigid parts by using node-pairs, where one node is selected on each of the two non-rigid components that are going to be joined (Lindau *et.al.,* 2012). The amount of weld points that are in an assembly and in which sequence they are positioned will affect the geometrical variation (Söderberg *et.al.,* 2012). The weld points can be used in variation simulation in RD&T to simulate a predetermined welding sequence (Wärmefjord *et.al.,* 2010).

2.7 Manual assemblies' impact on quality

There are many factors that can have an impact on the geometrical quality during assembly (Wärmefjord *et.al.,* 2010). One of these factors is the assembly sequence and the complexity of the manual assembly process (Wärmefjord *et.al.,* 2013) (Rosenqvist *et.al.,* 2014). A previous study has detected several factors when an assembly can be considered complex (Falck *et.al.,* 2012):

- “Many different ways of doing the task”
- “Many individual details and part operations”
- “Time demanding operations”
- “No clear mounting position of parts and components”

- “Poor accessibility”
- “Hidden operations”
- “Poor ergonomics conditions implying risk of harmful impact on operators”
- “Operator dependent operations requiring experience/knowledge to be properly done”
- “Operations must be done in a certain order”
- “Visual inspection of fitting and tolerances, i.e. subjective assessment of the quality results”
- “Accuracy/precision demanding”
- “Need of adjustment”
- “Geometric environment has a lot of variation (tolerances), i.e. level of fitting and adjustment vary between the products”
- “Need of clear work instructions”
- “Soft and flexible material”
- “Lack of (immediate) feedback of properly done work, e.g. a click sound and/or compliance with reference points”

Other factors that can affect the geometrical quality during manual assembly is if the operator mounts the parts in an incorrect order, if there is no response if the locators are in correct position, if clips are hard to mount and if the operator assembles the component incorrectly (Rosenqvist *et.al.,* 2013). In many cases when the geometrical quality is affected by an operator during manual assembly it is often due to that the product or process has been poorly designed. It is therefore important to create a robust design by acknowledging parts of the assembly process where the contribution to variation is high (Booker *et.al.,* 2005). One example of a robust design can be to have a plug-in solution where the locators would always be mounted in the correct position regardless of operator’s impact (Rosenqvist *et.al.,* 2013).

One intention with using Computer Aided Tolerancing (CAT) software is to ensure that the assembly process will function properly. CAT software does not consider all the aspects that contribute to variation, which affects the accuracy of the simulations. One aspect that is often not completely considered in CAT simulations is the contribution to variation from manual assembly performed by an operator. Assumptions are often made in CAT simulations that the positioning of the six reference points in a parts locating scheme are defined and that the six degrees of freedom are locked. This is not always achieved by the operator during manual assembly since it sometimes can be hard to determine if all the locators are in the correct position, which results in simulations that does not correspond with reality (Rosenqvist *et.al.,* 2013).

2.8 Assembly in relation to force

An assembly process is about mounting parts together and the force necessary to mount two components is referred to as the assembly force. The force that is used during assembly can impact the geometrical quality in the joining of the components. It is preferable to have low forces during an assembly process since it will then be less risk of joining failures and geometrical quality issues. The assembly sequence has a great impact on the assembly forces and it is therefore vital to consider in which sequence a product should be assembled in order to decrease the required assembly forces (Wärmefjord *et.al.*, 2013).

2.9 Coordinate Measuring Machine (CMM)

A Coordinate Measuring Machine (CMM) can obtain coordinate measurements in three dimensions and it is used to measure different parts and assemblies. A CMM consists of three orthogonal axes in X-, Y- and Z-direction and the location of each axis is determined by a scale. The CMM has a probe that is controlled by a measuring program that measures the predetermined values in all three directions. The CMM obtains measures in a point from a parts surface while the machine at the same time records the position in space in all three directions for the corresponding measurement point (Coord3_Metrology, 2016).

3 Method

The methodology in this project is based on a physical study of a front door and a virtual study of a front bumper. This section describes how the physical study and the virtual study were prepared and executed and figure 13 illustrates the main steps of the methodology.

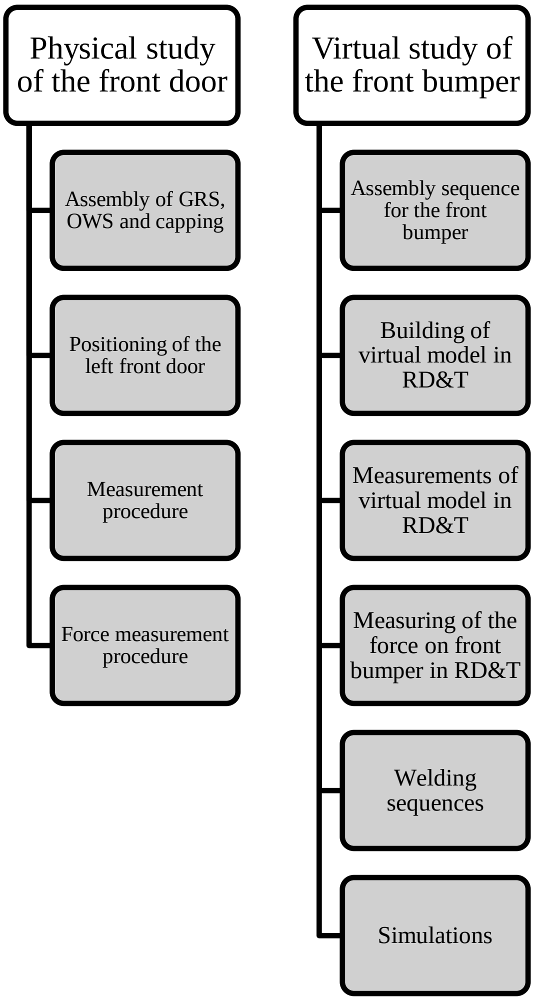
Physical study of the front door
Assembly of GRS, OWS and capping
Positioning of the left front door
Measurement procedure
Force measurement procedure
Virtual study of the front bumper
Assembly sequence for the front bumper
Building of virtual model in RD&T
Measurements of virtual model in RD&T
Measuring of the force on front bumper in RD&T
Welding sequences
Simulations

Figure 13. Main steps of the methodology

3.1 Physical study of the front door

The physical study of the front door was performed to evaluate if operators do contribute to variation during manual assembly. This was evaluated by manually assembling the three components Glass Run Seal (GRS), Outer Waist Seal (OWS) and capping for one car model on the left front door with the purpose of measuring deviations and forces. The preparations and execution of the physical study will be described in this section.

3.1.1 Assembly of GRS, OWS and capping

The study was performed in the pilot plant at VCC and a left front door was used that was collected from the production. The components that were manually assembled on the left front door were GRS, OWS and capping, see figure 14. The components were assembled in accordance with the assembly sequences that are used in production.

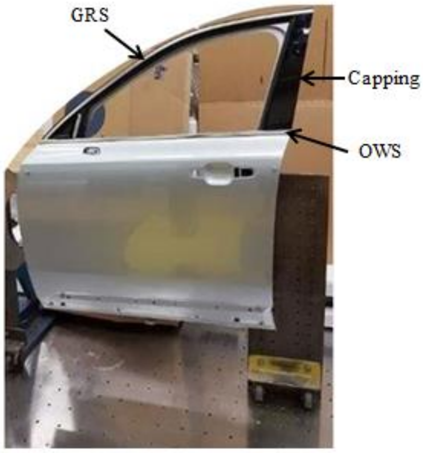

Figure 14. Components assembled on the left front door

3.1.1.1 Assembly sequence for the GRS

The Glass Run Seal (GRS) for the car model is mainly manufactured by a rubber material and it also has a chrome strip which is mounted on the front side of the component, which can be seen in figure 15.

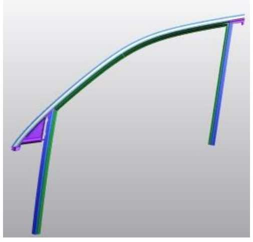

Figure 15. Glass Run Seal (GRS)

The GRS in relation to the left front door can be seen in figure 16 and the assembly sequence for how this component is mounted on the door in production consists of four main steps.

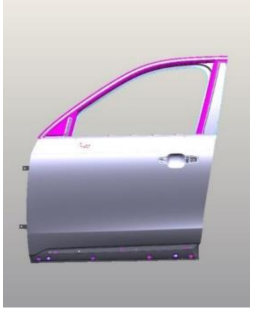

Figure 16. The GRS assembled on the left front door

The GRS has a reference pin on the inside of the component which consists of a rubber material that is used to position the GRS to the left front door, see figure 17. The reference pin is used to lock the movement for the GRS.

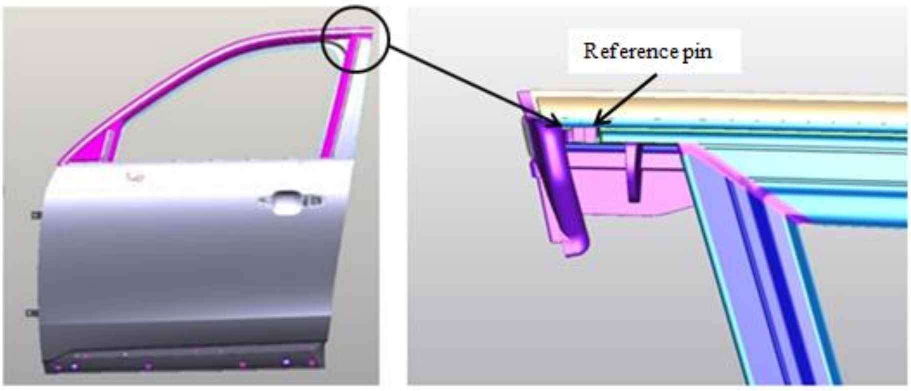

Figure 17. Reference pin on the GRS

The first step in the assembly sequence is to position the reference pin on the GRS in the cut out on the left front door, see figure 18 (C8450-0012, 2015).

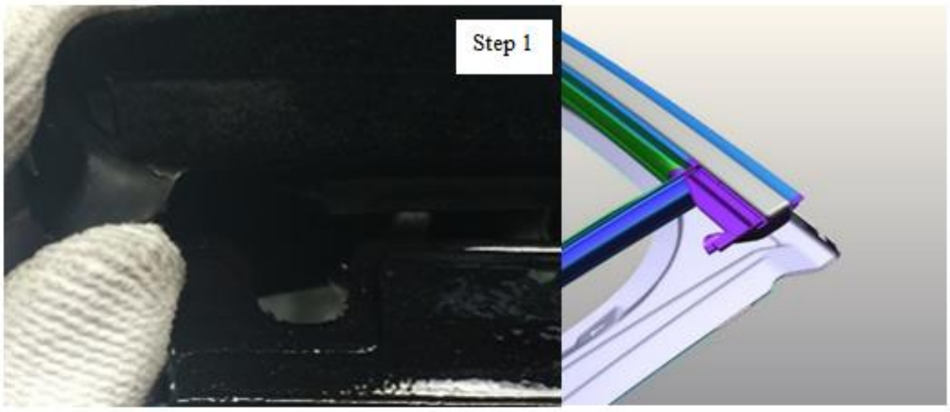

Figure 18. First step of the assembly process (C8450-0012, 2015)

The second step in the assembly sequence is to press on the component in order to assemble it on the door bow on the left side of the black marker, see figure 19 (C8450-0012, 2015).

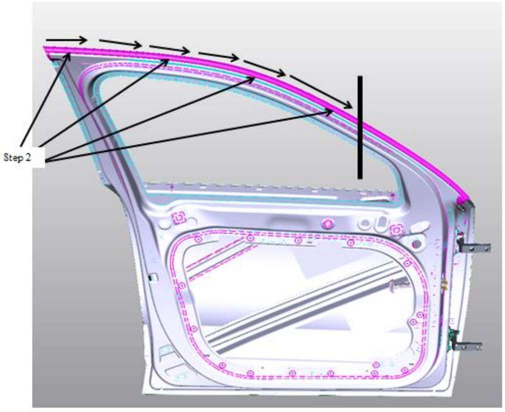

Figure 19. Second step of the assembly process (C8450-0012, 2015)

The third step in the assembly process is to position the left end of the GRS and to attach it against the left front door, see figure 20 (C8450-0012, 2015).

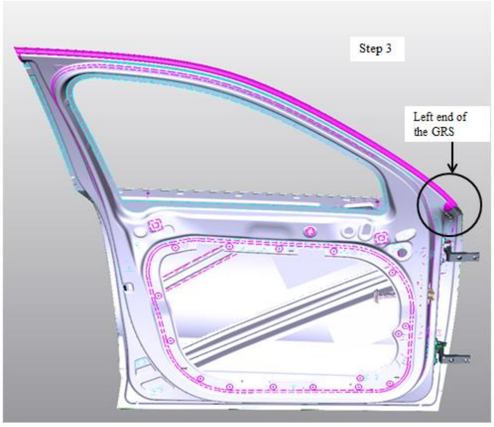

Figure 20. Third step of the assembly process (C8450-0012, 2015)

The fourth and last step in the assembly sequence is to assemble the GRS to the door bow on the right side of the black marker, see figure 21 (C8450-0012, 2015).

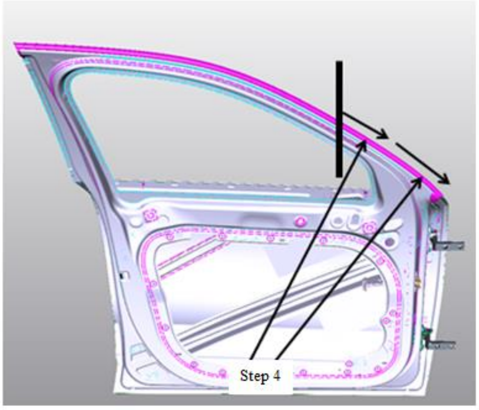

Figure 21. Fourth step of the assembly process (C8450-0012, 2015)

3.1.1.2 Assembly sequence for the capping

The capping is manufactured by a sheet metal material and the component can be seen in figure 22.

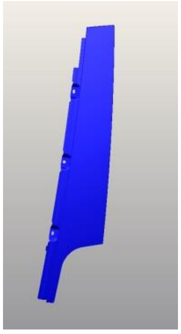

Figure 22. Capping

The capping in relation to the left front door can be seen in figure 23 and the assembly sequence for how this component is mounted on the door in production consists of four main steps.

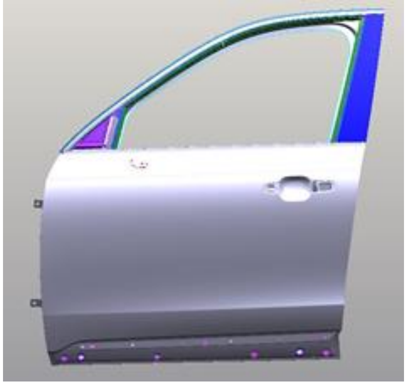

Figure 23. Capping assembled on the left front door

The first step in the assembly sequence is to attach one clip in each hole on the left front door, see figure 24 (C8414-0001, 2015).

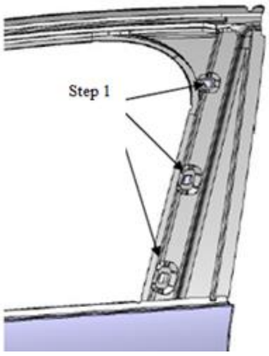

Figure 24. First step of the assembly process (C8414-0001, 2015)

The second step in the assembly process is to position the bottom of the capping inside of the left front door and to attach the folded edge on the right side of the capping to the right edge of the door bow, see figure 25 (C8414-0001, 2015).

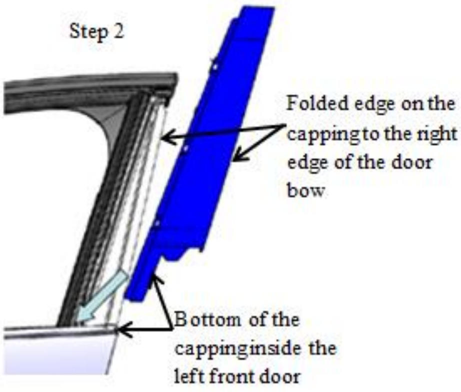
Step 2
Folded edge on the capping to the right edge of the door bow
Bottom of the capping inside the left front door

Figure 25. Second step of the assembly process (C8414-0001, 2015)

The capping has a reference pin at the top of the component which is used to lock the movement for the component, see figure 26.

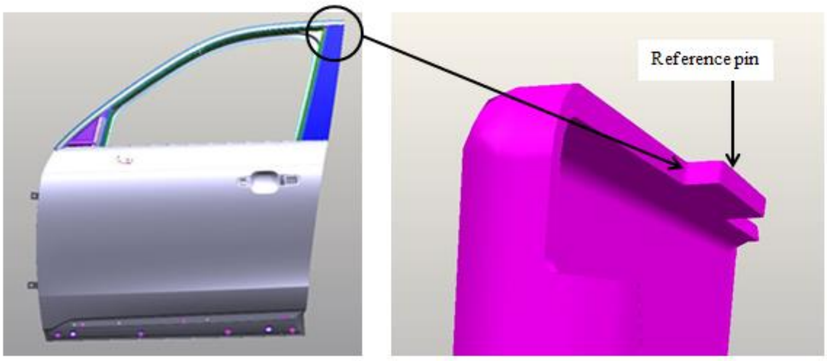

Figure 26. Reference pin on the capping

The third step in the assembly sequence is to mount the reference pin on the capping into the slot in the GRS, see figure 27 (C8414-0001, 2015).

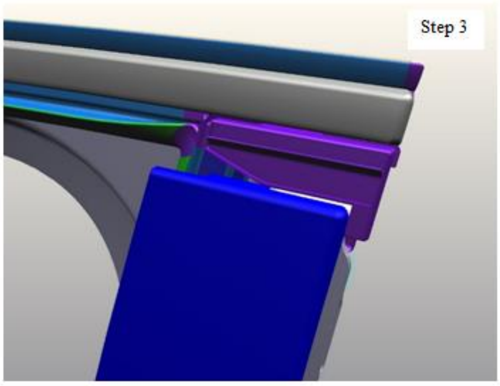

Figure 27. Third step of the assembly process (C8414-0001, 2015)

The fourth step in the assembly sequence is to hold away a part of the GRS in order to first mount one screw at the upper part of the capping in order to ensure that the component is positioned correctly against the GRS. A screw is after this mounted at the lower part of the capping and the middle screw is mounted last, see figure 28 (C8414-0001, 2015).

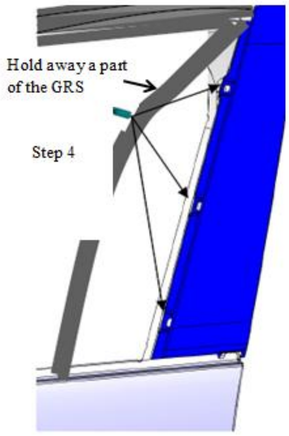

Figure 28. Fourth step of the assembly process (C8414-0001, 2015)

3.1.1.3 Assembly sequence for the OWS

The Outer Waist Seal (OWS) is mainly manufactured by a rubber material and it also has a chrome strip that is mounted on the front side of the component, which can be seen in figure 29.

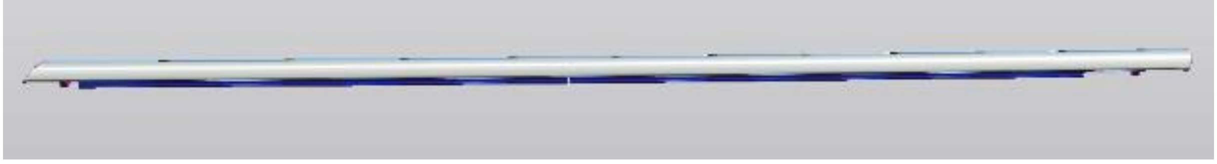

Figure 29. Outer Waist Seal (OWS)

The OWS in relation to the left front door can be seen in figure 30 and the assembly sequence for how this component is mounted on the door in production consists of two main steps.

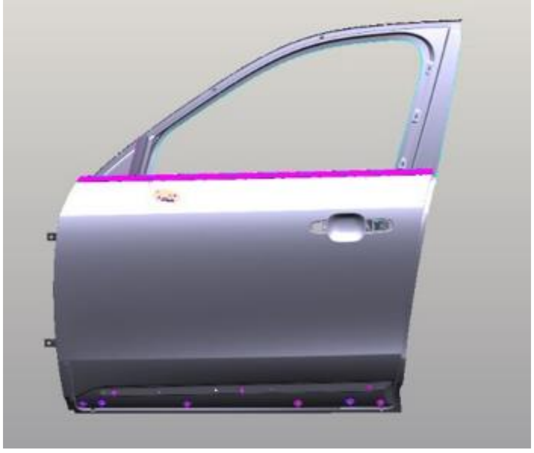

Figure 30. The OWS assembled on the left front door

The OWS has a reference pin on its right side, which consists of a rubber material that is used to position the component to the left front door, see figure 31. The reference pin is used to lock the movement for the OWS.

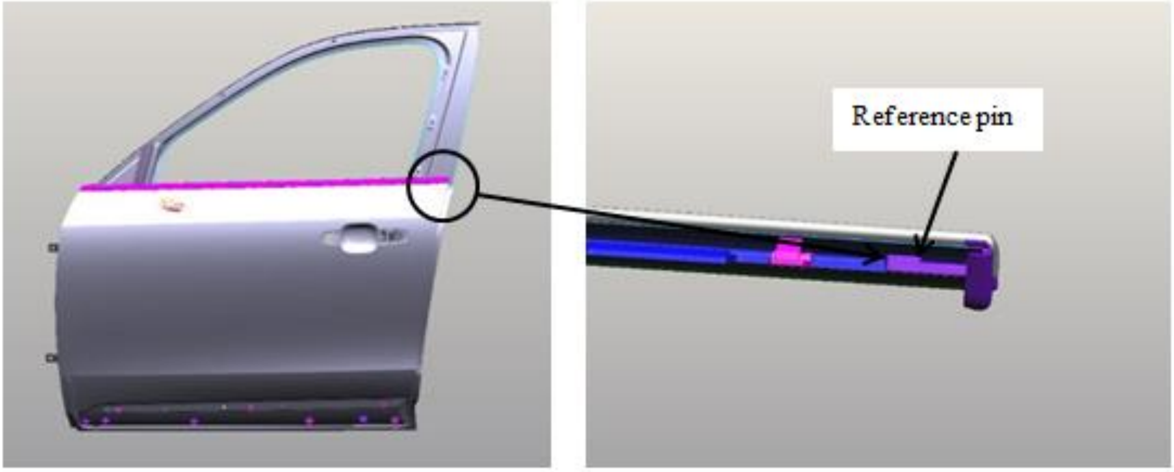

Figure 31. Reference pin on the OWS

The first step in the assembly process is to position the reference pin on the right side of the OWS into the cut out on the front door and then push this reference pin into the cut out on the right side of the door, see figure 32 (C8450-0001, 2015).

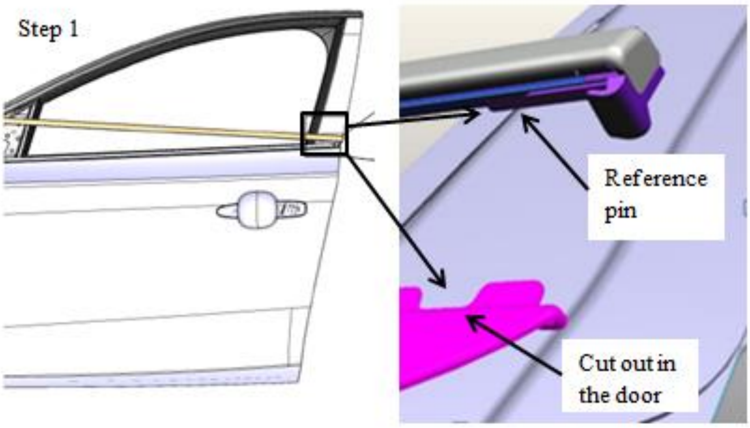
Step 1
Reference pin
Cut out in the door

Figure 32. First step of the assembly process (C8450-0001, 2015)

The OWS has one clip on the right side and one clip on the left side that is used to lock the movement for the OWS, see figure 33 (C8450-0001, 2015).

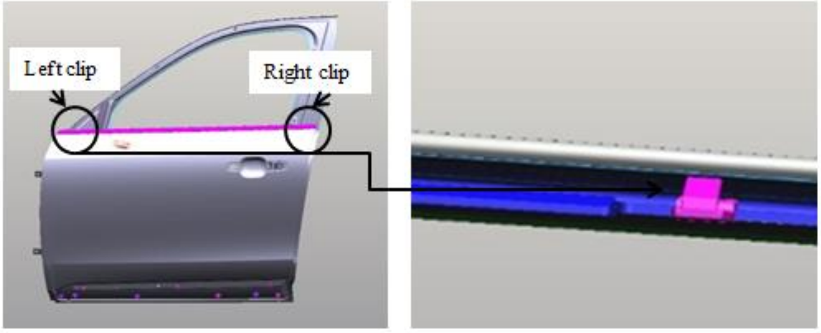
Left clip
Right clip

Figure 33. Clips on the OWS

The second step in the assembly sequence is to position the whole OWS on the door flange and then to press down the component in order to mount it against all the flanges and to attach the two clips, see figure 34 (C8450-0001, 2015).

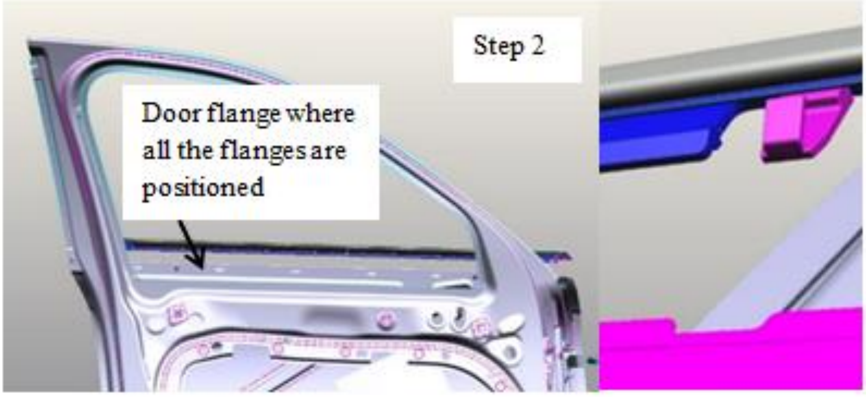
Step 2
Door flange where all the flanges are positioned

Figure 34. Second step of the assembly process (C8450-0001, 2015)

3.1.1.4 Assembly in the physical study of front door

The GRS was first assembled to the left front door, followed by the capping and lastly the OWS was mounted. This assembly process was repeatedly performed ten times during the physical study in which three assemblers performed three repetitions each, see figure 35.

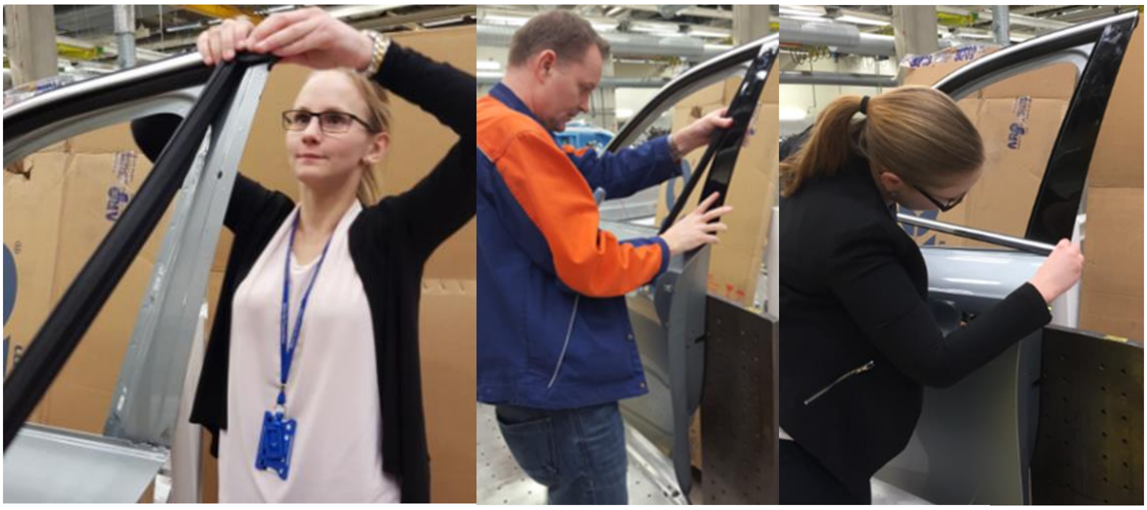

Figure 35. Mounting of GRS, OWS and capping by three assemblers

The assembly time that is used in production for the GRS, OWS and capping was not taken into account during the physical study. The amount of components included in the study were ten glass run seals, ten outer waist seals and ten cappings. Ten pieces of each component were used since there is a risk of destruction when the parts are disassembled from the door. The part variation was not taken into account during the physical study since it was insignificant in comparison to the total variation.

3.1.2 Positioning of the left front door

The left front door was attached in a fixture in which the right side of the door was positioned with a clamp that was fastened in a rack. The hinges on the left side of the door was attached to a plate that was fastened to a rack, see figure 36. Positioning the left front door in this type of fixture will allow perceiving it as a nominal door.

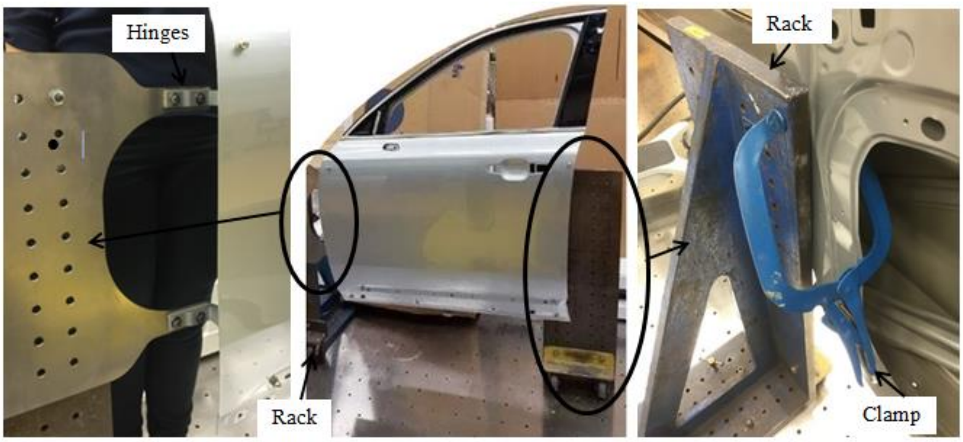

Figure 36. Positioning of the left front door in a fixture

The process of mounting the GRS, OWS and capping on the left front door and then disassembly these components could cause movement of the door in the fixture. The Coordinate Measuring Machine (CMM) was therefore used to reset the position of the door in order to compensate for any movement during assembly or disassembly. This was achieved by the use of three spheres that was glued to the left front door, see figure 37. The CMM measured the location of these three spheres after each assembly and after each disassembly in order to reset the position of the door. The fourth sphere in the left corner of the door and a point on the door bow was used as control points when the position of the door was reset.

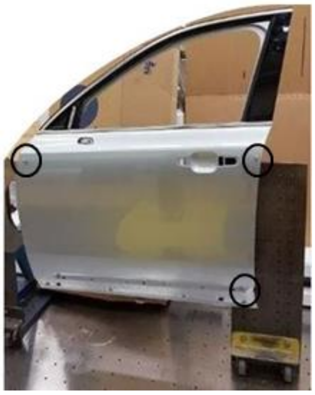

Figure 37. Positioning of spheres on the left front door

3.1.3 Measurement procedure

The measurement procedure in the physical study was performed with a CMM that measured deviations after each assembly process, which includes mounting of all three components. A measurement program was constructed by an operator and the first repetition was executed to see if the measurement program worked properly. The operator repeated the measurement procedure nine times since the study included nine assembly processes. Which measurements that were going to be obtained for the components was based on a visit to the production, in which observations could be taken on how the GRS, OWS and capping may deviate during manual assembly.

It was considered relevant to measure deviations in flush in X-direction for the GRS. The CMM used a point at the right side of the GRS to measure, which was compared against the corresponding point on the nominal CAD model to obtain the measurements in X-direction, see figure 38.

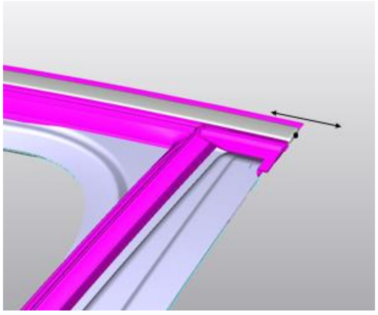

Figure 38. Measuring point on the GRS

It was also considered relevant to measure possible deviations in flush in X-direction for the OWS. The CMM used a point at the right side of the OWS to measure, which was compared against the corresponding point on the nominal CAD model to obtain the measurements in X-direction, see figure 39.

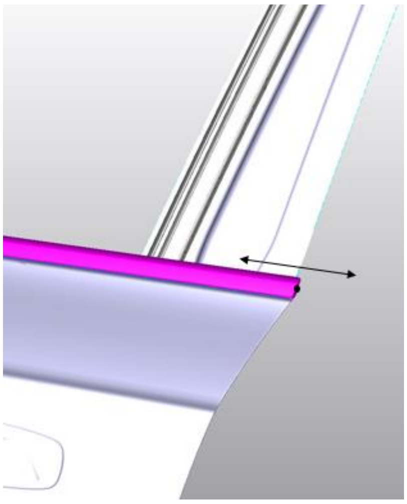

Figure 39. Measuring point on the OWS

There were several measurements that were considered to be relevant for the capping after observing from the visit in the production that the component could deviate in X-, Y-, and Z-direction. The capping is mounted to the left front door with three screws in which the upper and lower screws impacts the positioning of the component in X-direction since the holes are oval, see figure 40. The CMM used two points on the right side of the capping to measure, which were compared against the corresponding points on the nominal CAD model to obtain the measurements in flush in X-direction, see figure 40.

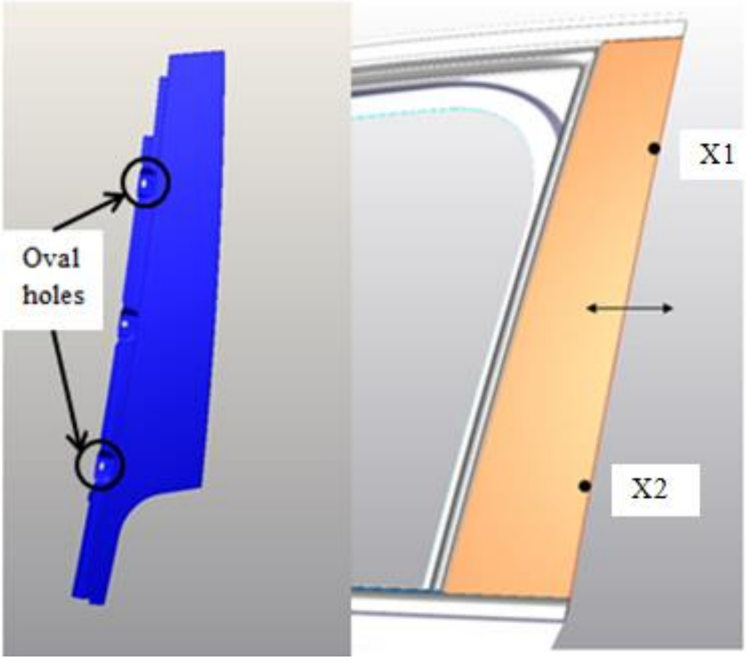

Figure 40. Measuring points on the capping in X-direction

The capping is mounted to the left front door with three screws and with a reference pin into a slot in the GRS that impacts the positioning of the component in Y-direction. The CMM used four points located at each corner of the capping to measure, which were compared against the corresponding points on the nominal CAD model to obtain the measurements in flush in Y-direction, see figure 41.

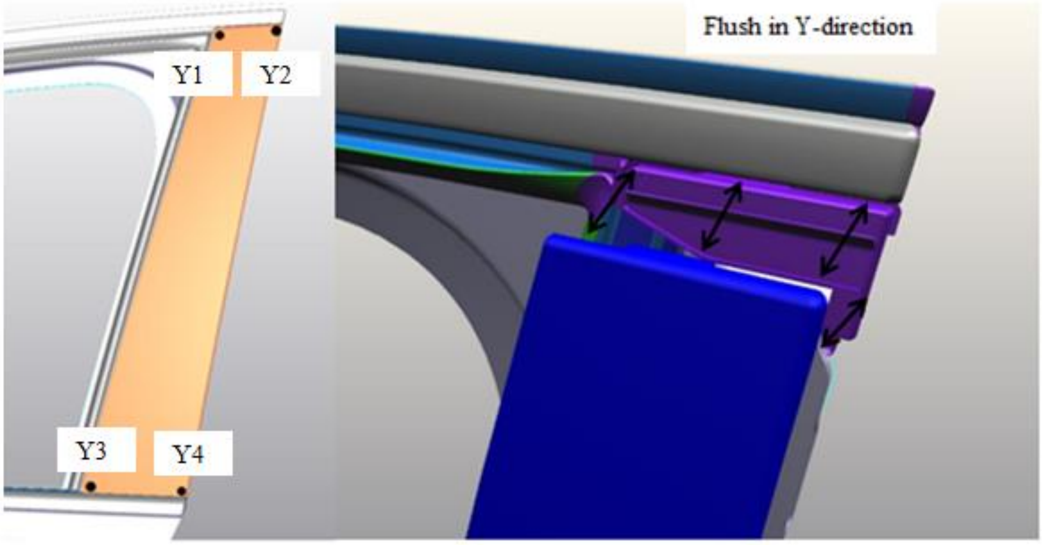

Figure 41. Measuring points on the capping in Y-direction

The capping is mounted with a reference pin into a slot in the GRS that also impacts the positioning of the component in Z-direction. The measuring point that was used for the Z-direction consisted of a punched whole on the upper part of the capping in order for the CMM to be able to measure this location on the component. The CMM measured the center point of the hole and this was then compared against the corresponding point on the nominal CAD model to obtain the measurements in Z-direction, see figure 42.

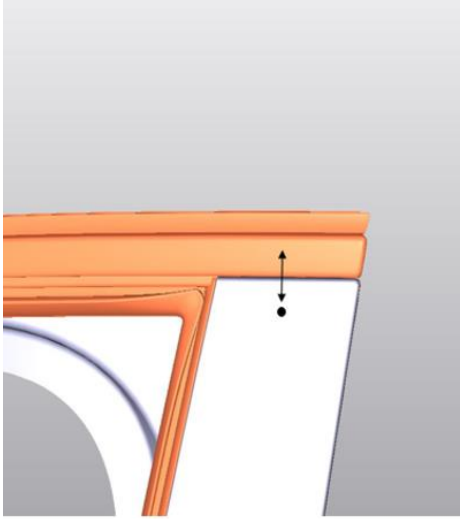

Figure 42. Measuring point on the capping in Z-direction

3.1.4 Force measurement procedure

The force was measured with a dynamometer during the physical study in which one pressure object was designed for each of the three components included in the study. The pressure objects were designed in order to enable measurement of the force in relation to the manual assembly. Each pressure object was designed so that the direction of the force would correspond with the main direction of the force that is applied during assembly of these components in the production. The pressure objects had a threaded hole that was attached to a screw on the dynamometer.

The force measurement procedure was performed after each assembly process and was therefore repeated nine times. After mounting the GRS, capping and OWS on the left front door, the operator performed the force measurement procedure by pressing the dynamometer with the attached pressure object against the component with approximately the same force that was used as during the assembly. This was performed for all the three components with the respective pressure object after assembly of the GRS, capping and OWS and the operator was standing in the same position in the force measurement procedure as during the assembly of the components.

The pressure object for the GRS with the direction of the force that is applied during assembly can be seen in figure 43.

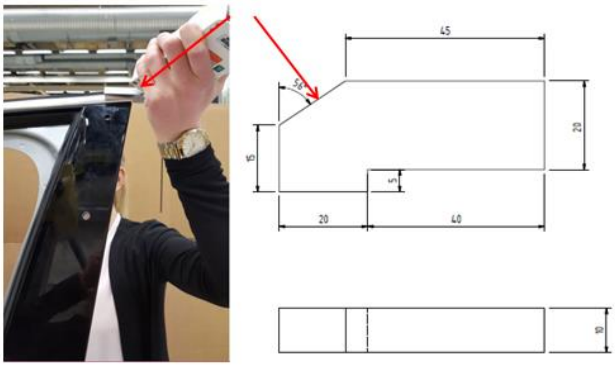

Figure 43. Pressure object for the GRS

The pressure object for the OWS with the direction of the force that is applied during assembly can be seen in figure 44.

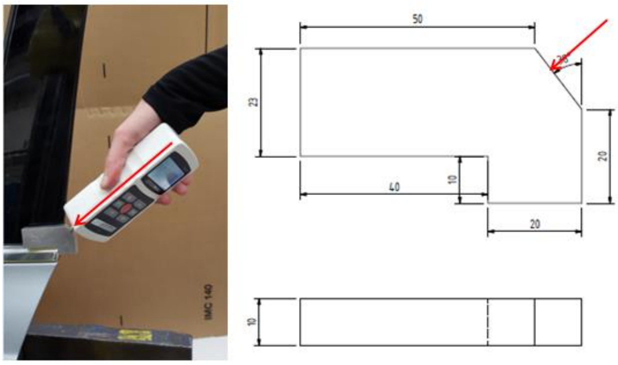

Figure 44. Pressure object for the OWS

The pressure object for the capping with the direction of the force that is applied during assembly can be seen in figure 45. A hole was drilled through the door in order for the pressure object for the capping to not move during the force measurement procedure.

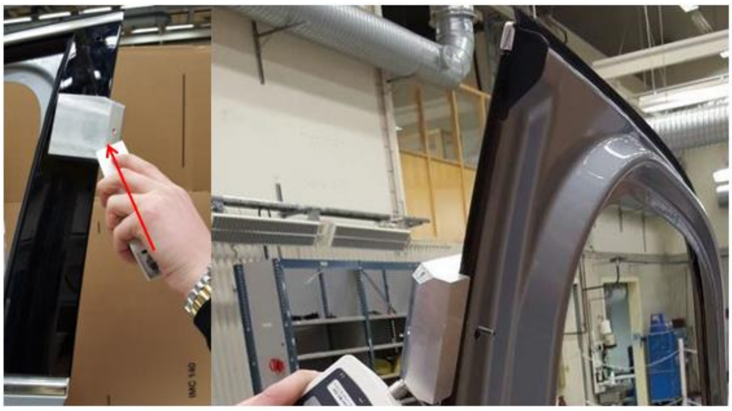

Figure 45. Pressure object for the capping

3.2 Virtual study of the front bumper

The virtual study of the front bumper was performed to evaluate if it is possible to find an optimal assembly sequence with regards to operators' contribution to variation. This was evaluated by creating a virtual model of the front bumper for one car model. The virtual model was created in RD&T in order to run simulations to obtain measurements of deviations and forces with regards to manual assembly sequences. The preparations and performance of the virtual study will be described in this section.

3.2.1 Assembly sequence for the front bumper

The front bumper for the car model can be seen in figure 46.

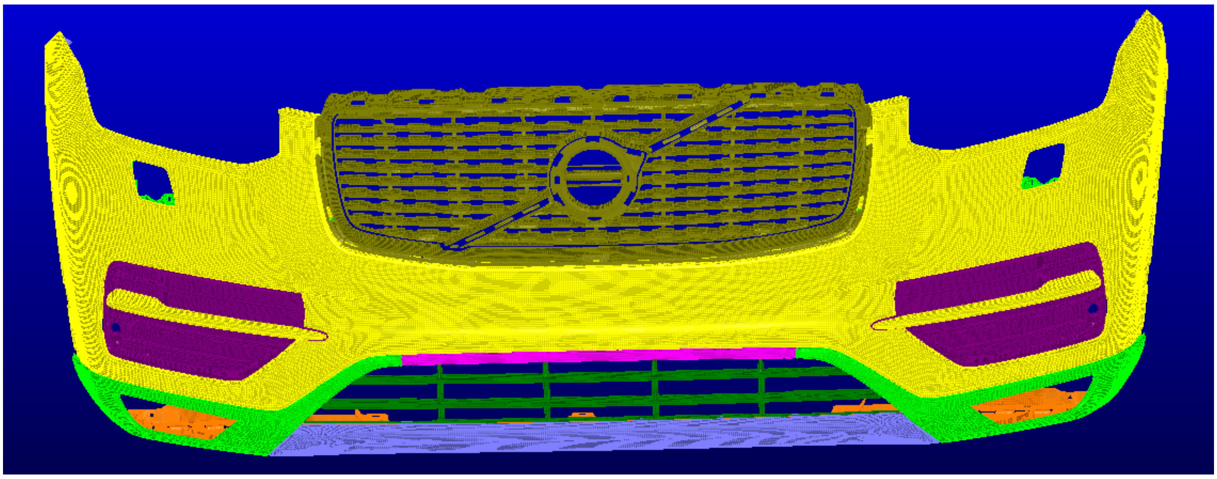

Figure 46. Front bumper

The front bumper in relation to the car body can be seen in figure 47 and the assembly sequence for how the front bumper is mounted on the car body in production consists of six main steps.

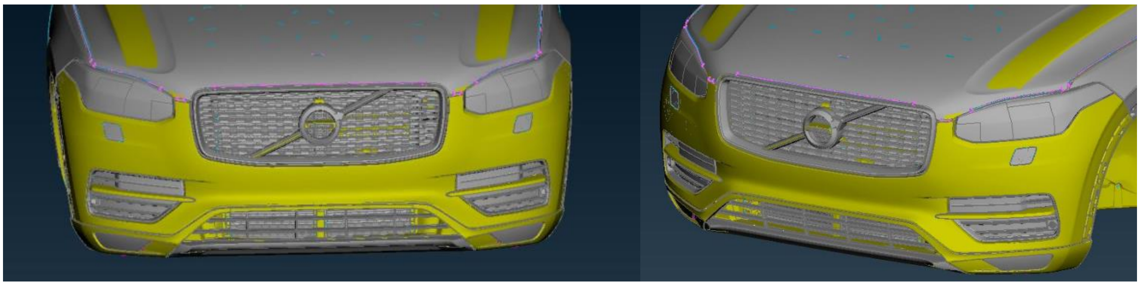

Figure 47. Front bumper mounted on the car body

The first step of the assembly process is to place the front bumper against the car body by positioning the grille on the front end carrier and the undershield under the cooling member (C8611-0002, 2016), see figure 48. Five clips are then mounted in the five reference points on the grille to attach it against the front end carrier (Andreasson, 2016) (Östergaard, 2016).

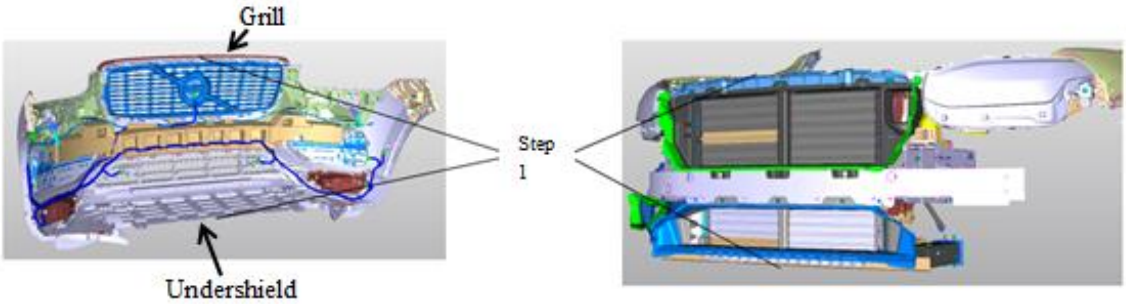

Figure 48. First step of the assembly process (C8611-0002, 2016)

There are one guide pin on the left combined bracket and one guide pin on the right combined bracket that are used to mount the front bumper on the car body, see figure 49.

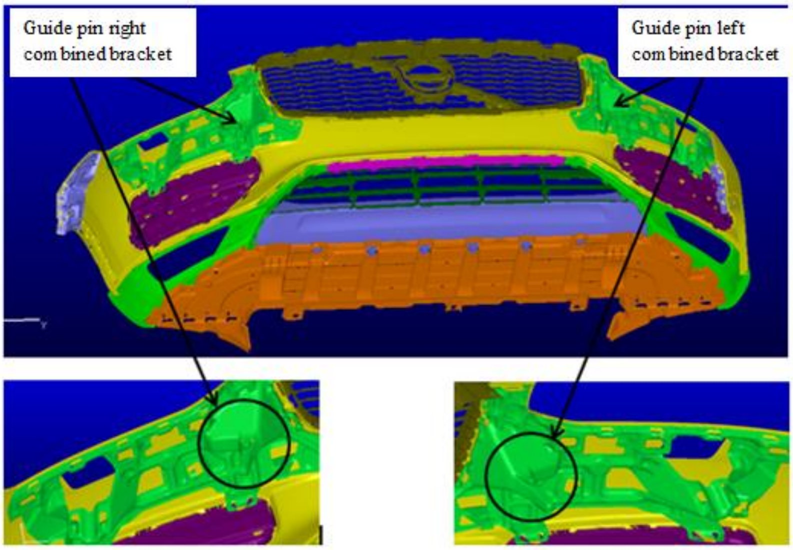
Guide pin right combined bracket
Guide pin left combined bracket

Figure 49. Guide pins on left and right combined bracket

The second step of the assembly process is to place the two guide pins that are attached to the left and right combined bracket on the front bumper into the bracket bumper carrier on the car body and then push the hooks in place, see figure 50 (C8611-0002, 2016).

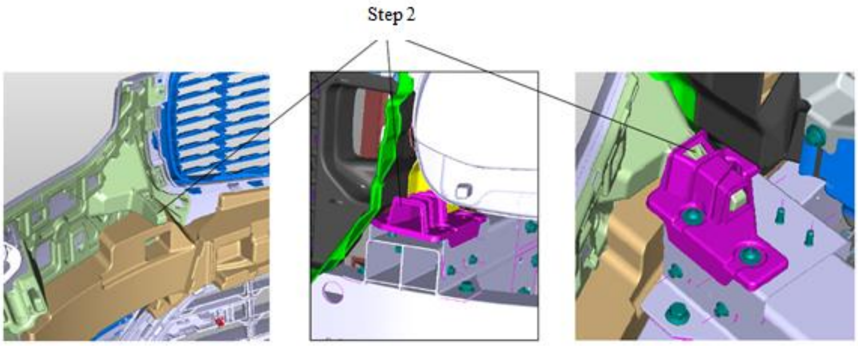

Figure 50. Second step of the assembly process (C8611-0002, 2016)

There are one guide pin on the left fender bracket and one guide pin on the right fender bracket that are used to mount the front bumper on the car body, see figure 51.

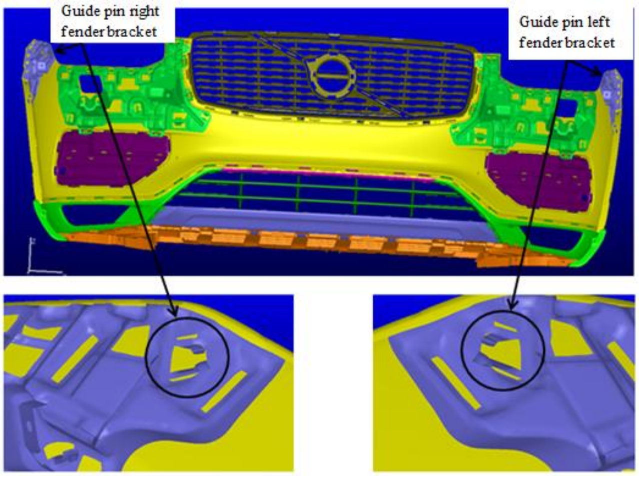

Figure 51. Guide pins on right and left fender bracket

The third step of the assembly process is to place the guide pines that are attached to the left and right fender bracket on the front bumper into the bracket bumper carrier on the car body and then push the hooks in place, see figure 52 (C8611-0002, 2016).

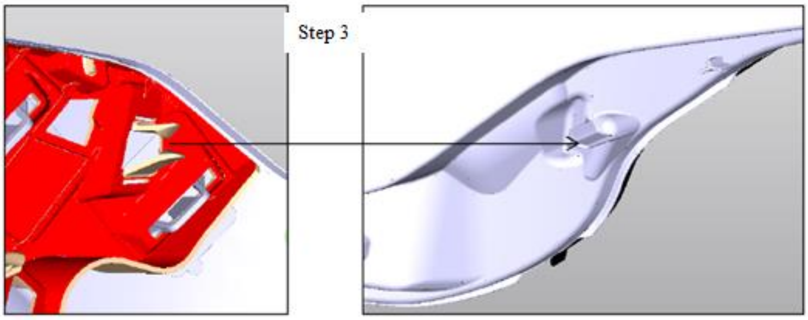

Figure 52. Third step of the assembly process (C8611-0002, 2016)

The left fender bracket and the right fender bracket has two guide pines each and two screw holes respectively, that are used to position the front bumper against the car body, see figure 53.

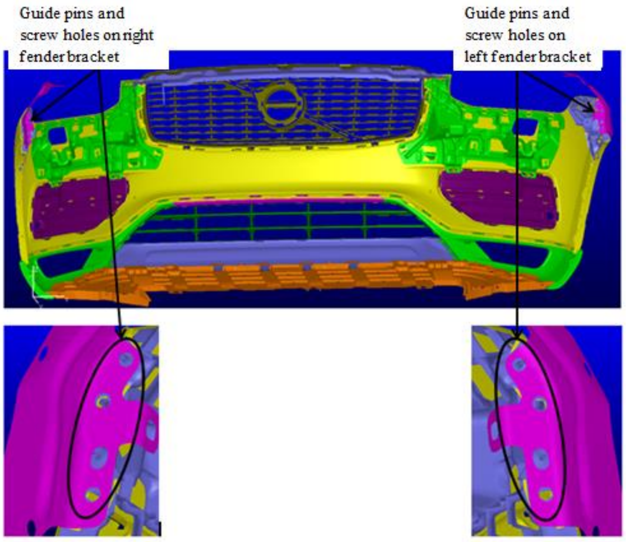
Guide pins and screw holes on right fender bracket
Guide pins and screw holes on left fender bracket

Figure 53. Guide pins and screw holes on right and left fender bracket

The fourth step in the assembly process is to position the guide pines on left fender bracket and right fender bracket into holes in front fender, see figure 54 (C8611-0002, 2016).

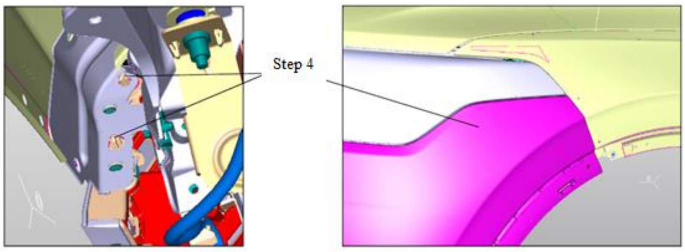

Figure 54. Fourth step of the assembly process (C8611-0002, 2016)

The fifth step in the assembly sequence is to tighten two screws into holes on left fender bracket and two screws into holes on right fender bracket against the front fender, the upper screw should be tighten before the lower screw, see figure 55 (C8611-0002, 2016).

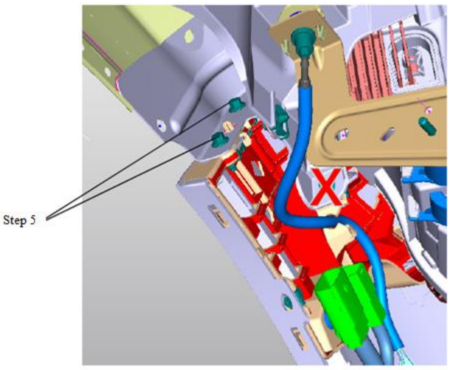

Figure 55. Fifth step of the assembly process (C8611-0002, 2016)

The sixth step in the assembly process is to mount three clips through the undershield into the front subframe, see figure 56 (C8611-0002, 2016).

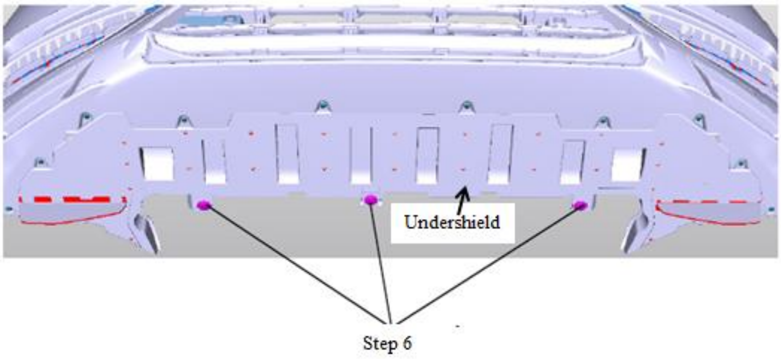
Undershield
Step 6

Figure 56. Sixth step of the assembly process (C8611-0002, 2016)

3.2.2 Building of virtual model in RD&T

The virtual model of the front bumper consists of eleven different parts, see figure 57 and for a more detailed image of each part see appendix A. All of these parts have been meshed in order to import them into RD&T through the compliant function that enables simulation for non-rigid parts. All the parts were mid-surface meshes and it was important in this process to check that all the nodes were connected to the rest of mesh in order for it to function in RD&T.

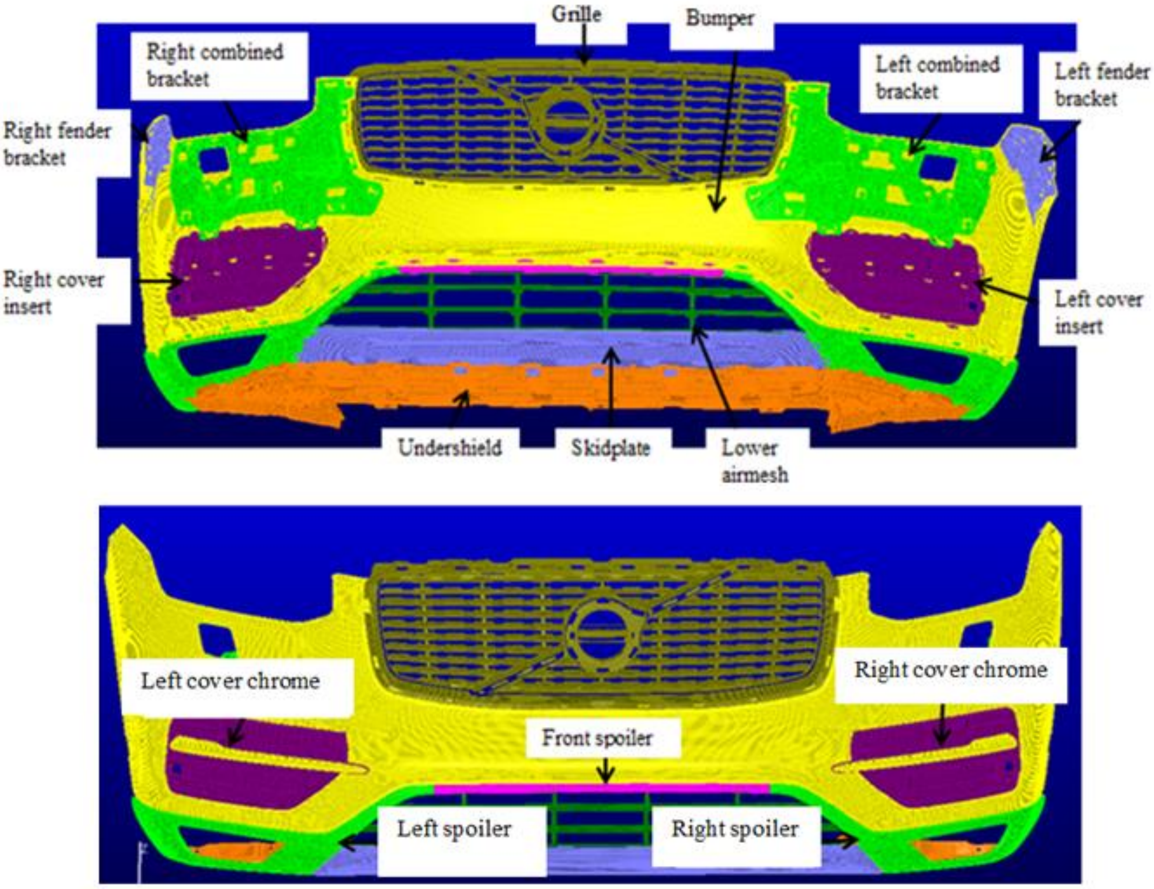
Grille
Bumper
Right combined bracket
Left combined bracket
Left fender bracket
Right fender bracket
Right cover insert
Left cover insert
Undershield
Skidplate
Lower airmesh
Left cover chrome
Right cover chrome
Front spoiler
Left spoiler
Right spoiler

Figure 57. Parts in the front bumper

3.2.2.1 Joining of front bumper components

When all the meshed parts that constituted the front bumper had been imported into RD&T, a new part was created in which all the meshed parts were included. This new part was then used to create a super part in which all the meshed components were joined by the use of weld points. Each weld point consisted of a node-pair in which a local node was selected on one of the components and an adjacent target node was selected on another component in order to join the two parts. Figure 58 illustrates one example of a weld point in which a node-pair was used to join the left fender bracket to the bumper.

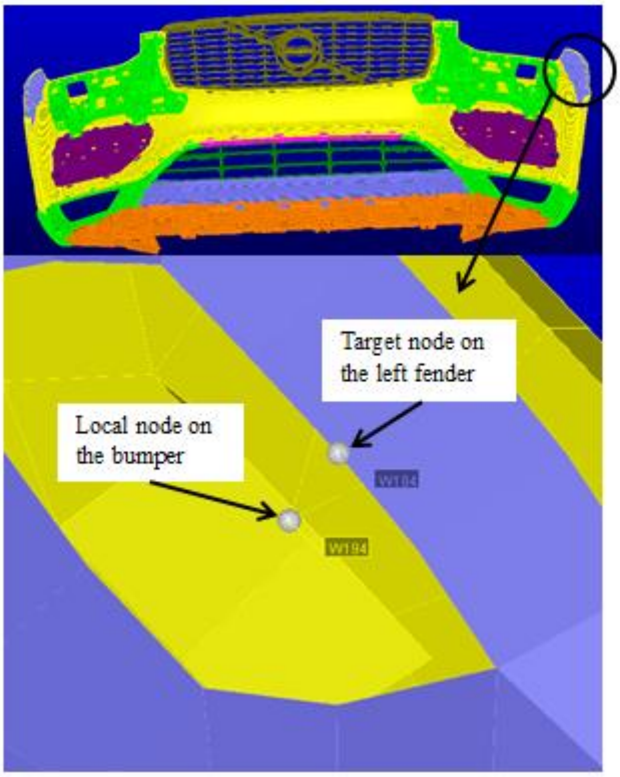

Figure 58. Node-pair

This procedure was repeated until all the meshed components in the super part were joined, see figure 59.

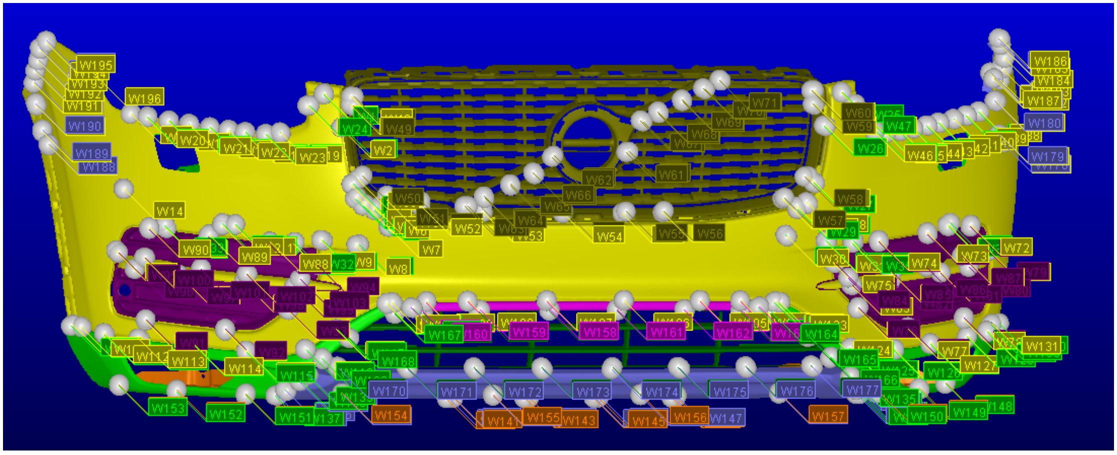

Figure 59. Weld points to join components in the super part

3.2.2.2 Assembly of car body components to front bumper

The next step in the process of creating the virtual model was to assemble the grille and the right and left side of the bumper against the car body. Three meshed car body components were therefore imported into RD&T, see figure 60 and for a more detailed image of each part see appendix B. Only these three car body components were selected to be included in the virtual model since their attachment against the grille, the right side and the left side on the front bumper are the relevant areas for the assembly sequences in the virtual study.

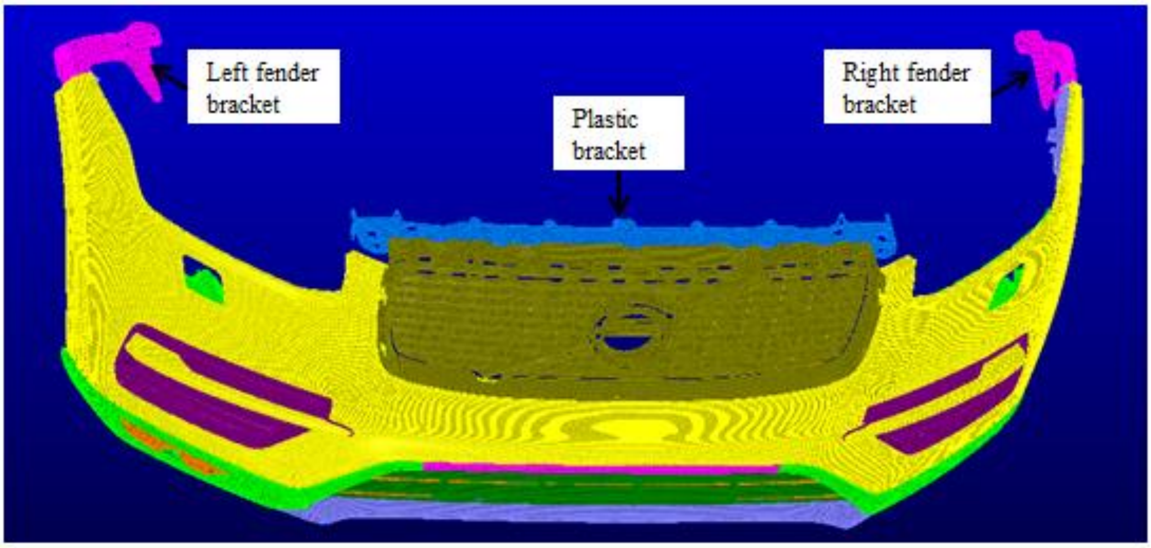
Left fender bracket
Plastic bracket
Right fender bracket

Figure 60. Car body components

A positioning scheme in the form of six directions was created for each car body component. These components constituted the local parts in the locating schemes and a fixture was used as a target part in order to lock the position of the components in space. Each locating scheme included six reference points, see figure 61.

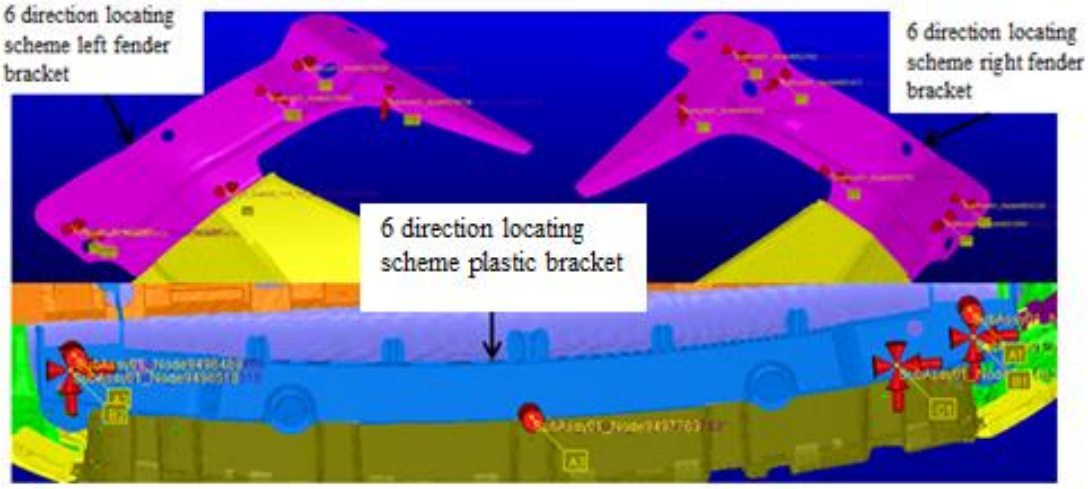
6 direction locating scheme left fender bracket
6 direction locating scheme right fender bracket
6 direction locating scheme plastic bracket

Figure 61. Positioning systems on car body components

A positioning scheme in the form of six directions was also created for the super part that includes all the assembled components in the front bumper. The super part was selected as the local part and the same fixture that was used in the car body components locating schemes was used as a target part. This positioning system was only created since the FEM solver in RD&T requires that all the degrees of freedom are locked. The locating scheme that included six reference points was therefore positioned on the undershield in the super part in order to not disrupt the simulations of the assembly process, see figure 62.

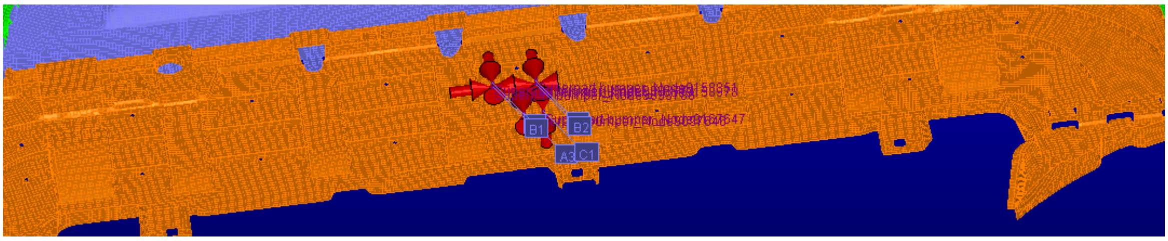

Figure 62. Positioning system on super part

A subassembly was created that included the super part with all the components in the front bumper, the car body components and the fixture in order to attach the front bumper to the car body. A positioning system was created for the subassembly by using the same reference points that were used in the three locating schemes on the car body components. The locating scheme for the subassembly did then include six reference points and twelve support points. The car body components were used as local parts and a second fixture was created as a target part in order to lock the position of the subassembly in space. The first fixture that was used in the locating schemes for the car body components and the super part was set as a local ground in the subassembly in order for it to not move during the assembly of the subassembly (Robust Design and Tolerancing, 2015).

The front bumper consists of several reference points that are used to attach the part against the car body, see figure 63. Weld points were added to all these reference points in order to further mount the front bumper against the car body and contact points were also added in order prevent mating surfaces from intersecting with one another during the simulation (Lindau *et.al.*, 2016). The technique of using weld points was only utilized to mount components in the virtual model but weld points are not used in production during the assembly process of the front bumper.

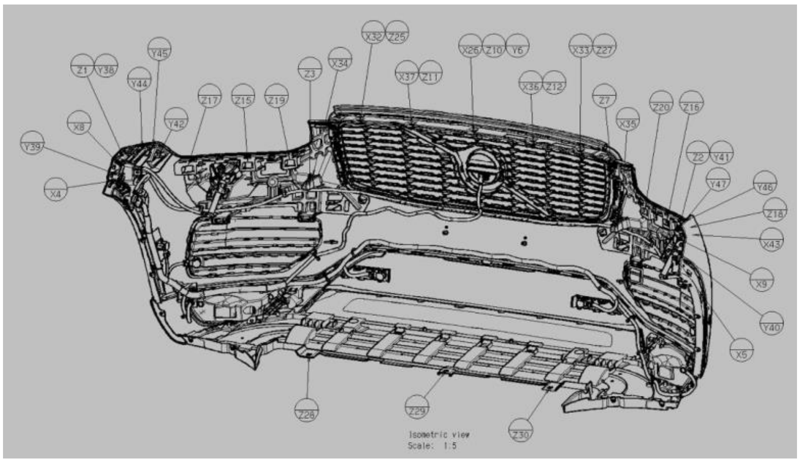

Figure 63. Reference points on the front bumper

3.2.2.3 Completion of the virtual model

Tolerances were added to the car body components in the weld points that are located in the reference points that are affected by the y-direction, which is illustrated by the circles in figure 64. The directions for the tolerances were automatically set to the direction of the vector in the node, it was therefore necessary to adjust the vector to y-direction in all the tolerances. It has been observed in production that the front bumper has a tendency to deviate in all directions during manual assembly, but it is only the y-direction that will be analyzed to limit the scope of the virtual study.

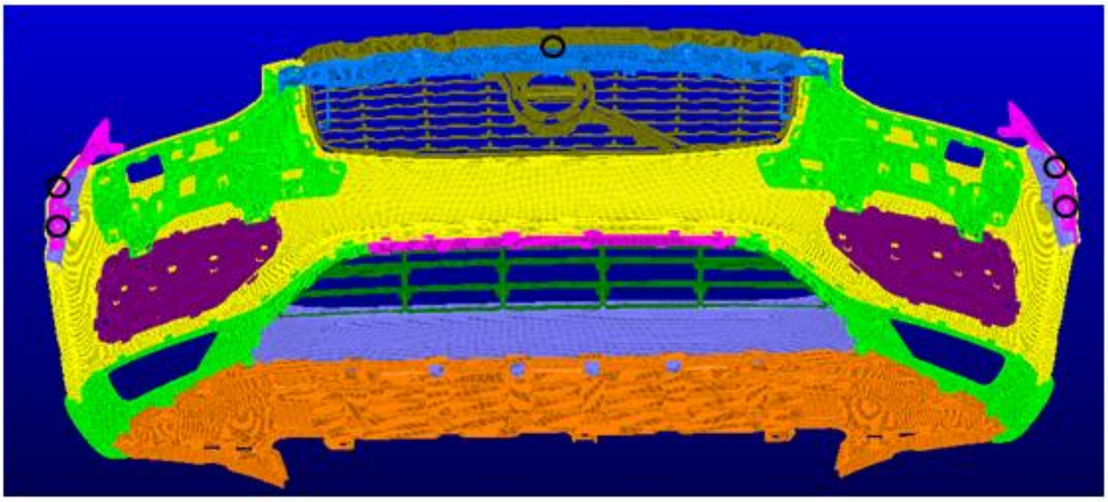

Figure 64. Reference points in which tolerances were added

Information about the elastic modulus and thickness had to be added for all the parts in order for the virtual model to deform in accordance with correct material properties, see appendix C to view data about material properties for the components. The car body components and the grille on the front bumper had the material properties of steel since they are assumed to be significantly more rigid than the other components.

3.2.3 Measurements of virtual model in RD&T

The areas for measurements that were chosen for the virtual model was located between the front bumper and the front lamps, see the black measurements in figure 65. These measurements were analyzed on the left and right side of the front bumper.

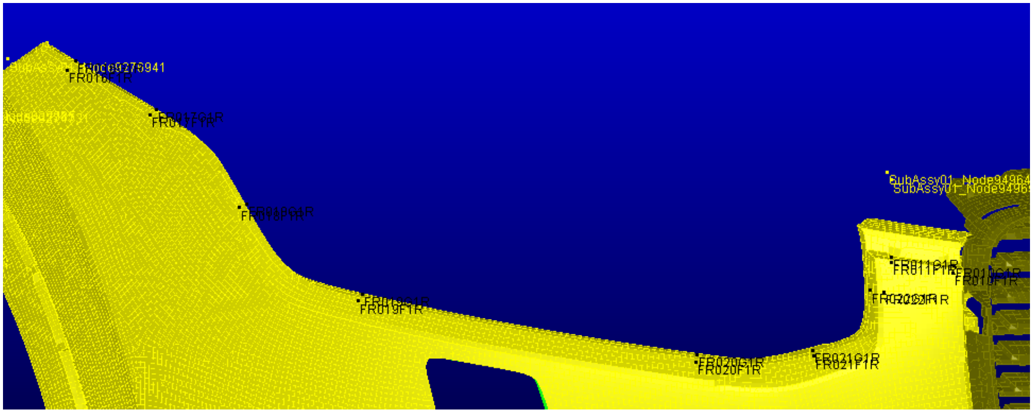

Figure 65. Measurements on the front bumper

Measurement points between the front bumper and the lamps were selected since deviations in the form of gap and flush between these two parts have been detected in production. Each area that was measured on the front bumper in relation to the lamp had one measurement point for gap (G) and one for flush (F). The gap is the space between front bumper and lamp. A negative deviation from the nominal value will result in a smaller gap and a positive deviation from the nominal value will result in a larger gap. Flush represent how the surfaces on the lamp and front bumper move in relation to each other. A negative deviation from the nominal value will result in flush in negative direction and a positive deviation from the nominal value will result in flush in positive direction, see figure 66.

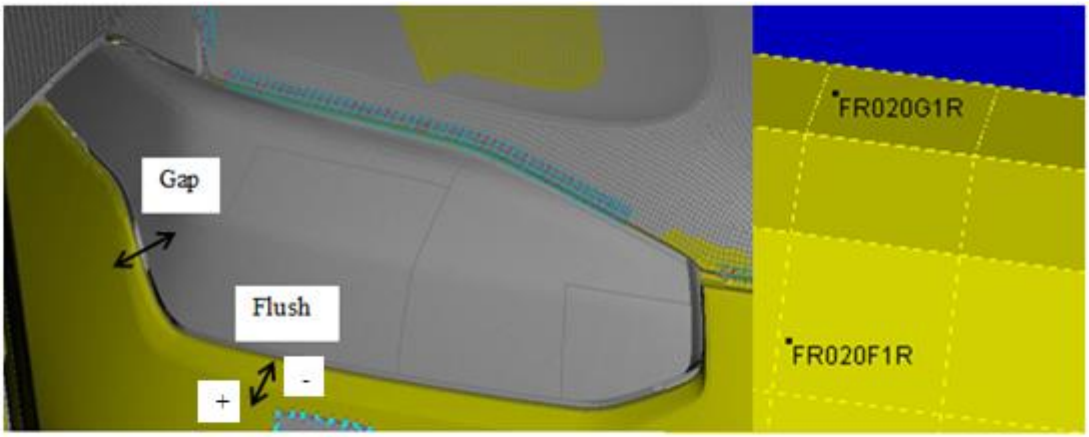

Figure 66. Gap and flush between front bumper and lamp

3.2.4 Measuring of the force on front bumper in RD&T

The function create contact force was used in RD&T to obtain measurements of the force during assembly. The forces will be measured in the form of welding forces, which are the forces required to assemble components together. Figure 67 illustrates the reference points on the front bumper in which the welding forces have been measured. The welding forces are measured in order to obtain possible differences in force between the two manual assembly sequences of the front bumper against the car body.

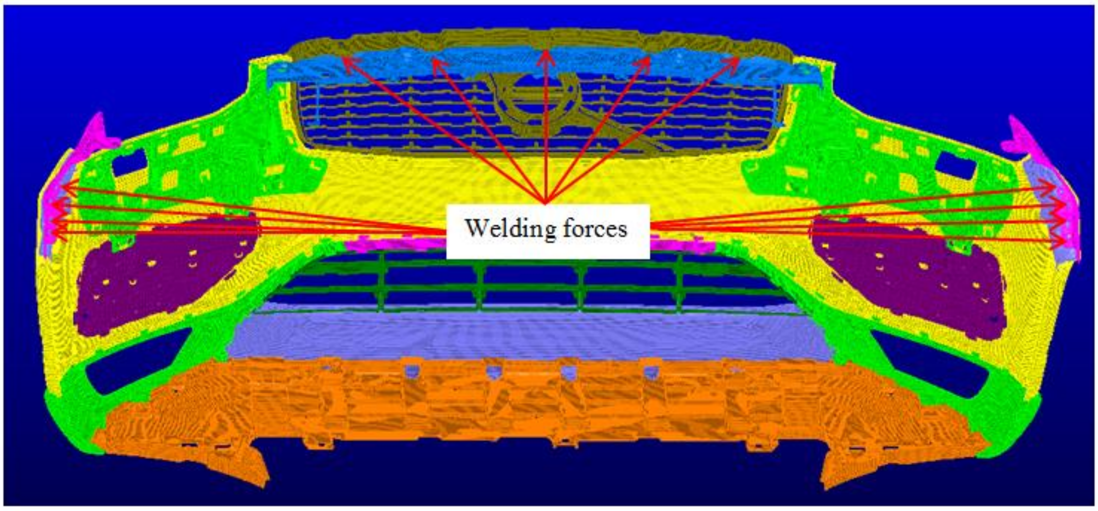

Figure 67. Welding forces for front bumper

3.2.5 Welding sequences

The virtual base model has now been created in which all the components have been assembled, relevant measurements for deviation have been created and a function for measuring forces has been added. This virtual base model is then used to create two welding sequences by choosing in which order the weld points should be assembled and then using the function create weld order model in RD&T. Welding sequences are used to be able to consider different assembly sequences in how the front bumper is attached to the car body during the simulations. All the welding points that were located in the reference points on the front bumper were used to create the welding sequences. The first assembly sequence consisted of four steps. In the first step, the weld points on the right side of the front bumper was attached to the car body followed by the second step in which the weld points on the left side of the front bumper was assembled. In the third step, the weld points in the middle of the grille was assembled to the car body and the fourth step included the assembly of the remaining weld points on the grille against the car body, see figure 68. This assembly sequence will now be referred to as the *right-left-middle* assembly sequence.

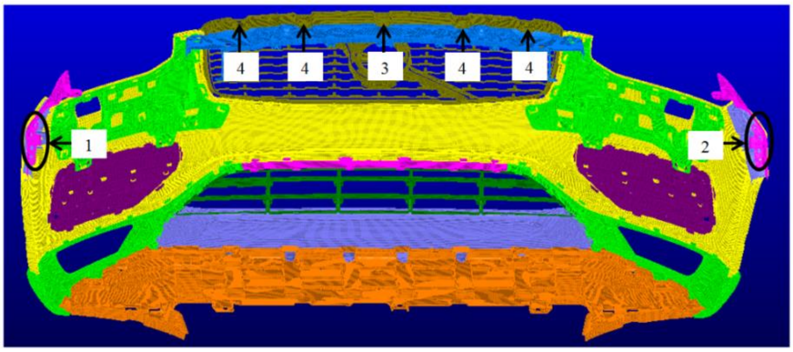

Figure 68. Right-left-middle assembly sequence

The second assembly sequence consisted of four steps. In the first step, the weld points in the reference point in the middle of the grille were assembled to the car body and the second step included the assembly of the remaining weld points on the grille against the car body. In the third step, the weld points on the right side of the front bumper were attached to the car body followed by the fourth step in which the weld points on the left side of the front bumper were assembled, see figure 69. This assembly sequence will now be referred to as the *middle-right-left* assembly sequence.

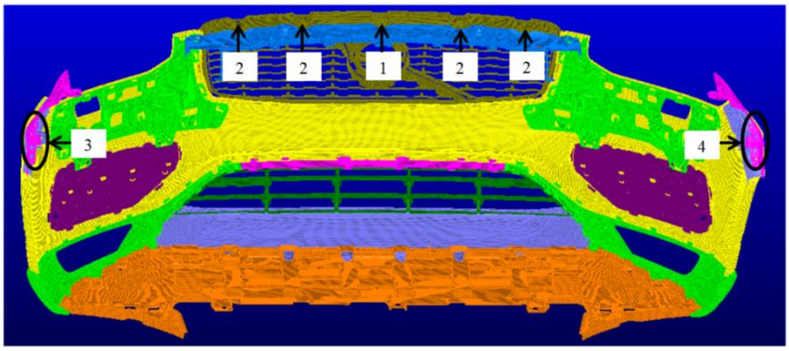

Figure 69. Middle-right-left assembly sequence

3.2.6 Simulations

After the two virtual welding sequence modules had been created, it was time to run simulations. Deviations in the reference points in y-direction on the left and right fender bracket of the car body have been measured in production after the front bumper has been manually assembled against the car body. The -3 sigma values of these measured deviations have been used in the virtual study to analyze deviations in relation to assembly sequence and theoretical values have been used for the y-direction in the middle of the grille, see table 1 that contains these values.

Table 1. -3 sigma values and theoretical values

Reference points	**Minus 3 sigma values in y-direction (mm)**
Front bumper left side	-1,69
Front bumper right side	-1,09
Reference points	**Theoretical values in y-direction (mm)**
Middle of the grille	1
Middle of the grille	2

These values have been added as an offset in the tolerances for the car body components in the weld points that represents the y-direction, located in the reference points on the front bumper, see figure 70. The car body components have been simulated with offsets from the nominal position.

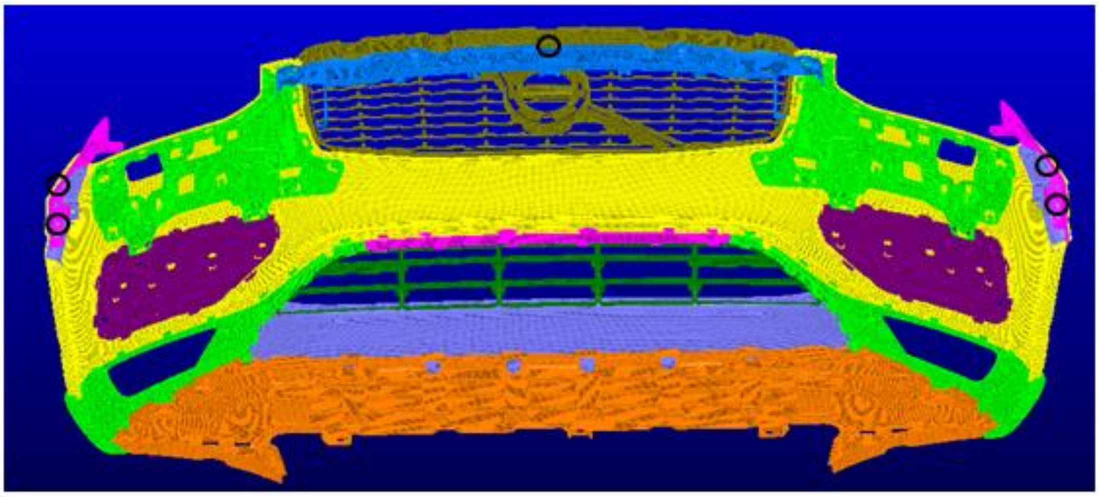

Figure 70. Reference points with added tolerances

After the values had been added as an offset a simulation was run in order to obtain deviations and welding forces. Two simulations were performed for each assembly sequence and the respective values that were used in each simulation can be seen in appendix D. The simulations in RD&T were based on offsets in y-direction in order to detect deviations, which mean that the simulations did not include Monte Carlo iterations. Because Monte Carlo is a method that uses iterations to achieve variation simulations and it is not applied in the virtual study since it is only the offset that is relevant.

4 Results

The result chapter is divided into two sections. The first one is the measured results from the physical study of the front door and the second section is the measured results from the virtual study of the front bumper.

4.1 Results from physical study of the front door

The physical study included nine measurement points for the components GRS, OWS and capping and nine deviations were obtained for each measurement point, see table in appendix E. The force was measured after each assembly process of the GRS, OWS and capping and the obtained forces for each assembler can be seen in appendix F.

4.1.1 Measurements of deviations and forces

One of the measurement points located on the capping in X-direction and the measured deviations and forces for each assembler can be seen in figure 71. Assembler one has an increase in force and a smaller deviation after each assembly process. This indicates that assembler one achieves smaller deviations when the applied force increases. The forces and the deviations decrease for assembler two after each assembly process, which indicates that smaller deviations are obtained when the applied force decreases. It is only a small difference between the forces that are applied by assembler three in each assembly process and the obtained deviations decreases after each mounting. The measured forces differ significantly among the assemblers. Assembler one applies for example a force over 70N in one of the assembly processes while assembler two applies a force under 30N in one assembly process. The measured deviations from the assembly processes differ for each assembler. The largest deviation that is above -0,5 mm was measured during one assembly process performed by assembler three and the smallest deviation that is around -0,25 mm was measured during one assembly process performed by assembler two. The diagrams for the remaining measurement points can be seen in appendix G.

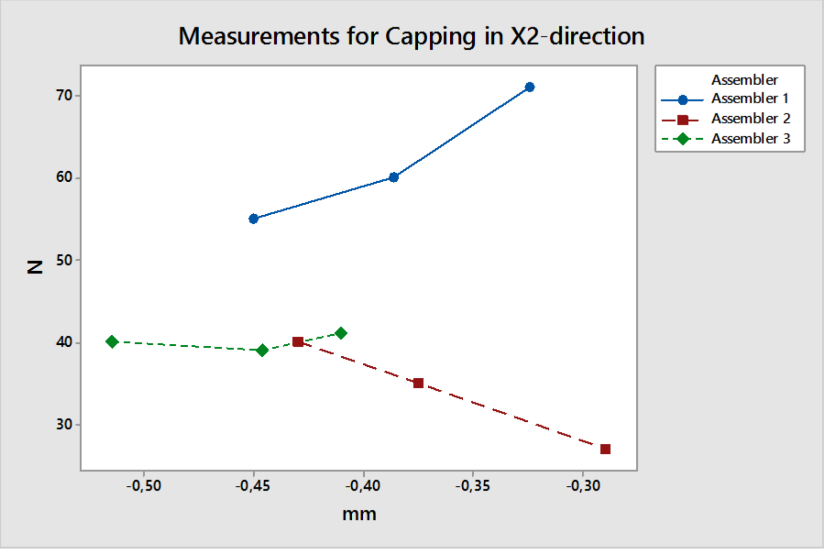

Figure 71. Measurements for Capping in X2-direction

4.2 Results from virtual study of the front bumper

The virtual study resulted in measurements of deviations and forces from simulations for two different assembly sequences.

4.2.1 Measurements of deviations

The first simulation was performed for both assembly sequences with a -3 sigma value of -1,69 mm on the left side of the bumper, a -3 sigma value of -1,09 mm on the right side of the front bumper and a theoretical value of 1 mm in the middle of the grille. The results from simulation one with measured deviations for all the measurement points can be seen in appendix H. The second simulation was also performed for both assembly sequences with the same -3 sigma values on the left and right side of the front bumper as in simulation one and a theoretical value of 2 mm in the middle of the grille. The results from simulation two with measured deviations can be seen in appendix I. The measured deviations from both simulations are based on the mean value. The obtained deviations are caused by deformations in the virtual model during the simulations.

4.2.1.1 Comparison between both assembly sequences for simulation 1

The difference in obtained deviations from simulation one between the *middle-right-left* assembly sequence and the *right-left-middle* assembly sequence can be seen in figure 72. There are deviations in all the measurement points for both assembly sequences since all the measurements deviates from the nominal value. There is more measurement points for the *right-left-middle* assembly sequence in which the deviation is larger in comparison to the *middle-right-left* assembly sequence. There is a small difference in deviation between the assembly sequences from point FR010F1L until point FR011G1R. The deviations differs more between the assembly sequences from point FR016F1L until point FR020F1R. The difference in deviation is smaller in the remaining measurement points. The *middle-right-left* assembly sequence has rather large deviations in the measurement points FR016F1L until FR016G1R that are located on the upper right and left side on the front bumper. The *right-left-middle* assembly sequence has rather large deviations in the measurement points FR018F1L, FR018F1R, FR019F1L and FR019F1R which are located towards the middle of the lamp area on the front bumper.

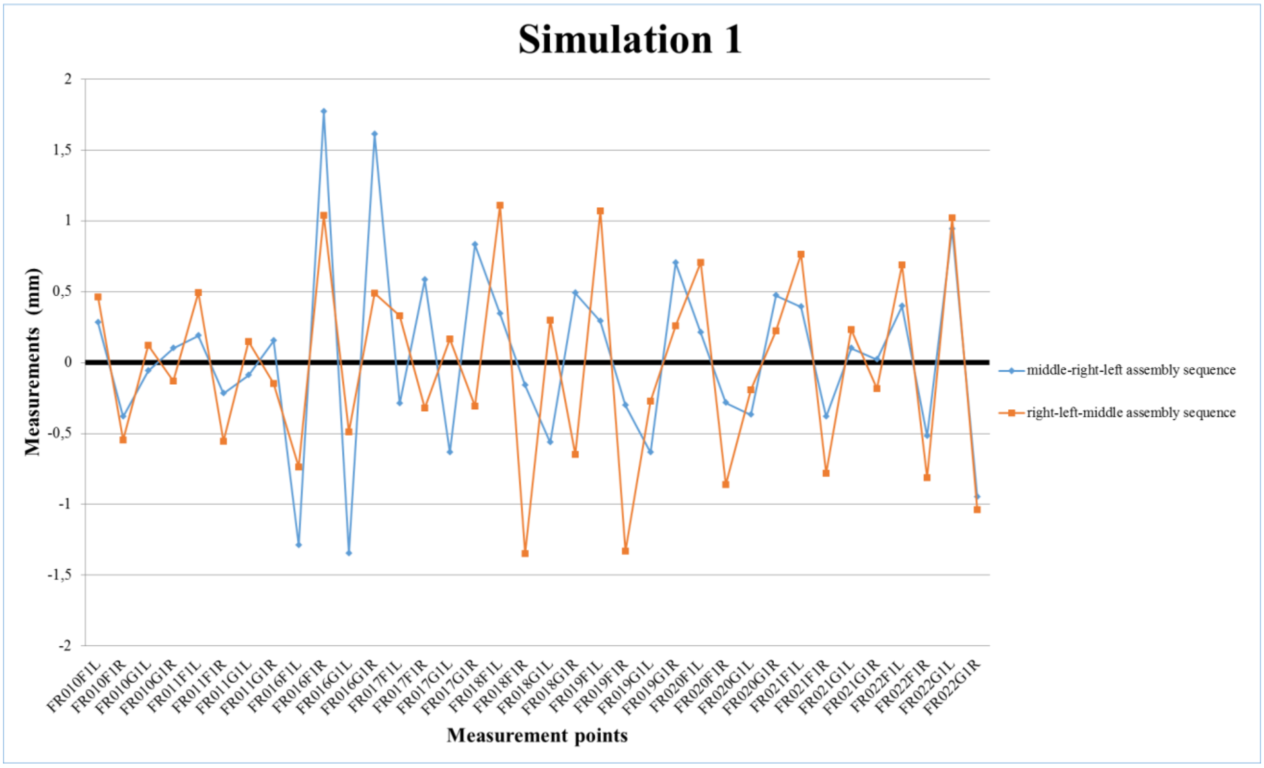

Figure 72. Measured deviations for both assembly sequences from simulation 1

The four measurement points with the largest difference in deviation between both assembly sequences can be seen in table 2.

Table 2. Difference between deviations from simulation 1

	Simulation 1: Measurements (mm)		
Measurement points	**middle-right-left assembly sequence**	**right-left-middle assembly sequence**	**Difference between deviations**
FR016G1R	1,61	0,492	1,118
FR017G1R	0,832	-0,308	1,14
FR018F1R	-0,159	-1,35	1,191
FR018G1R	0,491	-0,647	1,138

The four measurement points are all located on the upper left side of the front bumper, see figure 73.

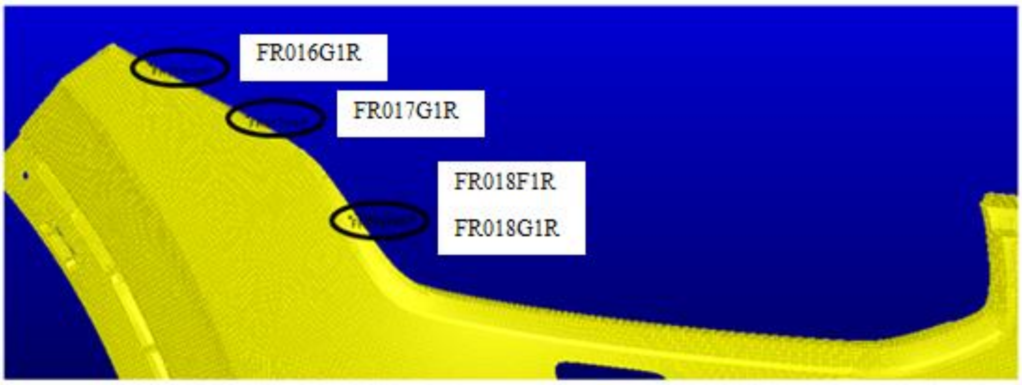

Figure 73. Four measurement points located on the upper left side of the front bumper

The difference in deviation between the assembly sequences for the four measurement points can be seen in figure 74. The deviations for point FR016G1R differ with 1,118 mm and both deviations are positive from the nominal value, which indicates that the gap has increased in both assembly sequences in comparison to the nominal gap. The deviations for point FR017G1R differ with 1,14 mm and the *middle-right-left* assembly sequence has a positive deviation from the nominal value while the *right-left-middle* assembly sequence has a negative deviation from the nominal value. This means that the *middle-right-left* sequence has a larger gap and that the *right-left-middle* assembly sequence has a smaller gap in comparison to the nominal. The deviations for point FR018F1R differ with 1,191 mm and both measurement points have resulted in flush deviations in negative direction from the nominal value. The measurement point FR018G1R has 1,138 mm as difference in deviation between the assembly sequences.

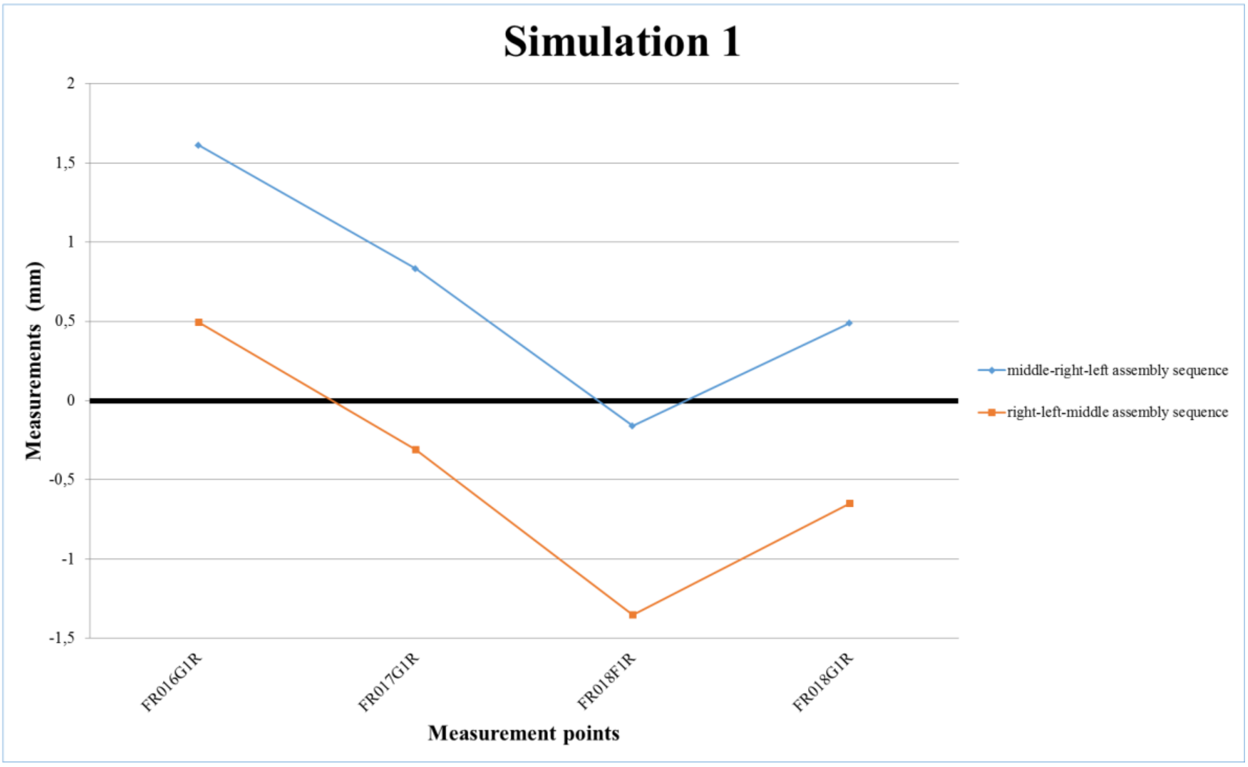

Figure 74. Difference in deviations for four measurements points from simulation 1

4.2.1.2 Comparison between both assembly sequences for simulation 2

The difference in obtained deviations from simulation two between the *middle-right-left* assembly sequence and the *right-left-middle* assembly sequence can be seen in figure 75. There are deviations in all the measurement points for both assembly sequences since all the measurements deviates from the nominal value. There is more measurement points for the *right-left-middle* assembly sequence in which the deviation is larger in comparison to the *middle-right-left* assembly sequence. There is a small difference in deviation between the assembly sequences from point FR010F1L until point FR011G1R. The deviations differs more between the assembly sequences from point FR016F1L until point FR020F1R. The difference in deviation is smaller in the remaining measurement points.

The *middle-right-left* assembly sequence has rather large deviations in the measurement points FR016F1L until FR016G1R that are located on the upper right and left side on the front bumper. The *right-left-middle* assembly sequence has rather large deviations in the measurement points FR018F1L, FR018F1R, FR019F1L and FR019F1R which are located towards the middle of the lamp area on the front bumper.

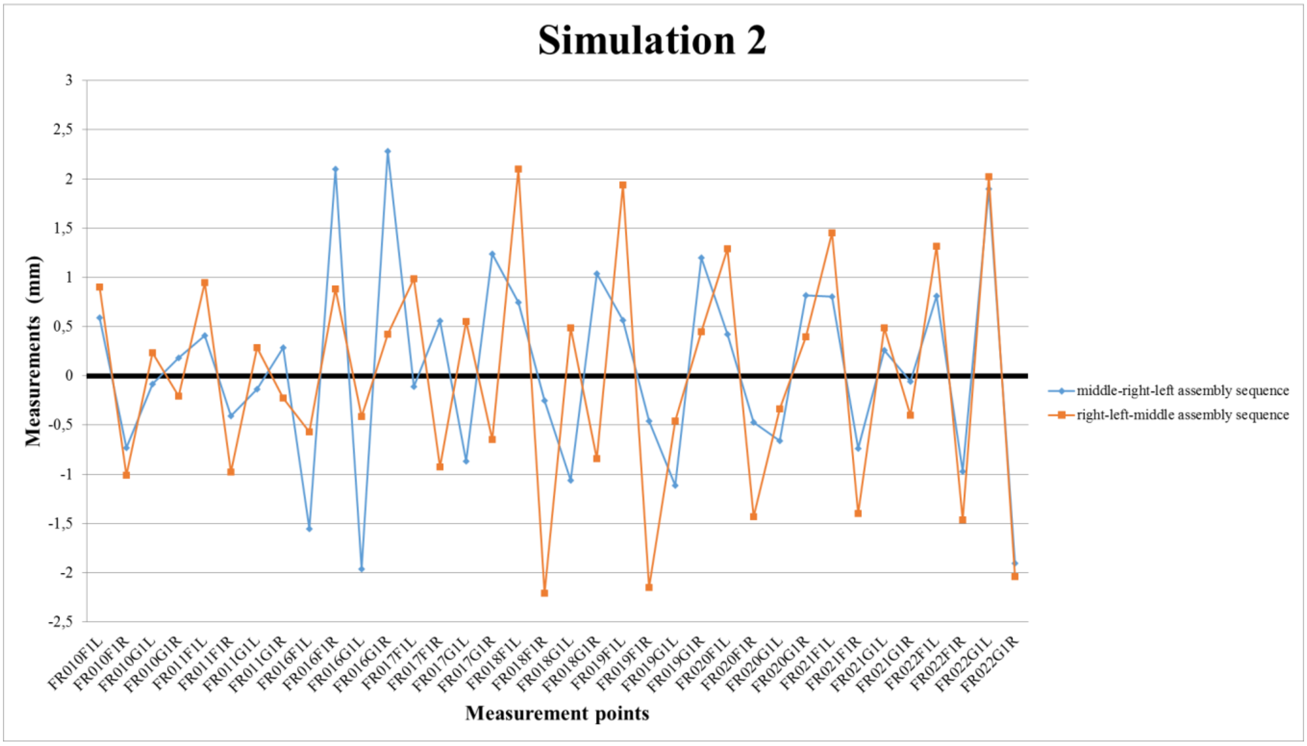

Figure 75. Measured deviations for both assembly sequences from simulation 2

The four measurement points with the largest difference in deviation between both assembly sequences can be seen in table 3.

Table 3. Difference between deviations from simulation 2

	Simulation 2: Measurements (mm)		
Measurement points	**middle-right-left assembly sequence**	**right-left-middle assembly sequence**	**Difference between deviations**
FR016G1R	2,28	0,423	1,857
FR017G1R	1,24	-0,644	1,884
FR018F1R	-0,252	-2,21	1,958
FR018G1R	1,04	-0,841	1,881

The four measurement points are all located on the upper left side of the front bumper, see figure 76.

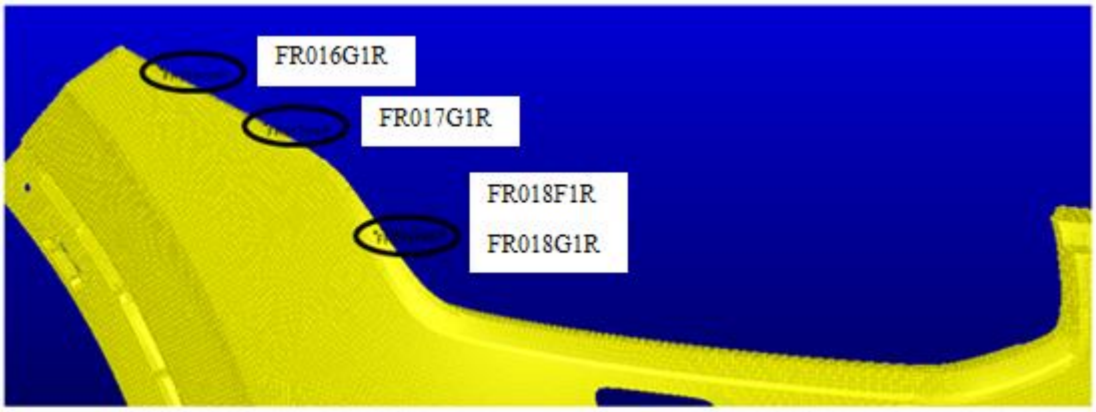

Figure 76. Four measurement points located on the upper left side of the front bumper

The difference in deviation between the assembly sequences for the four measurement points can be seen in figure 77. The deviations for point FR016G1R differ with 1,857 mm and both deviations are positive from the nominal value, which indicates that the gap has increased in both assembly sequences in comparison to the nominal gap. The deviations for point FR017G1R differ with 1,884 mm and the *middle-right-left* assembly sequence has a positive deviation from the nominal value while the *right-left-middle* assembly sequence has a negative deviation from the nominal value. This means that the *middle-right-left* sequence has a larger gap and that the *right-left-middle* assembly sequence has a smaller gap in comparison to the nominal. The deviations for point FR018F1R differ with 1,958 mm and both measurement points have resulted in flush deviations in negative direction from the nominal value. The measurement point FR018G1R has 1,881 mm as difference in deviation between the assembly sequences.

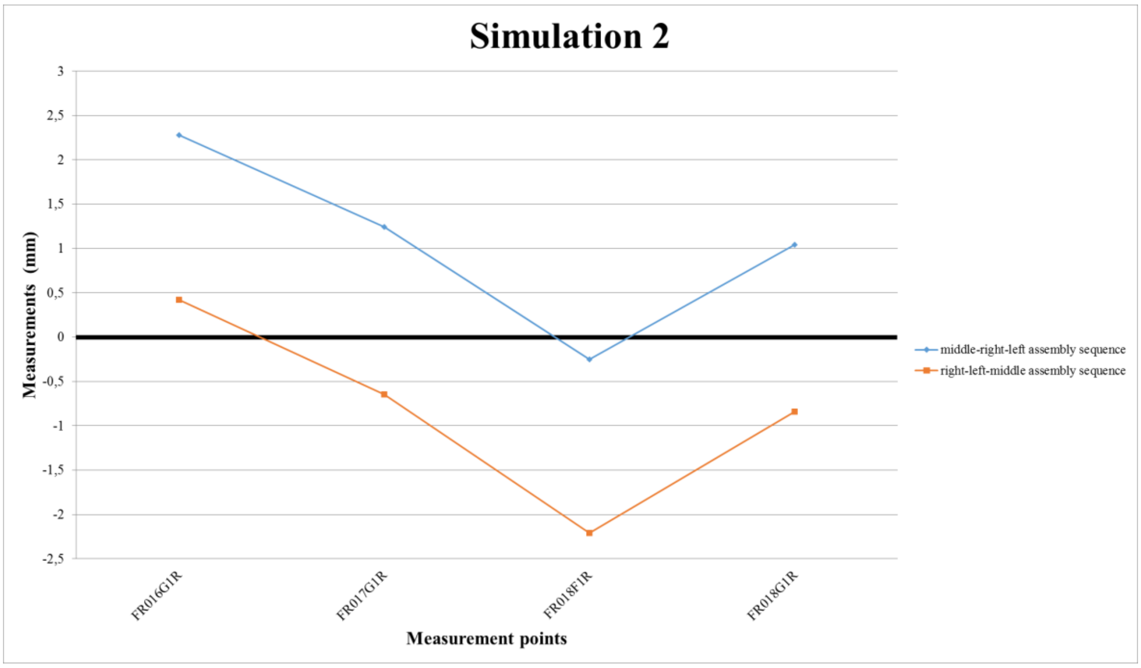

Figure 77. Difference in deviations for four measurements points from simulation 2

4.2.1.3 Comparison between middle-right-left assembly sequences from both simulations

The difference in obtained deviations for the *middle-right-left* assembly sequence between simulation one and simulation two can be seen in figure 78. The difference between these simulations is that the first one had a theoretical value of 1 mm in the reference points in the middle of the grille while the second simulation had a corresponding value of 2 mm.

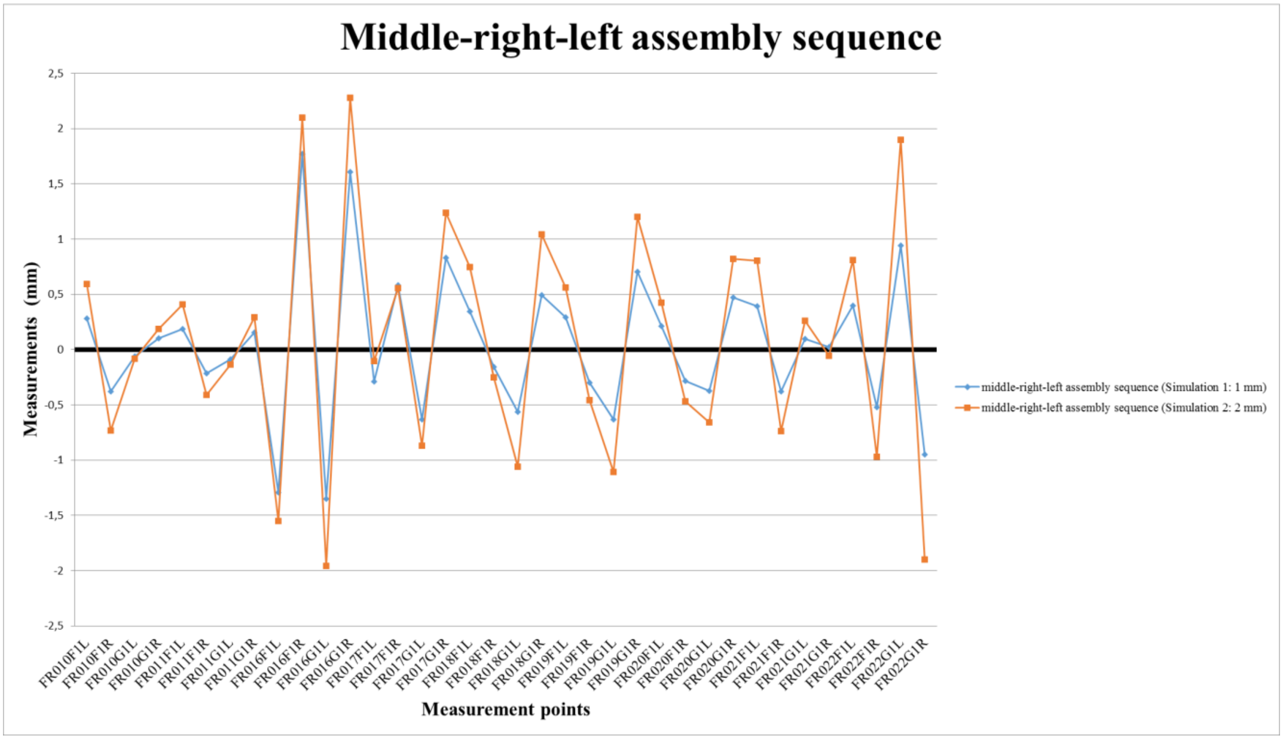

Figure 78. Measured deviations for middle-right-left assembly sequence from both simulations

The four measurement points with the largest difference in deviation for the *middle-right-left* assembly sequence between the two simulations can be seen in table 4.

Table 4. Difference between deviations from both simulations

	Simulation 1	**Simulation 2**	
Measurement points	**middle-right-left assembly sequence (Simulation 1: 1 mm)**	**middle-right-left assembly sequence (Simulation 2: 2 mm)**	**Difference between deviations**
FR016G1L	-1,35	-1,96	0,61
FR016G1R	1,61	2,28	0,67
FR022G1L	0,94	1,9	0,96
FR022G1R	-0,948	-1,9	0,952

Two of the measurement points are located on the left side of the front bumper and the other two measurement points are located on the right side of the front bumper, see figure 79.

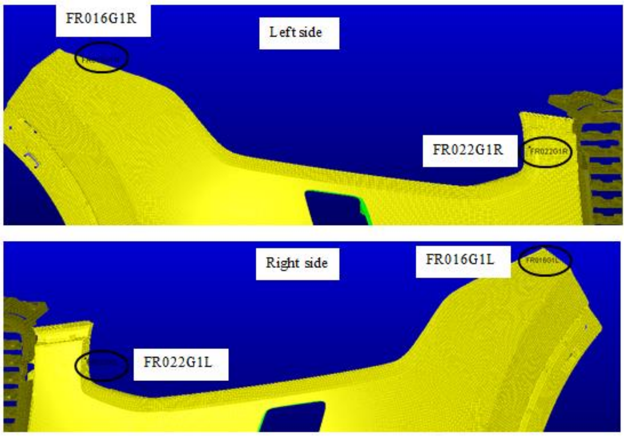

Figure 79. Four measurement points located on the right and left side on the front bumper

The difference in deviation between the two simulations for the *middle-right-left* assembly sequence for the four measurement points can be seen in figure 80. The deviations for point FR016G1L differ with 0,61 mm and this measurement point has negative deviations from both simulations, which indicate that the gap has become smaller after assembly in comparison to the nominal gap. The deviations for point FR016G1R differ with 0,67 mm and this measurement point has positive deviations from both simulations, which indicate that the gap has increased from the nominal gap. The difference in deviation for the measurement point FR022G1R is 0,952 mm and it differs 0,96 mm for the point FR022G1L. These measurement points are respectively located at each side of the grille. The measurements for FR022G1R resulted in negative deviations from the nominal value in both simulations, which means that the gap on the left side of the grille has become smaller and the measurements for FR022G1L resulted in positive deviations from the nominal value, which means that the gap on the right side of the grille has become larger in comparison to the nominal one.

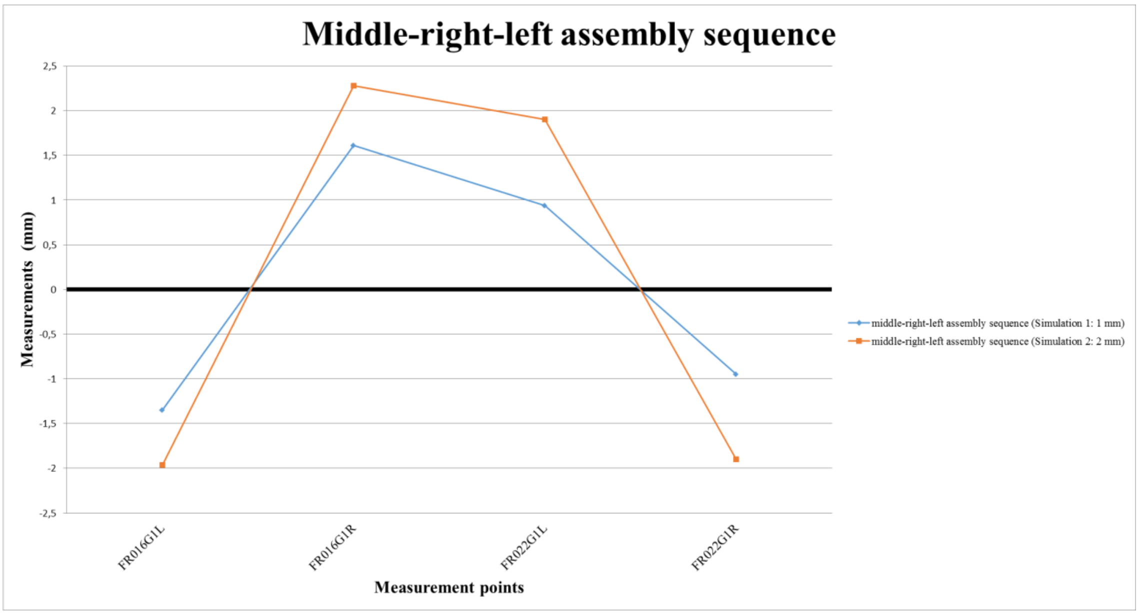

Figure 80. Difference in deviations for four measurements points from simulation 1 and 2

4.2.1.4 Comparison between right-left-middle assembly sequences from both simulations

The difference in obtained deviations for the *right-left-middle* assembly sequence between simulation one and simulation two can be seen in figure 81.

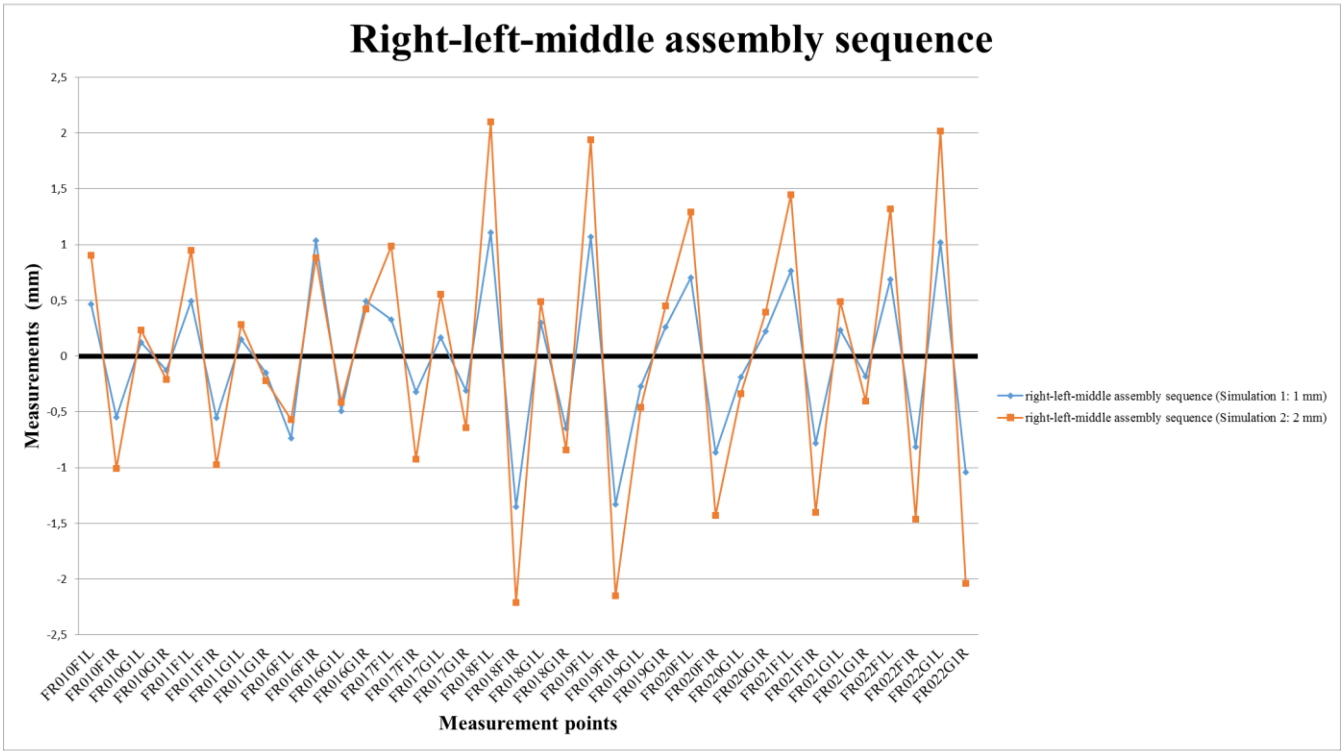

Figure 81. Measured deviations for right-left-middle assembly sequence from both simulations

The four measurement points with the largest difference in deviation for the *right-left-middle* assembly sequence between the two simulations can be seen in table 5.

Table 5. Difference between deviations from both simulations

	Simulation 1	Simulation 2	
Measurement points	**right-left-middle assembly sequence (Simulation 1: 1 mm)**	**right-left-middle assembly sequence (Simulation 2: 2 mm)**	**Difference between deviations**
FR018F1L	1,11	2,1	0,99
FR019F1L	1,07	1,94	0,87
FR022G1L	1,02	2,02	1
FR022G1R	-1,04	-2,04	1

One of the measurement points is located on the left side of the front bumper and the other three measurement points are located on the right side of the front bumper, see figure 82.

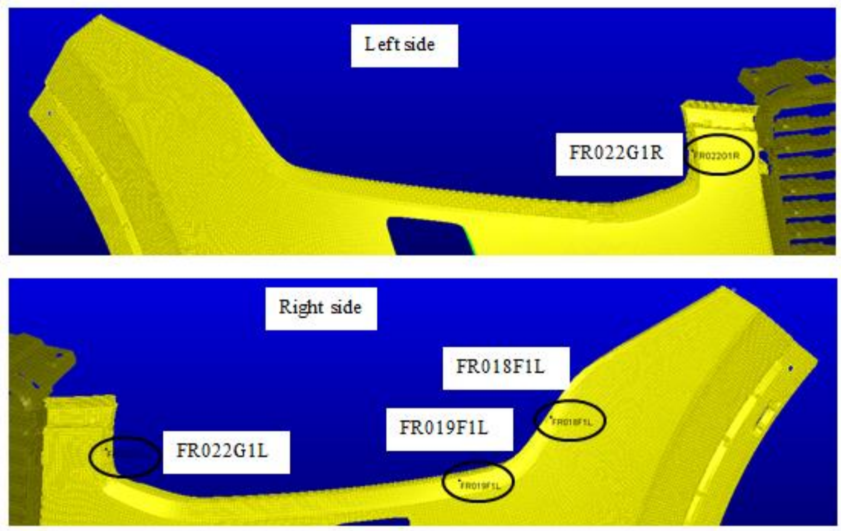

Figure 82. Four measurement points located on the right and left side on the front bumper

The difference in deviation between the two simulations for the *right-left-middle* assembly sequence for the four measurement points can be seen in figure 83. The deviations for point FR018F1L differ with 0,99 mm and it differs 0,87 mm for point FR019F1L. These two measurement points have resulted in flush deviations in positive direction from the nominal value. The difference in deviation for the measurement points FR022G1R and FR022G1L is 1 mm and these points are respectively located at each side of the grille. The measurements for FR022G1R resulted in negative deviations from the nominal value in both simulations, which means that the gap on the left side of the grille has become smaller and the measurements for FR022G1L resulted in positive deviations from the nominal value, which means that the gap on the right side of the grille has become larger in comparison to the nominal one.

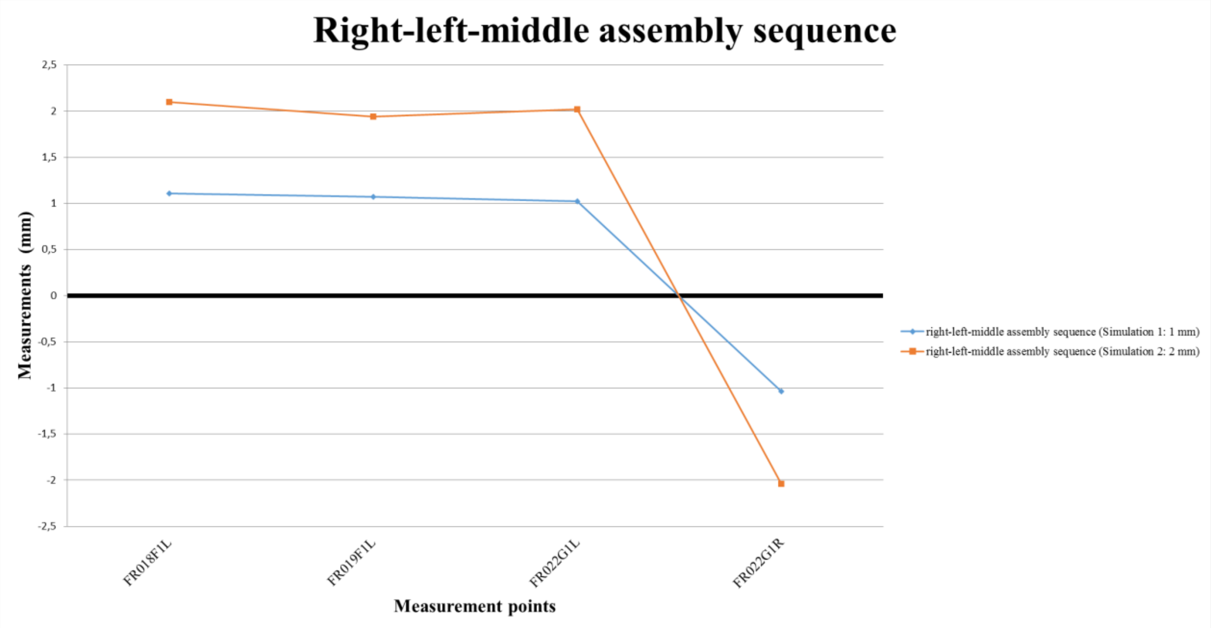

Figure 83. Difference in deviations for four measurement points from simulation 1 and 2

4.2.1.5 Measurements from production

Measurements from production have been obtained for the measurement points between the front bumper and the lamp. The red boxes represent the measurements that are most critical, see figure 84.

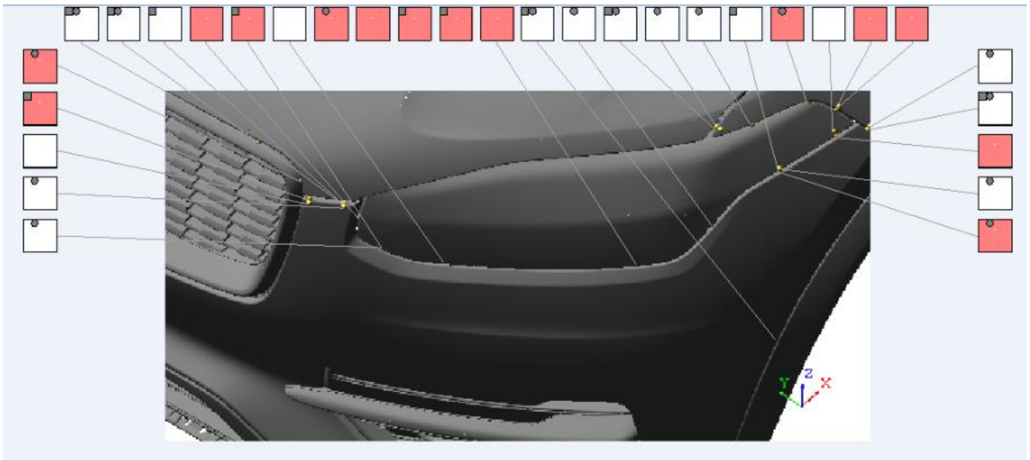

Figure 84. Critical measurements between front bumper and lamp

One measurement that was obtained from production for the point FR019G1L resulted in a +3 sigma value of 0,12 mm and -3 sigma value of -1,2 mm, see figure 85.

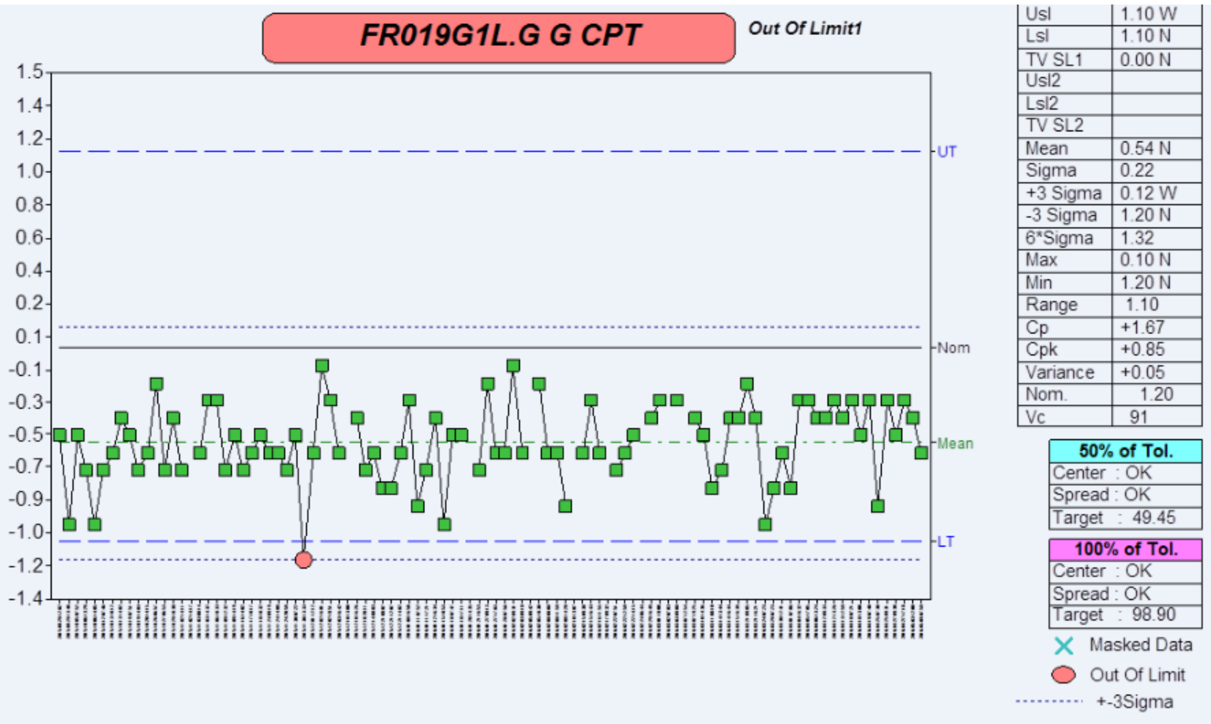

Usl	1.10 W
Lsl	1.10 N
TV SL1	0.00 N
Usl2	
Lsl2	
TV SL2	
Mean	0.54 N
Sigma	0.22
+3 Sigma	0.12 W
-3 Sigma	1.20 N
6*Sigma	1.32
Max	0.10 N
Min	1.20 N
Range	1.10
Cp	+1.67
Cpk	+0.85
Variance	+0.05
Nom.	1.20
Vc	91

50% of Tol.
Center : OK
Spread : OK
Target : 49.45

100% of Tol.
Center : OK
Spread : OK
Target : 98.90

Figure 85. Measurements from production for measurement point FR019G1L

Another measurement that was obtained from production for the point FR022G1L resulted in a +3 sigma value of 2,13 mm and -3 sigma value of -1,06 mm, see figure 86.

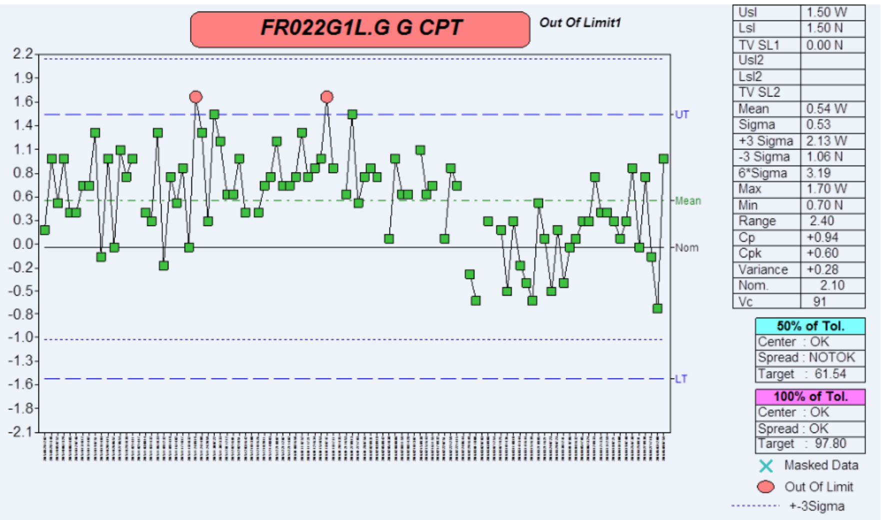

Usl	1.50 W
Lsl	1.50 N
TV SL1	0.00 N
Usl2	
Lsl2	
TV SL2	
Mean	0.54 W
Sigma	0.53
+3 Sigma	2.13 W
-3 Sigma	1.06 N
6*Sigma	3.19
Max	1.70 W
Min	0.70 N
Range	2.40
Cp	+0.94
Cpk	+0.60
Variance	+0.28
Nom.	2.10
Vc	91

50% of Tol.
Center : OK
Spread : NOTOK
Target : 61.54

100% of Tol.
Center : OK
Spread : OK
Target : 97.80

Figure 86. Measurements from production for measurement point FR022G1L

These measurements demonstrate that there are geometrical deviations between the front bumper and the lamp. This indicates that the manual assembly of the front bumper to the car body can result in geometrical defects in production.

4.2.1.6 Comparison between simulation results and measured data from production

Measurements from production for the measurement point FR019G1L resulted in a +3 sigma value of 0,12 mm and -3 sigma value of -1,2 mm. Measurements of deviations in the measurement point FR019G1L from simulation one and two for both assembly sequences in relation to the +3 sigma value and the -3 sigma value obtained from production can be seen in figure 87. The four measurements of deviations from the simulations are all within the limits of -3 sigma to +3 sigma. This indicates that the deviations from the virtual simulations do not exceed the +3 sigma or -3 sigma value for this measurement point.

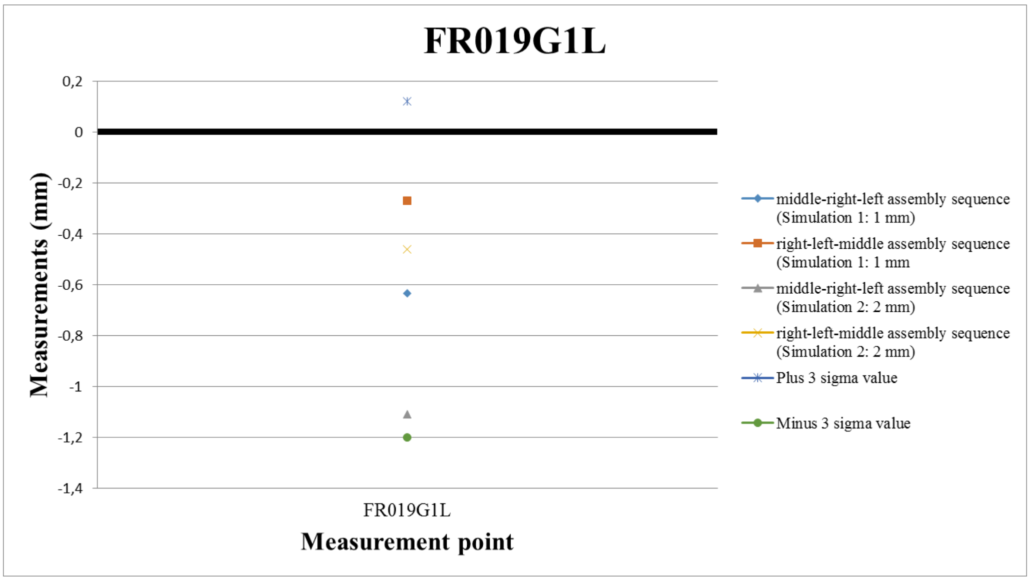

Figure 87. Comparison between data from production and simulations for FR019G1L

The measurement point are located on the right side of the front bumper, see figure 88.

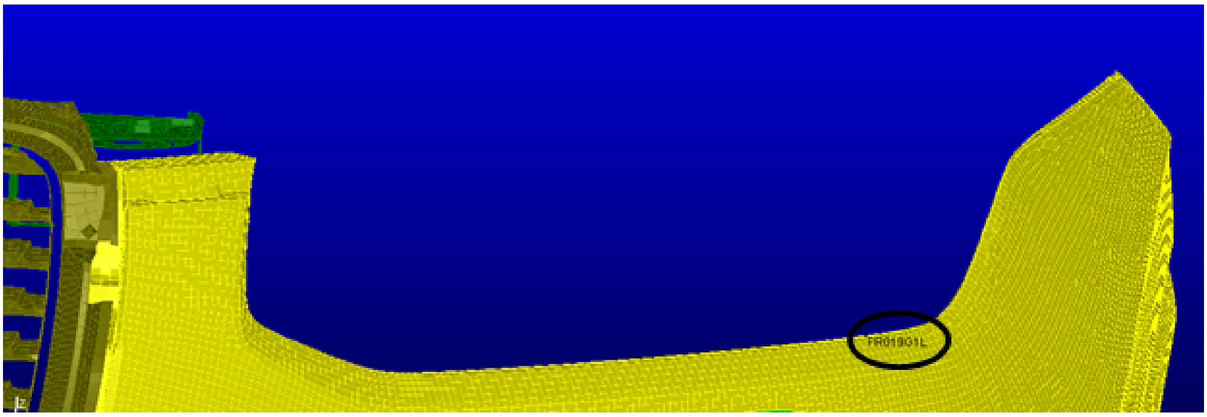

Figure 88. Measurement point located on the right side on the front bumper

Measurements from production for the measurement point FR022G1L resulted in a +3 sigma value of 2,13 mm and -3 sigma value of -1,06 mm. Measurements of deviations in the measurement point FR022G1L from simulation one and two for both assembly sequences in relation to the +3 sigma value and the -3 sigma value obtained from production can be seen in figure 89. The four measurements of deviations from the simulations are all within the limits of -3 sigma to +3 sigma. This indicates that the deviations from the virtual simulations do not exceed the +3 sigma or -3 sigma value for this measurement point.

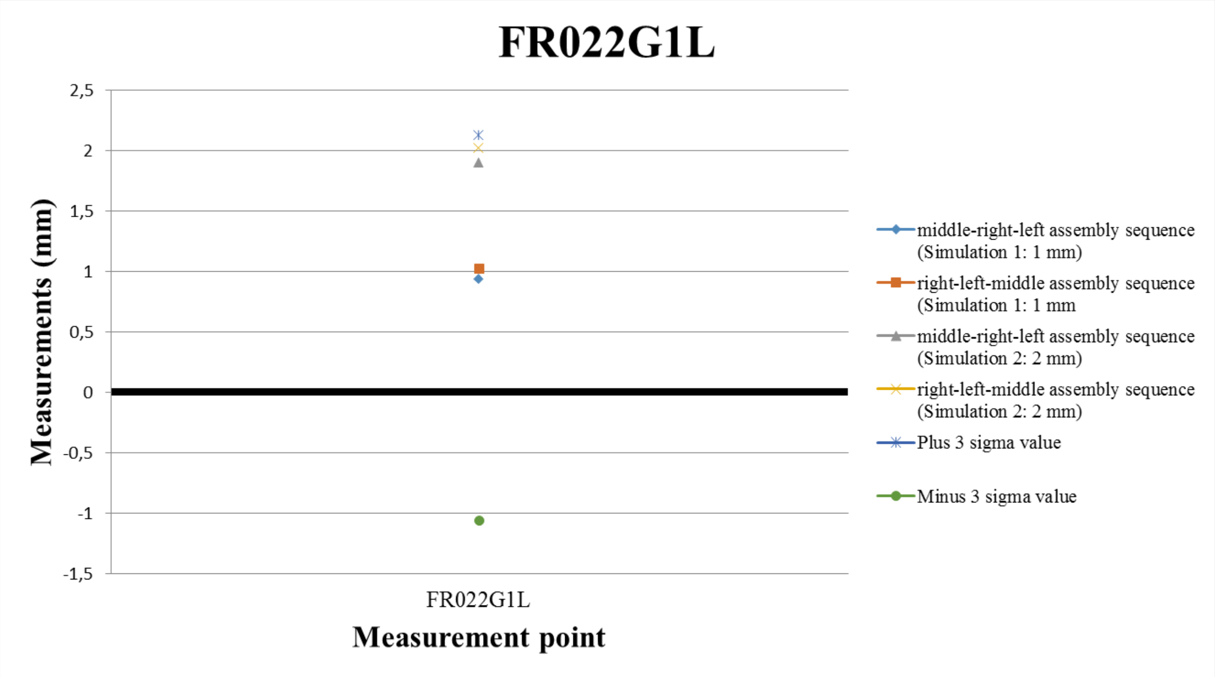

Figure 89. Comparison between data from production and simulations for FR022G1L

The measurement point are located on the right side of the front bumper, see figure 90.

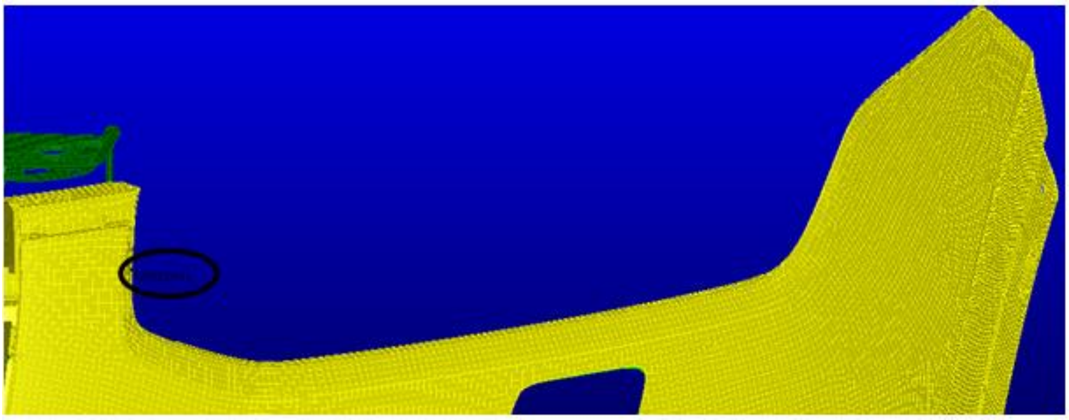

Figure 90. Measurement point located on the right side on the front bumper

4.2.2 Measurements of forces

The results from simulation one with measured welding forces for all the measurement points can be seen in appendix J. The results from simulation two with measured welding forces can be seen in appendix K.

4.2.2.1 Comparison between both assembly sequences for simulation 1

The difference in obtained forces from simulation one between the *middle-right-left* assembly sequence and the *right-left-middle* assembly sequence can be seen in figure 91. There is a rather small difference in force between the two assembly sequences for the measurement points WP_002 until WP_010. There is a pattern between small and large differences in force between the measurement points WP_012 until WP_030. The remaining measurement points have a small difference in force between the two assembly sequences. There is more measurement points for the *right-left-middle* assembly sequence in which the force is larger in comparison to the *middle-right-left* assembly sequence.

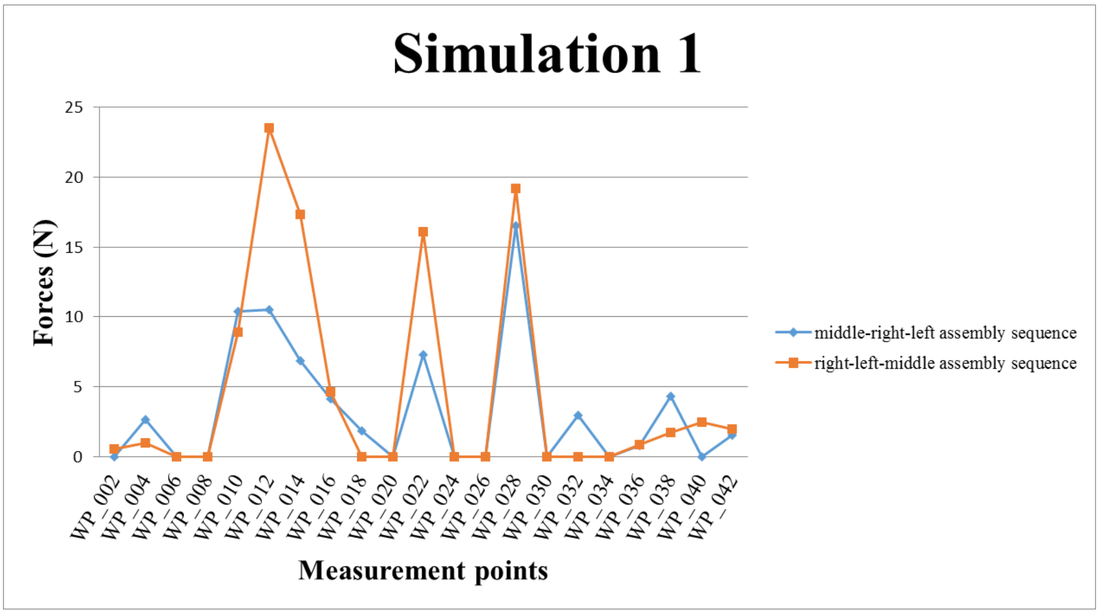

Figure 91. Measured forces for both assembly sequences from simulation 1

The three measurement points with the largest difference in force between both assembly sequences can be seen in table 6.

Table 6. Difference between forces from simulation 1

	Simulation 1: Measurements (N)		
Measurement points	**middle-right-left assembly sequence**	**right-left-middle assembly sequence**	**Difference between forces**
WP_012	10,5	23,5	13
WP_014	6,89	17,3	10,41
WP_022	7,29	16,1	8,81

The three measurement points are located in two reference points on the grille, see figure 92.

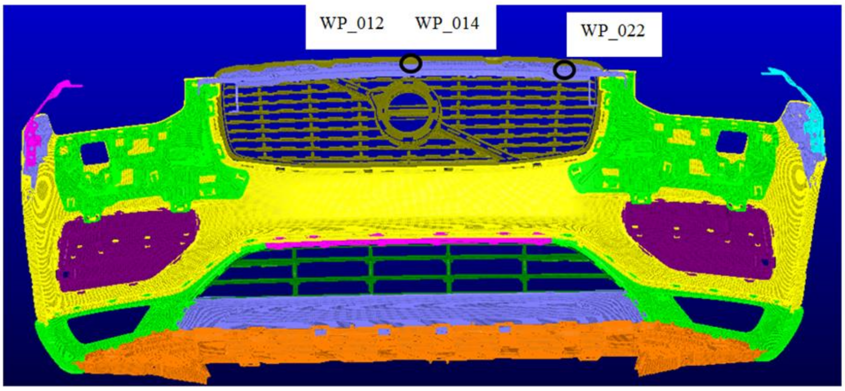

Figure 92. Measurement points located in the reference points on the front bumper

The difference in force between the assembly sequences for the three measurement points can be seen in figure 93. The force for measurement point WP_012 differs with 13 N, it differs 10,41 N for point WP_014 and it differs 8,81 N for point WP_022. The *right-left-middle* assembly sequence has a larger force than the *middle-right-left* assembly sequence in the three measurement points that are all located on the grille.

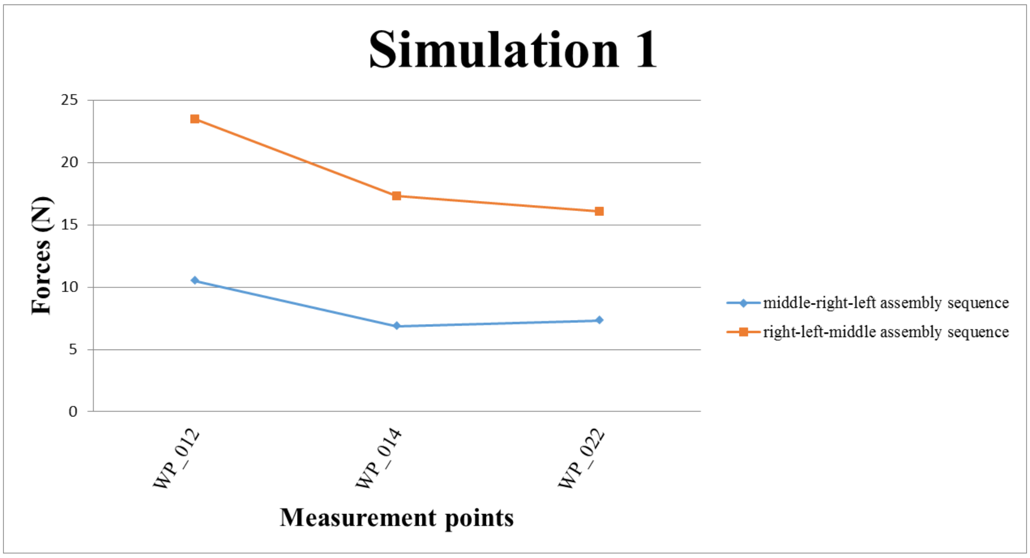

Figure 93. Difference in forces for three measurement points from simulation 1

4.2.2.2 Comparison between both assembly sequences for simulation 2

The difference in obtained forces from simulation two between the *middle-right-left* assembly sequence and the *right-left-middle* assembly sequence can be seen in figure 94. There is a rather small difference in force between the two assembly sequences for the measurement points WP_002 until WP_010. There is a pattern between small and large differences in force between the measurement points WP_012 until WP_032. The remaining measurement points have a small difference in force between the two assembly sequences. There is more measurement points for the *right-left-middle* assembly sequence in which the force is larger in comparison to the *middle-right-left* assembly sequence.

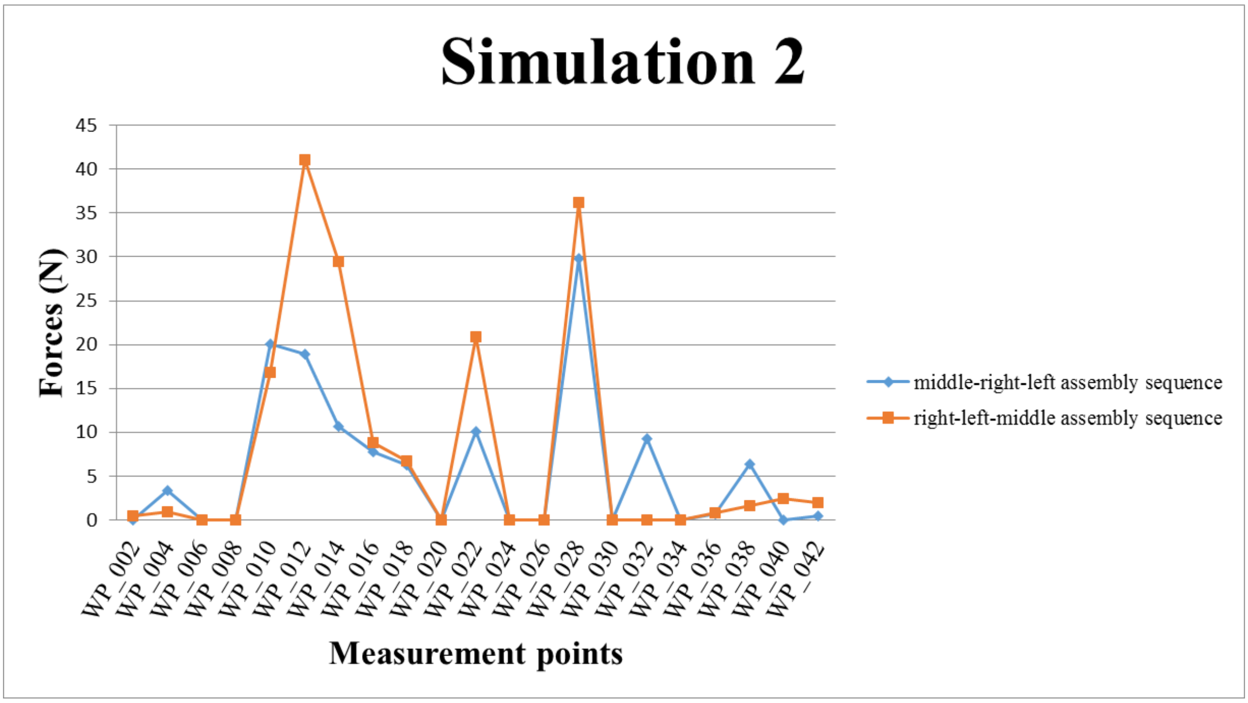

Figure 94. Measured forces for both assembly sequences from simulation 2

The three measurement points with the largest difference in force between both assembly sequences can be seen in table 7.

Table 7. Difference between forces from simulation 2

	Simulation 2: Measurements (N)		
Measurement points	**middle-right-left assembly sequence**	**right-left-middle assembly sequence**	**Difference between forces**
WP_012	18,9	41,1	22,2
WP_014	10,7	29,5	18,8
WP_022	10,1	20,9	10,8

The three measurement points are located in two reference points on the grille, see figure 95.

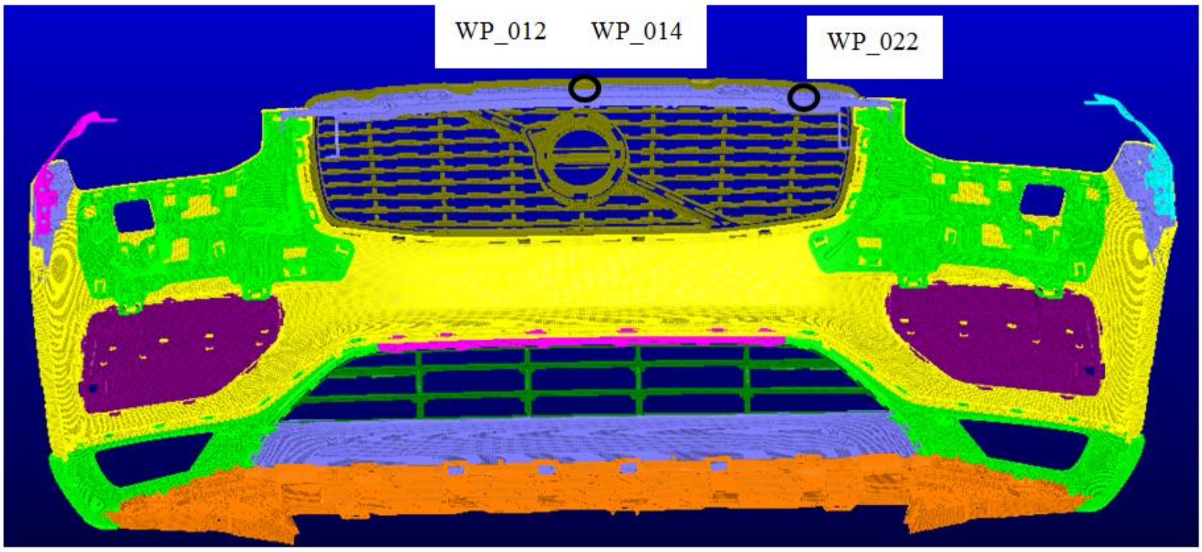

Figure 95. Measurement points located in the reference points on the front bumper

The difference in force between the assembly sequences for the three measurement points can be seen in figure 96. The force for measurement point WP_012 differs with 22,2 N, it differs 18,8 N for point WP_014 and it differs 10,8 N for point WP_022. The *right-left-middle* assembly sequence has a larger force than the *middle-right-left* assembly sequence in the three measurement points that are all located on the grille.

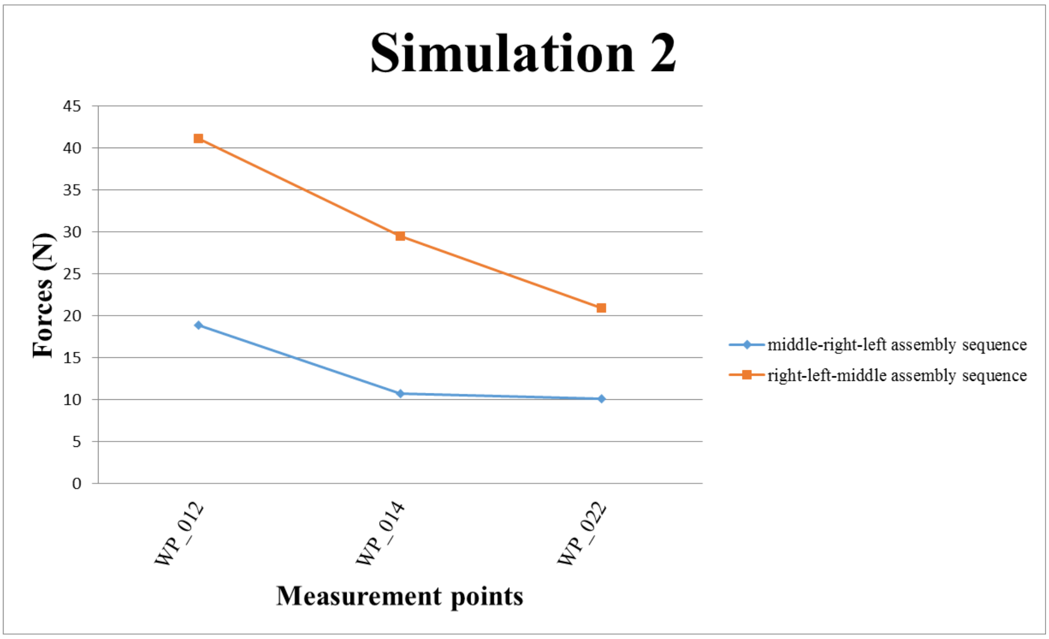

Figure 96. Difference in forces for three measurement points from simulation 2

4.2.2.3 Comparison between middle-right-left assembly sequences from both simulations

The difference in obtained forces for the *middle-right-left* assembly sequence between simulation one and simulation two can be seen in figure 97.

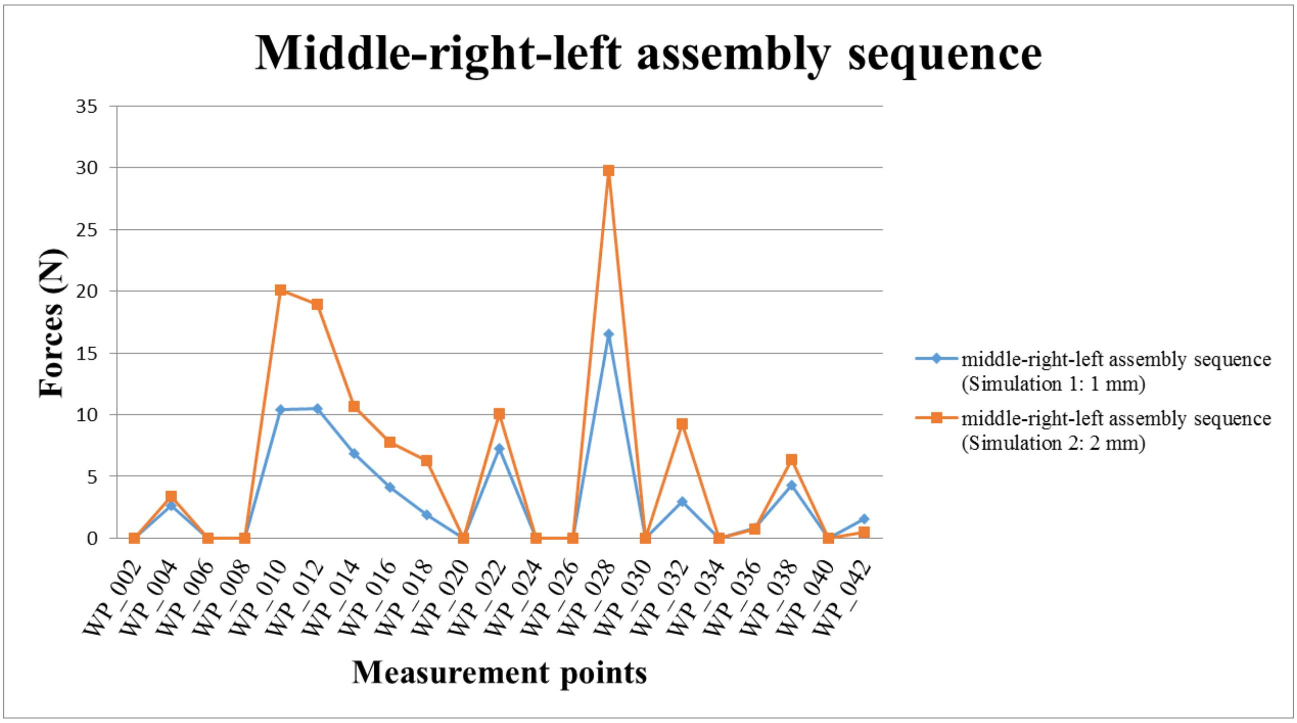

Figure 97. Measured forces for middle-right-left assembly sequence from both simulations

The three measurement points with the largest difference in force for the *middle-right-left* assembly sequence between the two simulations can be seen in table 8.

Table 8. Difference between forces from both simulations for the middle-right-left assembly sequence

	Simulation 1	Simulation 2	
Measurement points	**middle-right-left assembly sequence (Simulation 1: 1 mm)**	**middle-right-left assembly sequence (Simulation 2: 2 mm)**	**Difference between forces**
WP_010	10,4	20,1	9,7
WP_012	10,5	18,9	8,4
WP_028	16,5	29,8	13,3

The three measurement points are located in two reference points on the grille, see figure 98.

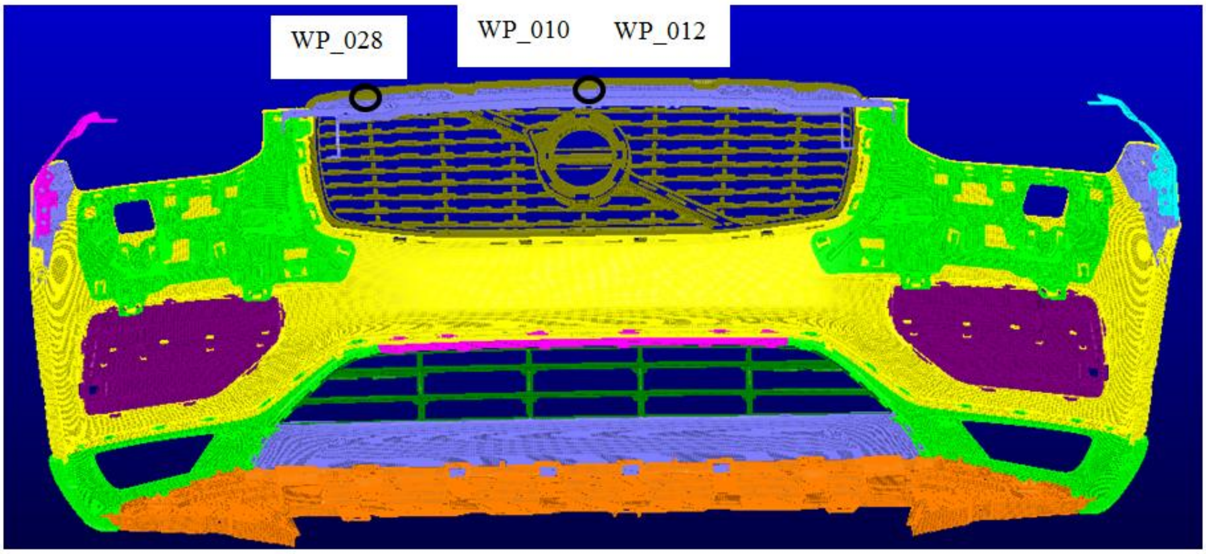

Figure 98. Measurement points located in the reference points on the front bumper

The difference in force between the two simulations for the *middle-right-left* assembly sequence for the three measurement points can be seen in figure 99. The force for measurement point WP_010 differs with 9,7 N and it differs 8,4 N for point WP_012. The *middle-right-left* assembly sequence has a larger force in these two measurement points from simulation two that are both located in the middle of the grille. The largest difference in force between the simulations for this assembly sequence is 13,3 N in measurement point WP_028 which is located in the reference point on the right side of the grille.

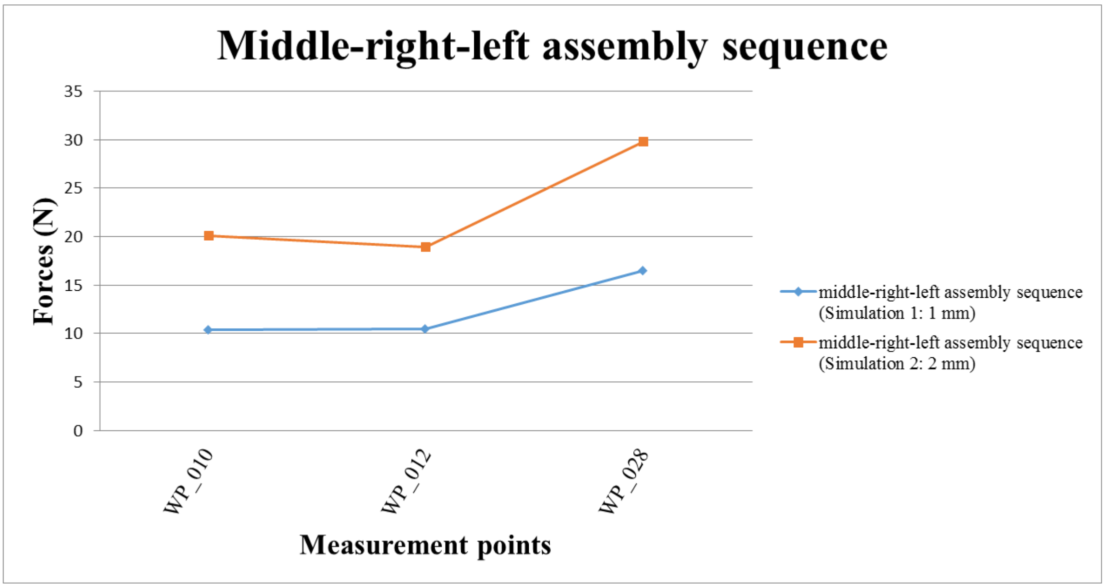

Figure 99. Difference in forces for three measurement points from simulation 1 and 2

4.2.2.4 Comparison between right-left-middle assembly sequences from both simulations

The difference in obtained forces for the *right-left-middle* assembly sequence between simulation one and simulation two can be seen in figure 100. The difference in force for the *right-left-middle* assembly sequence is zero for the measurement points WP_002 until WP_008. There is a pattern between small and large differences in force between the measurement points WP_010 until WP_028. The difference in force for the remaining measurement points is zero.

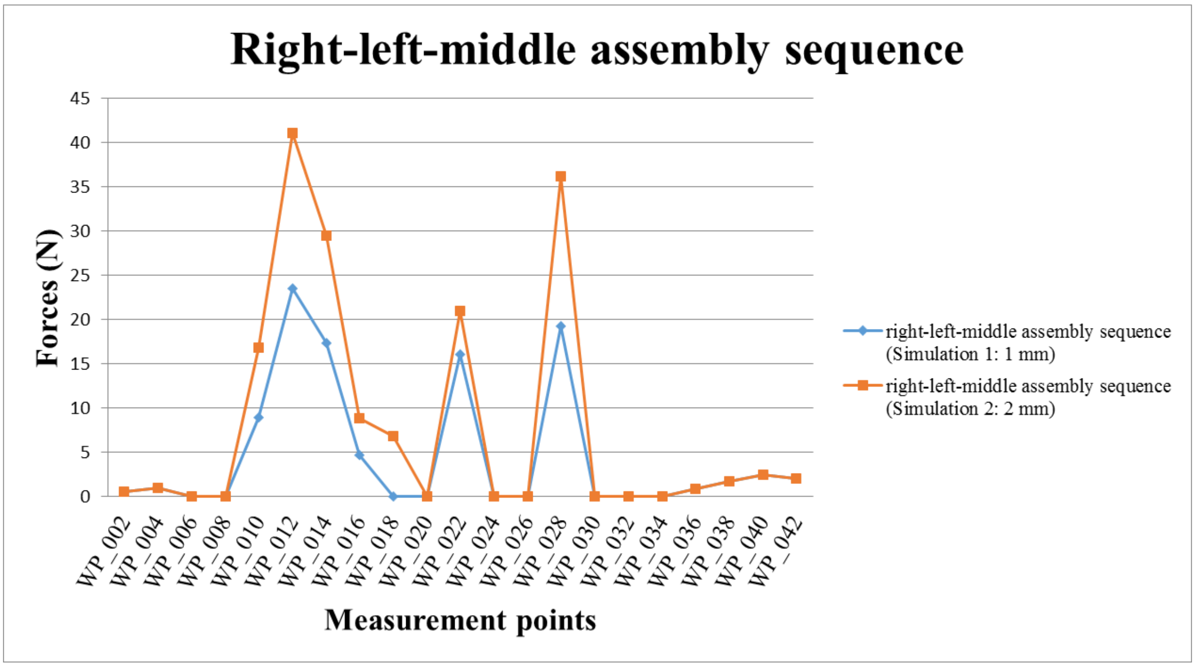

Figure 100. Measured forces for right-left-middle assembly sequence from both simulations

The three measurement points with the largest difference in force for the *right-left-middle* assembly sequence between the two simulations can be seen in table 9.

Table 9. Difference between forces from both simulations for the right-left-middle assembly sequence

	Simulation 1	**Simulation 2**	
Measurement points	**right-left-middle assembly sequence (Simulation 1: 1 mm)**	**right-left-middle assembly sequence (Simulation 2: 2 mm)**	**Difference between forces**
WP_012	23,5	41,1	17,6
WP_014	17,3	29,5	12,2
WP_028	19,2	36,2	17

The three measurement points are located in two reference points on the grille, see figure 101.

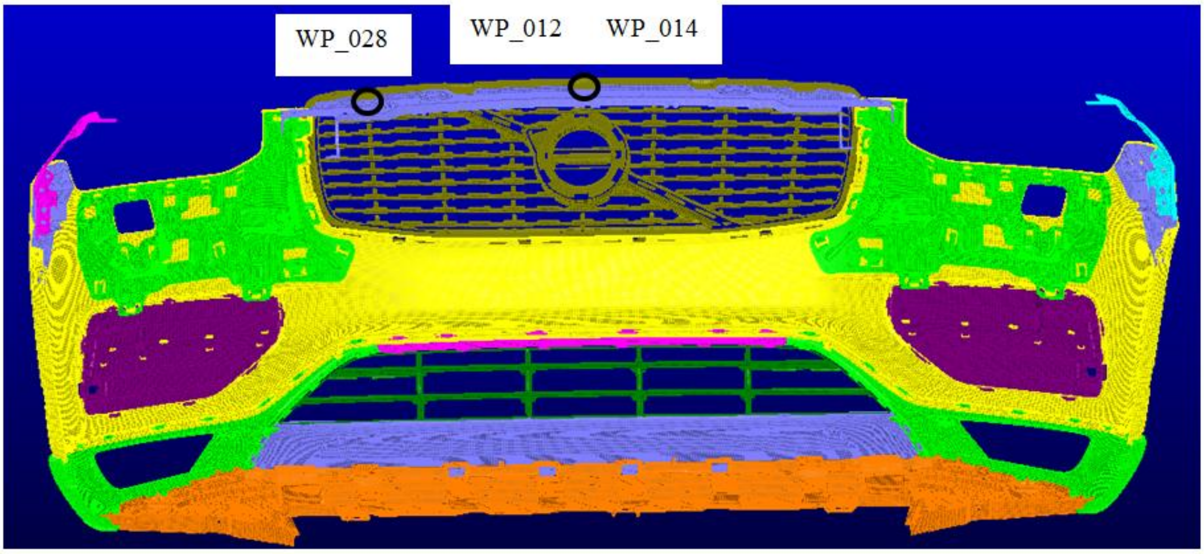

Figure 101. Measurement points located in the reference points on the front bumper

The difference in force between the two simulations for the *right-left-middle* assembly sequence for the three measurement points can be seen in figure 102. The force for measurement point WP_028 differs with 17 N and it differs 12,2 N for point WP_014. The *right-left-middle* assembly sequence has a larger force in these two measurement points from simulation two that are both located on the grille. The largest difference in force between the simulations for this assembly sequence is 17,6 N in measurement point WP_012 which is located in the reference point in the middle of the grille.

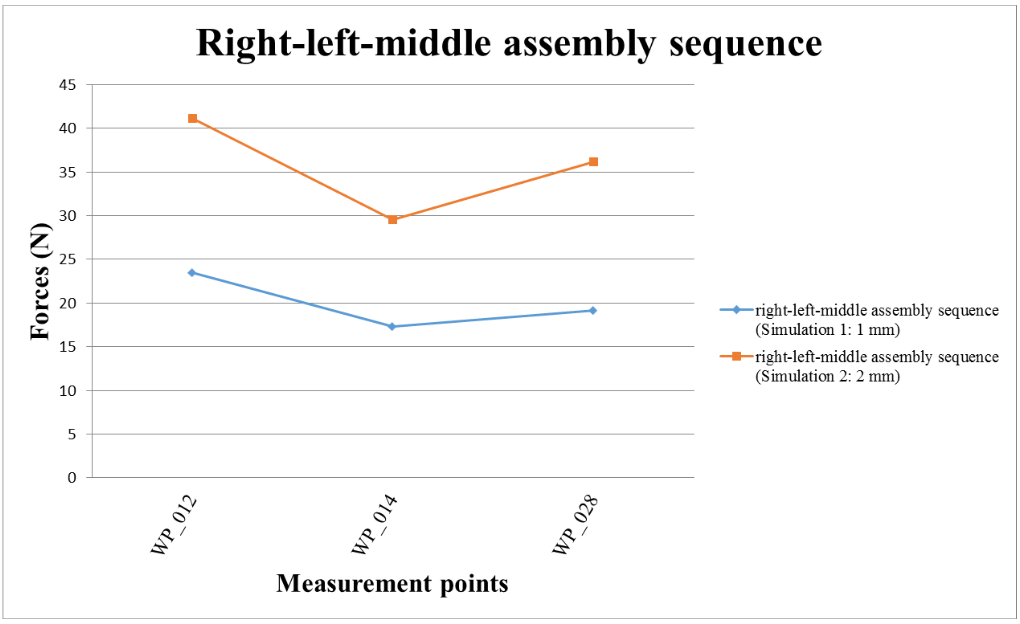

Figure 102. Difference in forces for three measurement points from simulation 1 and 2

5 Discussions

This chapter will include discussions of the obtained results from the physical study of the front door and the virtual study of the front bumper. Results that will be discussed from the physical study of the front door are obtained deviations and contributing factors to these deviations. Results that will be discussed from the virtual study of the front bumper are obtained deviations and forces in relation to the assembly sequences and the contributing factors to these deviations and forces.

5.1 Physical study of the front door

The main objective of the physical study of the front door was to see if the assemblers contribute to variation during manual assembly. All the measurements that were obtained for the measurement point on the capping in X2 direction from the physical study resulted in different deviations. This means that the obtained deviations differ between the assemblers, which indicate that the outcome in deviation depends on which operator that is performing the manual assembly. The outcome in deviation did not only vary between the assemblers, there was also a difference in the obtained deviations from the manual assemblies performed by each operator. This clearly shows that operators do contribute to variation during manual assembly and that the degree of contributing variation differs between assemblers.

5.1.1 Contributing factors to obtained deviations from physical study of the front door

One of the factors that can cause deviations during manual assembly is the force that is applied by the assemblers. The force that was measured after assembly of the capping in the physical study differed among the assemblers, which resulted in different deviations. This implies that the applied force has an impact on which deviation that will be obtained and that it depends on which operator that performs the manual assembly. One reason to why operators might apply different forces during manual assembly can be that they need to apply different amounts of pressure in order to be able to assemble a component. One example is from the physical study when the capping was assembled, where the amount of pressure affected if the component was pressed all the way in against the side of the front door in X-direction, which will have an impact on the obtained deviations for the capping in X2-direction. The assemblers positioning and the direction in which the force is applied during manual assembly can be another reason to why operators might apply different forces. One example is when one assembler was positioned in front of the door when assembling the capping while another assembler was positioned at the right side of the door while mounting the component. This causes the two assemblers to apply the force in different directions during assembly, which will lead to a difference in the amount of force used and this can also have an impact on the obtained deviations for the capping in X2-direction. The results from the physical study demonstrates that the deviations and forces differ between assemblers, but a larger amount of measurement data is required by performing more tests in order to prove if the deviations and forces has a linear correlation.

Another factor that can probably have an impact on why these deviations are obtained during manual assembly is the method of how these components are assembled. Two aspects that according to Falck *et.al.* (2012) makes an assembly complex is if operations must be performed in a certain order and if clear work instructions are necessary. These two aspects have a direct impact on the method of how components are assembled. If operations in an assembly sequence are not performed in a certain order it can probably have an impact on the outcome of measured deviations since it affects the positioning of a part. One example of this is that the upper screw had to be mounted first when the capping was assembled on the front door in order to ensure that the component was positioned correctly against the GRS. If the lower or middle screw was mounted before the upper screw it would affect the positioning of the capping in relation to the GRS, which would probably have an impact on the obtained deviations for the capping. If there are no clear work instructions that describe the method of how to assemble components it can be hard for an operator to know how and in which order the assembly should be performed. This could lead to that the operators' uses different methods to assemble the same component, which could cause different positions of the component and therefore have an impact on the deviations that are obtained during manual assembly.

Two aspects that according to Falck *et.al.* (2012) makes an assembly complex is if there is no feedback if reference points are in the correct position and if the material is soft and flexible. A third factor that can have an impact on why deviations occur during manual assembly is the design of the component and the two aspects mentioned are both affected by the design. One example of this is the reference pin on the GRS that is made of a rubber material. The reference pin was vital in the positioning of the component against the front door. But it was difficult to know if the reference pin was in the correct position in the cut out in the door since the rubber material allowed the GRS to move along the door bow, which caused the component to deviate from its nominal position. This demonstrates that the design of the component in both the reference pin and choice of material had an impact on the obtained deviations during manual assembly.

5.2 Virtual study of the front bumper

The physical study of the front door gave indications that the method in how components are assembled and the force that is applied during manual assembly are two factors that might have an impact on the deviations that can result from manual assembly. These two factors were therefore selected to be further investigated in the virtual study of the front bumper. The main objective of the virtual study for the front bumper was to see if it is possible to find an optimal assembly sequence with regards to operators' contribution to variation and the applied force.

5.2.1 Optimal assembly sequence in relation to obtained deviations from virtual study of the front bumper

The method of how components are assembled was investigated by analyzing two assembly sequences in RD&T by obtaining measurements on the front bumper in relation to the lamp in order to see if an optimal assembly sequence with regards to operators' contribution to variation could be found. The two assembly sequences was compared in two simulations with the difference of applying an offset of 1 mm in the reference point in the middle of the grille in simulation one and by applying 2 mm in simulation two. Both these simulations that compared the two assembly sequences showed similar patterns with the difference that simulation two obtained larger deviations overall. It was the same four measurement points that resulted in the largest difference in deviation between the assembly sequences from both simulations and these points were located on the upper left side of the front bumper, see tables 2 and 3. These four measurement points resulted in quite large differences in deviation between the assembly sequences from both simulations, which indicate that the choice of assembly sequence for the front bumper against the car body has an impact on the obtained deviations from the manual assembly.

It is clear that there are differences in deviation in the measurement points between the assembly sequences from both simulations and it is therefore important to find an optimal assembly sequence in order to obtain as small deviations as possible from the manual assembly of the front bumper to the car body. There were more measurement points from both simulations in which the obtained deviations were larger for the *right-left-middle* assembly sequence in comparison to the *middle-right-left* assembly sequence. The *middle-right-left* assembly sequence from both simulations showed a trend of being closer to the nominal value in the majority of the measurement points in comparison to the *right-left-middle* assembly sequence. This implies that the *middle-right-left* assembly sequence is more optimal than the *right-left-middle* assembly sequence since it will allow for smaller deviations in the majority of the measurement points from the manual assembly of the front bumper against the car body, which will cause less geometrical defects.

5.2.1.1 Contributing factors to the difference in deviations between assembly sequences

There are many factors that could be contributing to why there is a difference in the obtained deviations between the two assembly sequences. One of these factors could be that the *middle-right-left* assembly sequence should result in larger deviations on the edges of the front bumper and the *right-left-middle* assembly sequence should result in larger deviations further towards the grille on the front bumper (Andreasson, 2016) (Östergaard, 2016). One example of this is that the *middle-right-left* assembly sequence had some distinguishing values where large deviations were obtained in several measurement points that were located towards the edges of the front bumper. The *right-left-middle* assembly sequence had some distinguishing values where large deviations were obtained in several measurement points that were located further towards the grille. This could be one of the reasons to why the obtained deviations differs between the assembly sequences since the area of where the largest deviations can be located depends on in which order the assembly is performed.

Another factor that could have caused differences in deviations between the two assembly sequences is that the front bumper is made of a flexible material while the grille is made of a material that is significantly more rigid. If the *middle-right-left* assembly sequence is used in which the grille is mounted first to the car body it will cause the front bumper to deform differently than if the *right-left-middle* assembly sequence would be applied, since a more rigid material will be attached to the car body first in comparison to if a more flexible material would be attached first.

5.2.3 Comparison between simulation results and measured data from production

Two measurement points in which deviations were obtained for the assembly sequences from both simulations was compared to the +3 sigma and -3 sigma values that have been obtained from measurements in production for the corresponding measurement points. The obtained deviations from both measurement points lied within the +3 sigma and -3 sigma values that were obtained from measurements in production. This indicates that the deviations from the virtual simulations do not exceed the +3 sigma or -3 sigma values. This results shows that the obtained deviations from the measurement points are stable. It also shows that the virtual simulations of the front bumper give more credible results in relation to reality since the spread of the obtained deviations in the two measurement points is rather small and that they are within the +3 sigma and -3 sigma limits. The obtained deviations from the virtual simulations and the +3 sigma and -3 sigma values from the physical results cannot be completely compared. Because there were different offsets in the reference points in y-direction on the right and left fender bracket of the car body and in the middle of the grille, between the virtual simulations and the physical measurement procedure in production when the values for these two measurement points were obtained.

5.2.4 Optimal assembly sequence in relation to obtained forces from virtual study of the front bumper

The method of how components are assembled was investigated by analyzing two assembly sequences in RD&T by obtaining measurements of the force to see if an optimal manual assembly sequence could be found. Simulation one and two that compared the two assembly sequences showed similar patterns with the difference that simulation two obtained larger forces overall. It was the same three measurement points that resulted in the largest difference in force between the assembly sequences from both simulations and these points were located on the grille, se tables 6 and 7. The *right-left-middle* assembly sequence had a larger force than the *middle-right-left* assembly sequence in the three measurement points that were located on the grille in both simulations. There are also more measurement points for the *right-left-middle* assembly sequence in which the force is larger in comparison to the *middle-right-left* assembly sequence in both simulations. It is according to Wärmefjord *et.al.* (2013) preferable to have low forces during an assembly process since it will then be less risk of joining failures and geometrical quality issues. This indicates that the *middle-right-left* assembly is more optimal since it will allow for smaller forces in more measurement points in comparison to the *right-left-middle* assembly sequence in the manual assembly of the front bumper against the car body, which will reduce the risk of joining failures and geometrical quality issues.

5.2.4.1 Contributing factor to the difference in forces between assembly sequences

The assembly sequence has according to Wärmefjord *et.al.* (2013) a great impact on the force and it is therefore vital to consider in which sequence a product should be assembled in order to decrease the required forces. This could be one of the main reasons to why there is a difference in force between the two assembly sequences since the order in which a part is assembled affects which force that is required during the assembly.

6 Conclusions

This chapter will answer the research questions by presenting the conclusions from the physical study of the front door and the virtual study of the front bumper.

6.1 Physical study of the front door

The physical study of the front door indicates that it is possible to identify and quantify how operators can contribute to variation during manual assembly since deviations were obtained from the assembly of the GRS, OWS and capping. However, larger amounts of measurement data need to be obtained by performing more tests in the physical study of the front door, in order to quantify operators' contribution to variation. The main conclusion from the physical study is that operators do contribute to variation during manual assembly and that the degree of contributing variation differs between assemblers. The physical study indicated also that the applied force during manual assembly differs between assemblers and that the force has an impact on which deviations that will be obtained.

6.2 Virtual study of the front bumper

The virtual study of the front bumper shows that it is possible to find an optimal manual assembly sequence with regards to operators' contribution to variation in RD&T. The main conclusion from the virtual study is that the *middle-right-left* assembly sequence is more optimal than the *right-left-middle* assembly sequence since it will allow for smaller deviations in the majority of the measurement points from the manual assembly of the front bumper against the car body, which will reduce the operators contribution to variation and cause less geometrical defects. The two assembly sequences caused deformations in different areas on the front bumper since the obtained deviations differed between the sequences. The virtual study indicated also that the *middle-right-left* assembly is more optimal since it will allow for smaller forces in more measurement points in comparison to the *right-left-middle* assembly sequence in the manual assembly of the front bumper against the car body, which will reduce the risk of joining failures and geometrical quality issues. The conclusion that it is possible to find an optimal assembly sequence with regards to operators' contribution to variation indicates that it might be beneficial for the department Robust Design and Tolerancing to consider different manual assembly sequences in RD&T for parts of the car where it seems necessary, in order to select an optimal assembly sequence with the least contribution to variation from the operators.

For further studies it is recommended to include the front lamps in the virtual model to analyze if it has an impact in finding an optimal manual assembly sequence. The virtual study of the front bumper did not include the front lamps in the model in RD&T.

7 References

7.1 Articles

Cai, N., Qiao, L. & Anwer, N. (2015). Assembly model representation for variation analysis. *13th CIRP conference on Computer Aided Tolerancing – Procedia CIRP 27.* p. 241-246.

Booker, J.D., Swift, K.G. & Brown, N.J. (2005). Designing for assembly quality: strategies, guidelines and techniques. *Journal of Engineering Design.* Vol. 16, No. 3, June 2005, p.279-295.

Falck, A., Örtengren, R. & Rosenqvist, M. (2012). Relationship between complexity in manual assembly work, ergonomics and assembly quality. *Department of Product and Production Development, Chalmers University of Technology, SE-412 96 Gothenburg Sweden.*

Forslund, K., Wagerstern, O., Tafuri, S., Segerdahl, D., Carlsson, J.S., Lindkvist, L. & Söderberg, R. (2011). Parameters influencing the perception of geometrical deviations in a virtual environment. *Proceedings of the ASME 2011 International Design Engineering Technical Conferences & Computers and Information in Engineering Conference – August 28-31 Washington, DC, USA.* p.1-10.

Lindau, B., Andersson, A., Lindkvist, L. & Söderberg, R. (2012). Body in white geometry measurements of non-rigid components: a virtual perspective. *Proceedings of the ASME 2012 International Design Engineering Technical Conferences & Computers and Information in Engineering Conference, August 12-15, Chicago, IL, USA.* p.1-9

Lindau, B., Lorin, S., Lindkvist, L. & Söderberg, R. (2016). Efficient Contact Modeling in Nonrigid Variation Simulation. *Journal of Computing and Information Science in Engineering,* Vol. 16, p.1-7

Rosenqvist, M., Falck, A-C., Söderberg, R. & Wärmefjord, K. (2013). Operator related causes for low correlation between CAT simulations and physical results. *Proceedings of the ASME 2013 International Mechanical Engineering Congress & Exposition, November 13-21, San Diego, California, USA.* p.1-10.

Rosenkvist, M., Falck, A-C., Lindkvist, L. & Söderberg, R. (2014). Geometrical robustness analysis considering manual assembly complexity. *Procedia CIRP 23 (2014),* pp. 98-103.

Söderberg, R., Wickman, C. & Lindkvist, L. (2008). Improving decision making by simulating and visualizing geometrical variation in non-rigid assemblies. *CIRP Annals – Manufacturing Technology 57.* p.175-178

Söderberg, R. & Lindkvist, L. (1999). Computer Aided Assembly Robustness Evaluation. *Journal of Engineering Design,* 10:2, p. 165-181.

Söderberg, R., Lindkvist, L. & Carlson, J. (2006). Virtual geometry assurance for effective product realization. *1st Nordic Conference on Product Lifecycle Management – NordPLM'06, Göteborg, January 25-26 2006.* p.75-87

Söderberg, R., Lindkvist, L. & Carlson J.S. (2007). Managing physical dependencies through location system design. *Journal of Engineering Design, Chalmers University of Technology, Sweden.*Vol. 17, No. 4, August 2006, p.325-346.

Söderberg, R. (1998) Robust Design by Support of CAT Tools. *Proceedings of the ASME Design Automation Conference, September 13-16, Atlanta, GA, USA DETC98/DAC-5633*

Söderberg, R., Wärmefjord, K., Lindkvist, L. & Berlin, R. (2012). The influence of spot welding position variation on geometrical quality. *Department of Product and Production Development, Chalmers University of Technology, Gothenburg, Sweden. CIRP Annals – Manufacturing Technology 61 (2012) 13-16.*

Wärmefjord, K., Söderberg, R. & Lindkvist, L. (2010). Variation Simulation of Spot Welding Sequence for Sheet Metal Assemblies. *Department of Product and Production Development, Chalmers University of Technology, SE-412 96 Gothenburg Sweden, August 25-27, 2010.*

Wärmefjord, K., Söderberg, R. & Lindkvist, L. (2013). Simulation of the effect of geometrical variation on assembly and holding forces. *Int. J. Product Development, Vol 18, No. 1, 2013.* p.88-108.

7.2 Books

Bergman, B. & Klefsjö, B. (2010). *Quality from Customer Needs to Customer Satisfaction.* 3rd edition., Lund Studentlitteratur AB.

Ottosen, N. & Petersson, Hans (1992). *Introduction to the Finite Element Method*. University of Lund, Sweden. Pearson Education Limited. Prentice Hall Europe.

7.3 Lecture from Chalmers University of Technology

Lindkvist, L. (2016). *Advanced Computer Aided Design: Geometry Assurance 1 – Robust Design & Variation Simulation.* Chalmers University of Technology.

7.4 Web-pages

Coord3_Metrology. (2016). Coordinate Measuring Machine History – Fifty Years of CMM History leading up to a Measuring Revolution. *Coord3 Metrology*. Available at: http://www.coord3-cmm.com/50-years-of-coordinate-measuring-machine-industry-developments-and-history/ [Accessed May 6, 2016].

Mathportal. (2016). About standard deviation. *Mathportal.* Available at: http://www.mathportal.org/calculators/statistics-calculator/standard-deviation-calculator.php [Accessed May 6, 2016].

MSC Apex. (2016). Midsurface Introduction. *MSC Apex.* Available at: http://www.mscapex.com/midsurface/ [Accessed May 5, 2016].

MatWeb. (2016). Covestro Bayblend T45 PG Polycarbonate + ABS. *MatWeb.* Available at: http://www.matweb.com/search/DataSheet.aspx?MatGUID=7dcc31a45883429ab98c24c693f11a7c&ckck=1 [Accessed May 5, 2016].

MatWeb. (2016). Borealis Daplen EE225AE Polypropylene TPO Compound. *MatWeb.* Avaliable at: *http://www.matweb.com/search/DataSheet.aspx?MatGUID=fabf3bb4bfec4bd195cc9bc203b14f4d&ckck=1* [Accessed May 5, 2016].

MatWeb. (2016). Borealis Xmod GD302HP Polypropylene, Glass Fiber Reinforced. *MatWeb.* Available at: http://www.matweb.com/search/DataSheet.aspx?MatGUID=2ec5482835524b6db21ab593a8604400 [Accessed May 5, 2016].

MatWeb. (2016). Borealis Daplen MD206U Polypropylene Compound 20% Mineral Filled. *MatWeb.* Available at: http://www.matweb.com/search/DataSheet.aspx?MatGUID=25db367bc38c4d67bf447bc3a343ab8f

RD&T_Technology. (2016). The Tool RD&T. *RD&T Technology*. Available at: http://rdnt.se/tool.html [Accessed May 4, 2016].

Stat yale education. (2016). The Normal Distribution. *Stat yale education.* Available at: http://www.stat.yale.edu/Courses/1997-98/101/normal.htm [Accessed May 6, 2016].

The Engineering Toolbox. (2016). Engineering Materials. *The Engineering Toolbox* Available at: http://www.engineeringtoolbox.com/engineering-materials-properties-d_1225.html [Accessed May 5, 2016].

The Engineering Toolbox. (2016). Modulus of Elasticity. *The Engineering Toolbox* Available at: http://www.engineeringtoolbox.com/young-modulus-d_417.html [Accessed May 10, 2016].

The Engineering Toolbox. (2016). Poisson's ratio. *The Engineering Toolbox* Available at: http://www.engineeringtoolbox.com/poissons-ratio-d_1224.html [Accessed May 10, 2016].

Ultra Polymers. (2016). Hifax TRC 228P 2 C12637. *Ultra Polymers.* Available at: http://catalog.ides.com/Datasheet.aspx?I=26119&U=0&E=294179 [Accessed May 5, 2016].

7.5 Documents from VCC

VCC. (2015). Standard VCS 5060,6. Capability. Available from http://www.volvocars.net [Accessed 2016-05-4].

VCC. (2013). Standard VCS 5026,4 Master Location System. Available from http://www.volvocars.net. [Accessed 2016-05-4].

VCC Manufacturing Engineering. (08-Jan-2015). Process-/Inspection Instruction (PII). Description B-pillar capping to front door. PII no C8414-0001.

VCC Manufacturing Engineering. (21-May-2015). Process-/Inspection Instruction (PII). Description Outer waist seal to front door. PII no C8450-0001.

VCC Manufacturing Engineering. (06-Oct-2015). Process-/Inspection Instruction (PII). Description Glass run seal to door bow front door. PII no C8450-0012.

VCC Manufacturing Engineering. (07-Mar-2016). Process-/Inspection Instruction (PII). Front bumper to car. PII no C8611-0002.

7.6 Software manual

Robust Design and Tolerancing (2015). Robustness evaluation and tolerance analysis. *Software Manual.* Ver. 1.17

7.7 Interviews

Andreasson, John. “GAE Front End.” *Geometry Assurance Program.* Volvo Car Corporation. Gothenburg. (May 16, 2016).

Östergaard, Ben. “Program Manager.” *Geometry Program and Development.* Volvo Car Corporation. Gothenburg. (May 16, 2016).

8 Appendices

8.1 Appendix A: Parts included in the front bumper

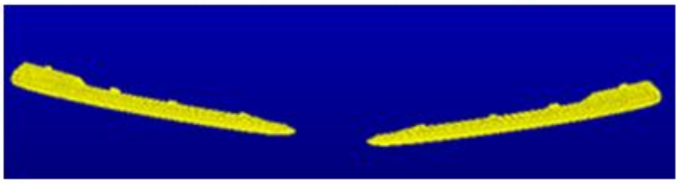

Left cover chrome Right cover chrome

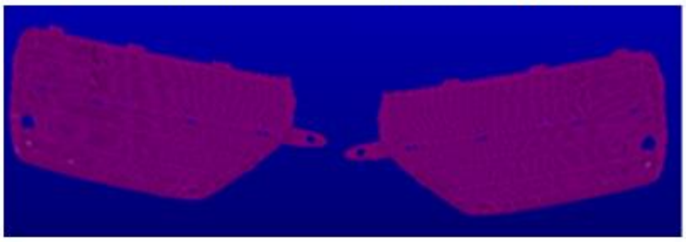

Left cover insert Right cover insert

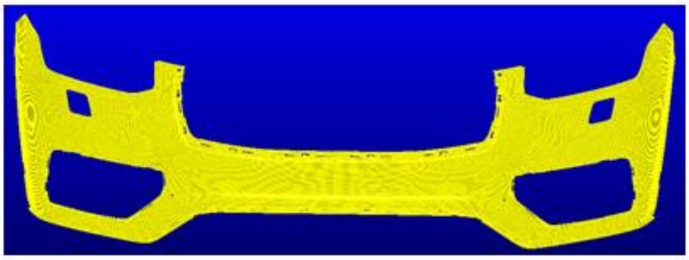

Bumper

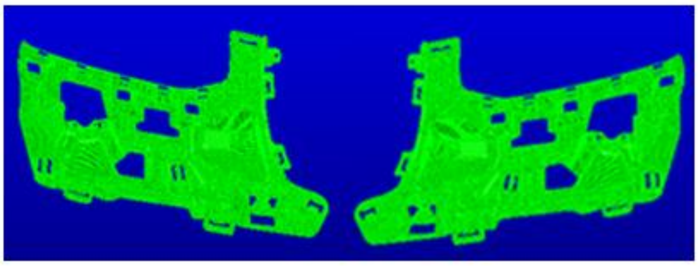

Left combined bracket Right combined bracket

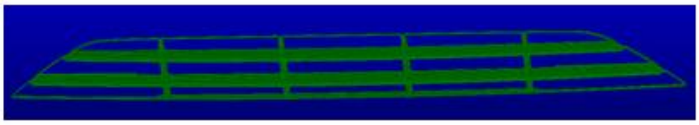

Lower airmesh

Skidplate

Left fender bracket Right fender bracket

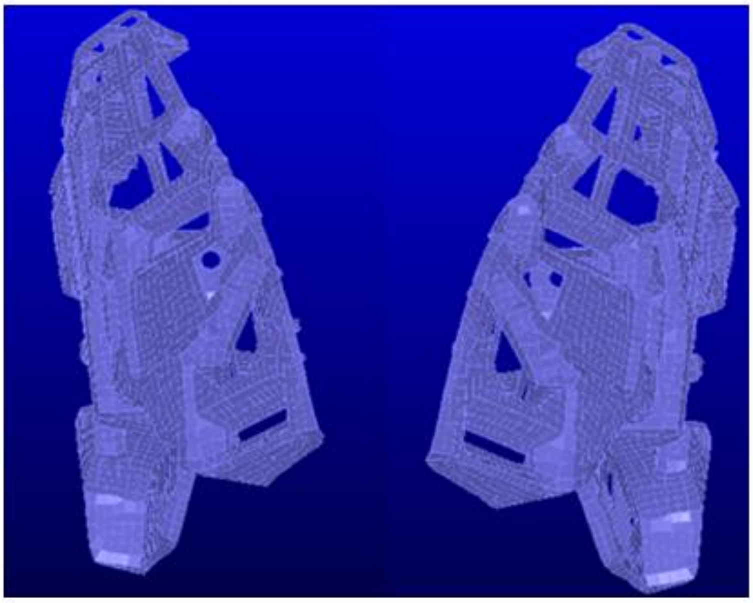

Front spoiler

Left spoiler Right spoiler

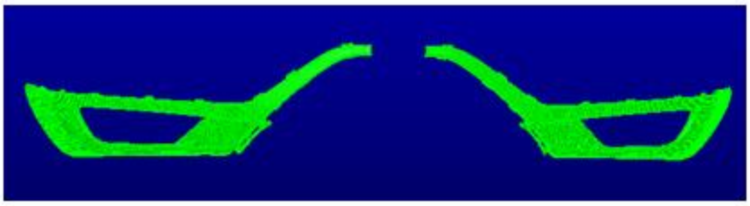

Undershield

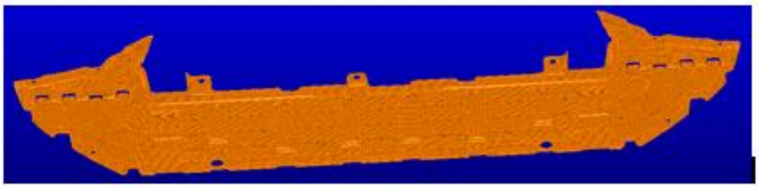

Grille

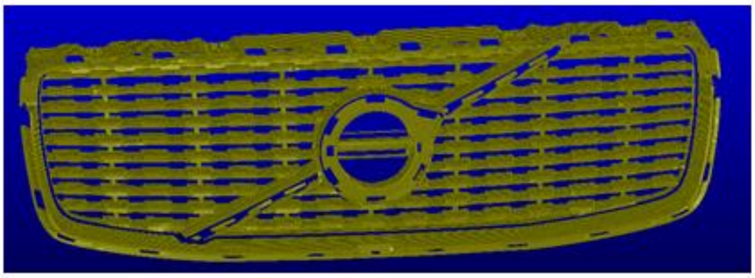

8.2 Appendix B: Parts included in the car body

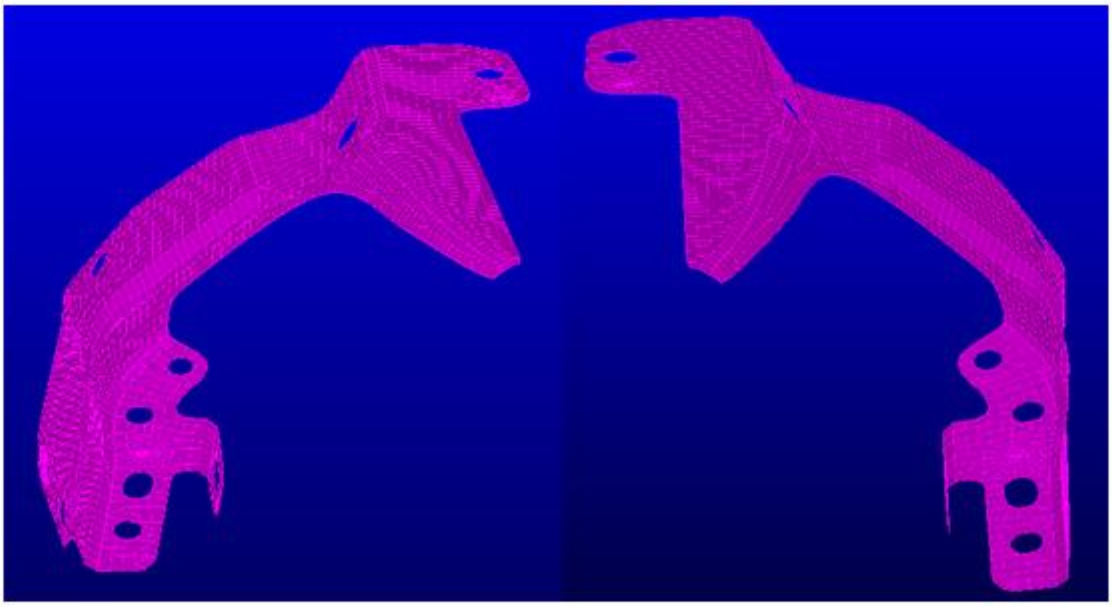

Left fender bracket

Right fender bracket

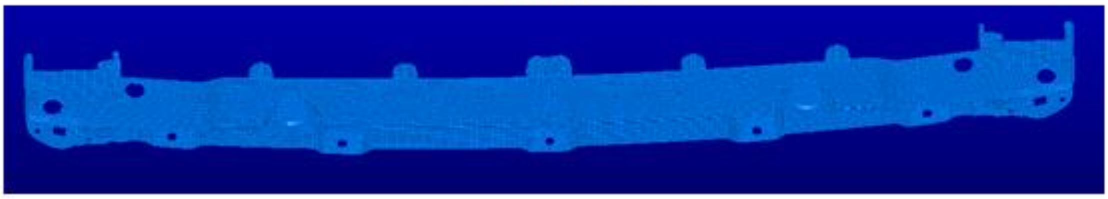

Plastic bracket

8.3 Appendix C: Data included in the elastic modulus

Front bumper	**Material**	**Thickness (mm)**	**Elastic modulus**	**Density kg/m3**	**Poissons ratio**	**References**
Cover chrome	Bayblend T45 PG	2,5	2,10 Gpa	1100	0,3	(MatWeb, 2016)
Cover insert	Basell Hifax TRC 228P-2	2,5	Flexular modulus: 1300 Mpa	1000	0,3	(Ultra Polymers, 2016)
Bumper	Borealis Daplen EE255AE	2,9	1,5 Gpa	1050	0,3	(MatWeb, 2016)
Combined bracket	Borealis GD 302 (MuCell)	2,5	5,60 Gpa	1160	0,3	(MatWeb, 2016)
Lower airmesh	Basell Hifax TRC 228P-2	2,5	Flexular modulus: 1300 Mpa	1000	0,3	(Ultra Polymers, 2016)
Skidplate	Borealis Daplen EE255AE	2,9	1,5 Gpa	1050	0,3	(MatWeb, 2016)
Front spoiler	Borealis Daplen EE255AE	2,9	1,5 Gpa	1050	0,3	(MatWeb, 2016)
Spoiler	Borealis Daplen EE255AE	2,9	1,5 Gpa	1050	0,3	(MatWeb, 2016)
Undershield	Borealis MD206U	2,9	Flexular modulus: 2,25 Gpa	1040	0,3	(MatWeb, 2016)
Grille	Steel	2,5	210 Gpa	7800	0,3	(The Engineering Toolbox, 2016)
Fender bracket	Borealis MD206U	2,5	Flexular modulus: 2,25 Gpa	1040	0,3	(MatWeb, 2016)
Car body	**Material**	**Thickness (mm)**	**Elastic modulus**	**Density kg/m3**	**Poisson`s ratio**	
Fender bracket	Steel	5	210 Gpa	7800	0,3	(The Engineering Toolbox, 2016)
Plastic bracket	Steel	5	210 GPa	7800	0,3	(The Engineering Toolbox, 2016)

8.4 Appendix D: Data used in the simulations

Simulation 1: right-left-middle assembly sequence	
Parts	**Minus 3 sigma values in y-direction (mm)**
Front bumper left side	-1,69
Front bumper right side	-1,09
Parts	**Theoretical value in y-direction (mm)**
Middle of the grille	1
Simulation 2: right-left-middle assembly sequence	
Parts	**Minus 3 sigma values in y-direction (mm)**
Front bumper left side	-1,69
Front bumper right side	-1,09
Parts	**Theoretical value in y-direction (mm)**
Middle of the grille	2
Simulation 1: middle-right-left assembly sequence.	
Parts	**Minus 3 sigma values in y-direction (mm)**
Front bumper left side	-1,69
Front bumper right side	-1,09
Parts	**Theoretical value in y-direction (mm)**
Middle of the grille	1
Simulation 2: middle-right-left assembly sequence.	
Parts	**Minus 3 sigma values in y-direction (mm)**
Front bumper left side	-1,69
Front bumper right side	-1,09
Parts	**Theoretical value in y-direction (mm)**
Middle of the grille	2

8.5 Appendix E: Measured deviations from the physical study

	Assembler 1			Assembler 2			Assembler 3		
Measurement points	**Measure 2 (mm)**	**Measure 3 (mm)**	**Measure 4 (mm)**	**Measure 5 (mm)**	**Measure 6 (mm)**	**Measure 7 (mm)**	**Measure 8 (mm)**	**Measure 9 (mm)**	**Measure 10 (mm)**
GRS X-direction	-2,389	0,989	-1,640	-2,329	-1,562	-2,349	-0,889	0,404	0,369
OWS X-direction	-0,179	-0,254	-0,508	-0,571	-1,749	-1,033	-0,575	-0,060	-0,882
Capping X1-direction	0,229	0,855	0,933	0,679	0,361	0,770	0,280	1,021	0,612
Capping X2-direction	-0,324	-0,450	-0,386	-0,289	-0,375	-0,430	-0,515	-0,446	-0,410
Capping Y1-direction	-0,948	-1,678	-1,660	-1,423	-1,667	-0,843	-1,178	-1,866	-1,322
Capping Y2-direction	-1,759	-1,582	-1,518	-1,499	-1,649	-1,555	-1,428	-1,637	-1,658
Capping Y3-direction	-0,358	-0,212	-0,388	-0,461	-0,224	-0,369	-0,202	-0,194	-0,473
Capping Y4-direction	0,799	0,770	0,830	0,877	0,767	0,823	0,830	0,782	0,891
Capping Z-direction	0,514	0,560	0,816	0,197	0,365	0,594	-0,263	0,550	0,868

8.6 Appendix F: Measured forces from the physical study

	Force measurements (N)								
Type of component	**Assembler 1**	**Assembler 1**	**Assembler 1**	**Assembler 2**	**Assembler 2**	**Assembler 2**	**Assembler 3**	**Assembler 3**	**Assembler 3**
GRS	45	60	52	33	45	50	34	29	32
OWS	48	50	59	32	28	53	31	45	48
Capping	71	55	60	27	35	40	40	39	41

8.7 Appendix G: Results from the physical study

Measurements for GRS

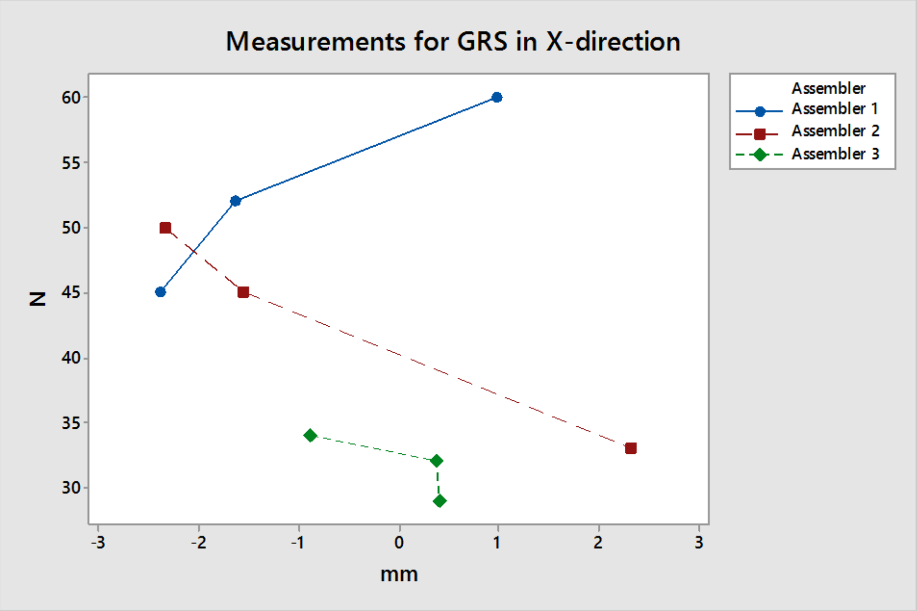

Measurements for OWS

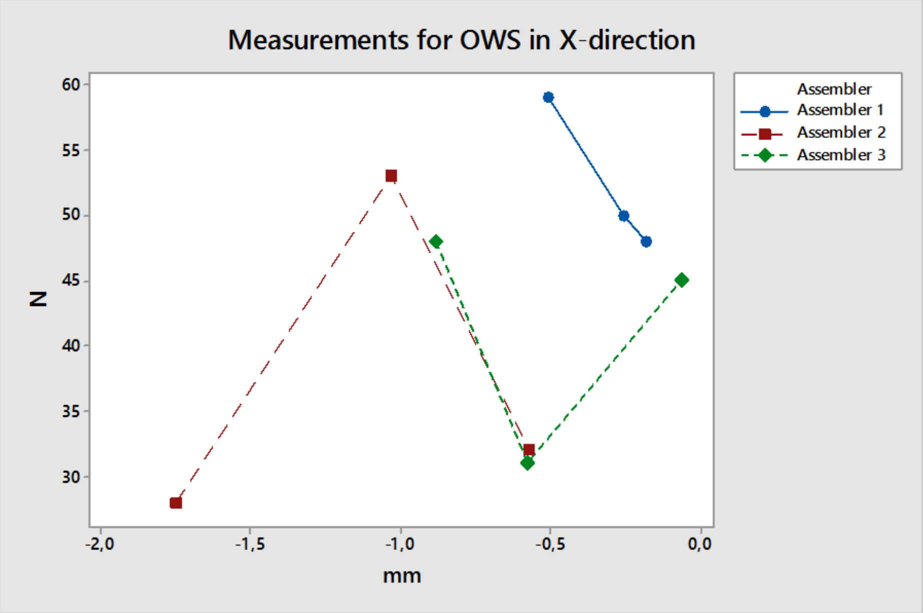

Measurements for Capping

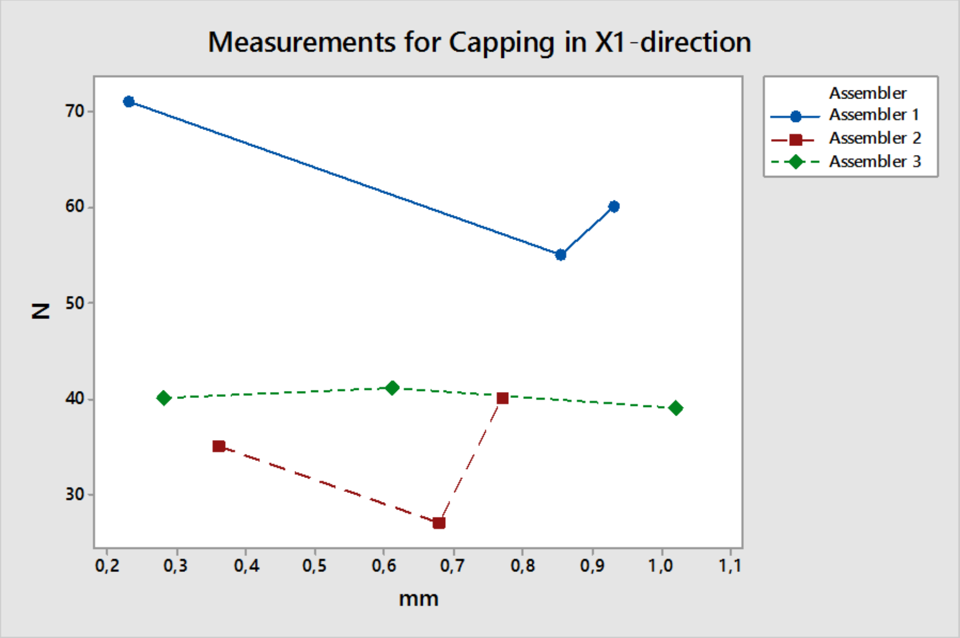

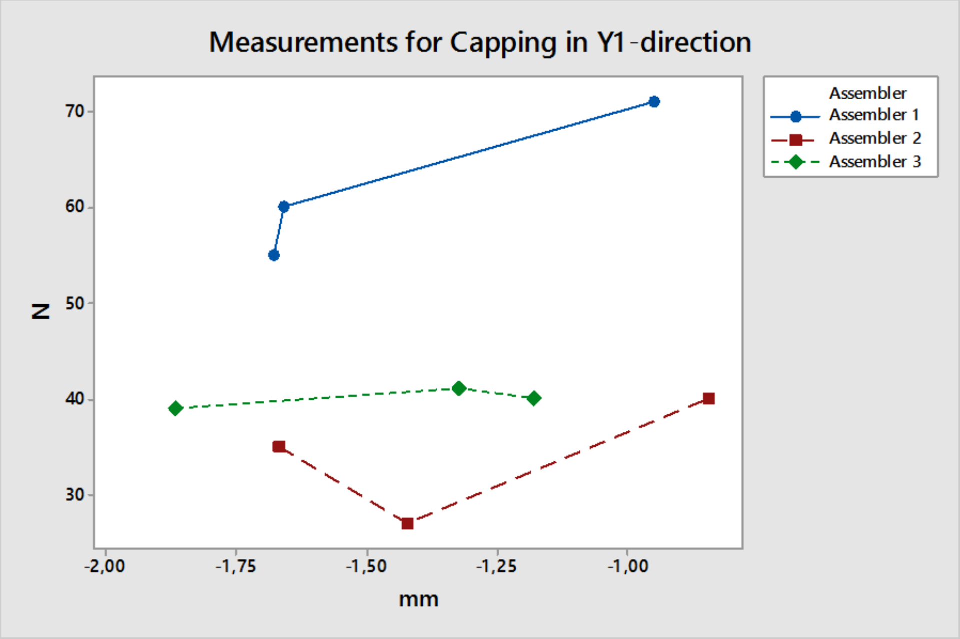

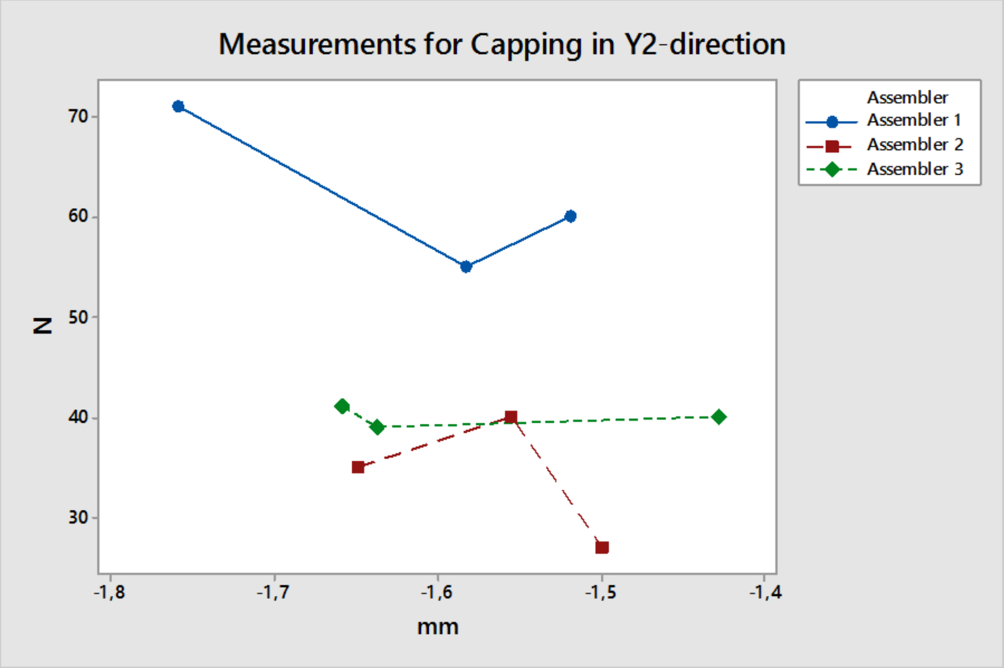
Measurements for Capping in Y2-direction
N
70
60
50
40
30
-1,8
-1,7
-1,6
-1,5
-1,4
mm
Assembler
Assembler 1
Assembler 2
Assembler 3

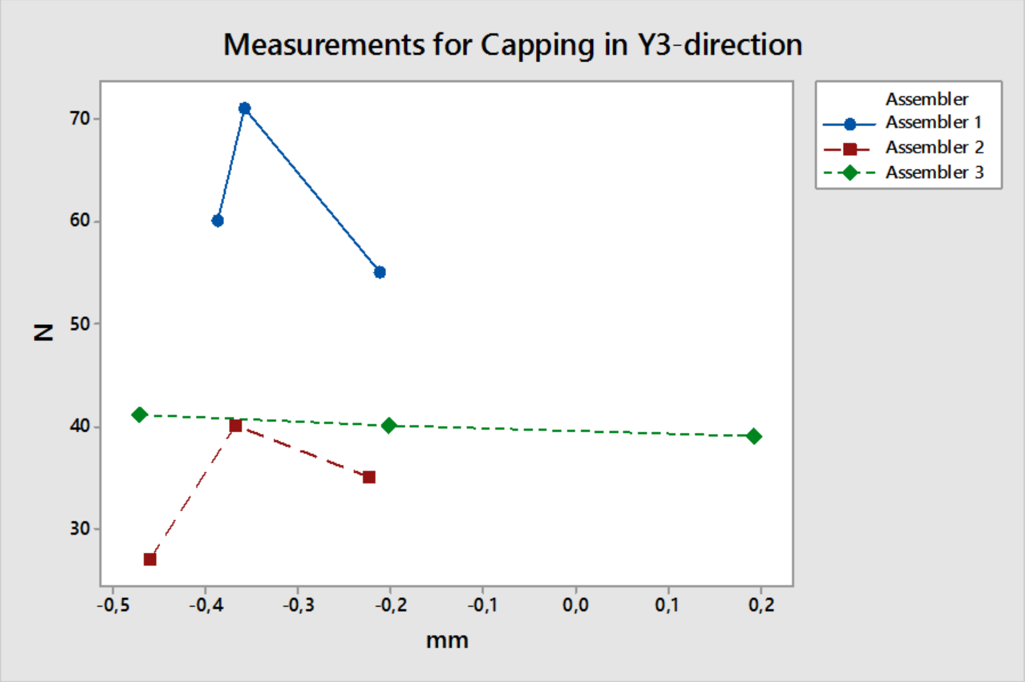
Measurements for Capping in Y3-direction
N
70
60
50
40
30
-0,5
-0,4
-0,3
-0,2
-0,1
0,0
0,1
0,2
mm
Assembler
Assembler 1
Assembler 2
Assembler 3

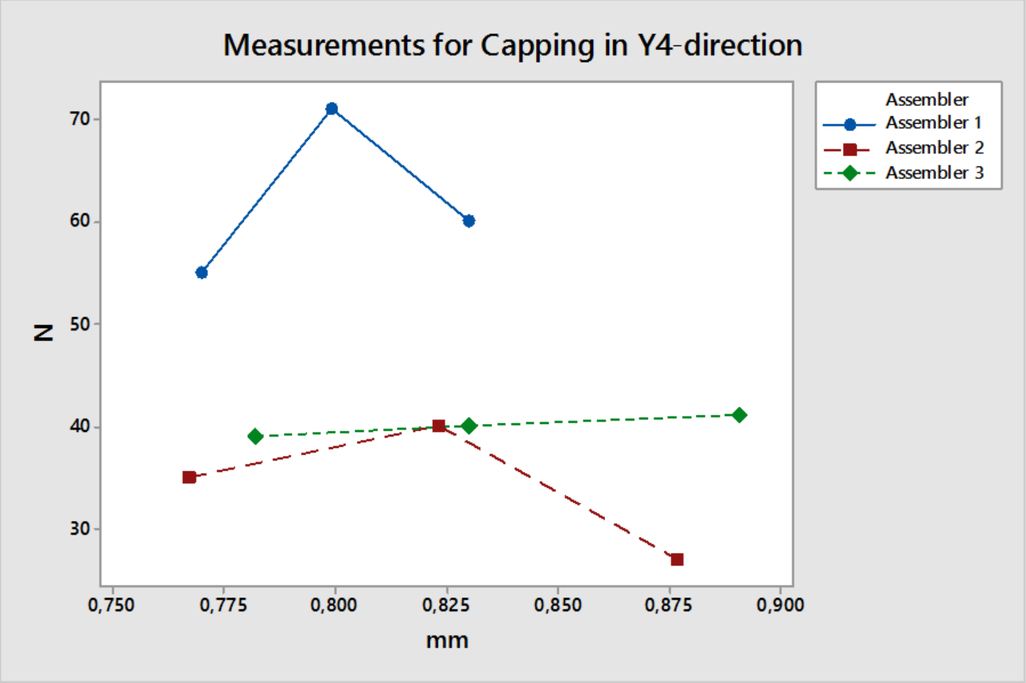
Measurements for Capping in Y4-direction
N
70
60
50
40
30
0,750
0,775
0,800
0,825
0,850
0,875
0,900
mm
Assembler
Assembler 1
Assembler 2
Assembler 3

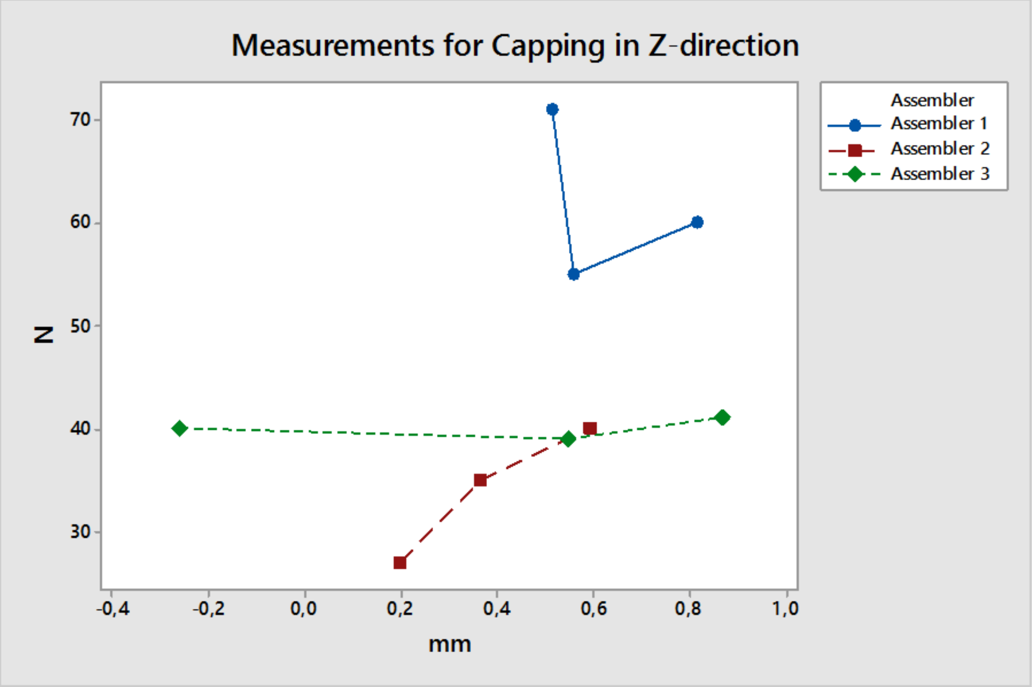
Measurements for Capping in Z-direction
N
70
60
50
40
30
-0,4
-0,2
0,0
0,2
0,4
0,6
0,8
1,0
mm
Assembler
Assembler 1
Assembler 2
Assembler 3

8.8 Appendix H: Measurements of deviations from simulation 1

	Simulation 1: Measurements (mm)	
Name of measurements	**middle-right-left assembly sequence**	**right-left-middle assembly sequence**
FR010F1L	0,284	0,464
FR010F1R	-0,381	-0,545
FR010G1L	-0,0592	0,122
FR010G1R	0,101	-0,128
FR011F1L	0,187	0,494
FR011F1R	-0,217	-0,555
FR011G1L	-0,0902	0,15
FR011G1R	0,155	-0,147
FR016F1L	-1,29	-0,736
FR016F1R	1,77	1,04
FR016G1L	-1,35	-0,49
FR016G1R	1,61	0,492
FR017F1L	-0,288	0,329
FR017F1R	0,583	-0,32
FR017G1L	-0,633	0,165
FR017G1R	0,832	-0,308
FR018F1L	0,346	1,11
FR018F1R	-0,159	-1,35
FR018G1L	-0,565	0,3
FR018G1R	0,491	-0,647
FR019F1L	0,291	1,07
FR019F1R	-0,301	-1,33
FR019G1L	-0,633	-0,271
FR019G1R	0,705	0,259
FR020F1L	0,213	0,707
FR020F1R	-0,285	-0,863
FR020G1L	-0,371	-0,19
FR020G1R	0,473	0,224
FR021F1L	0,394	0,763
FR021F1R	-0,381	-0,781
FR021G1L	0,0982	0,232
FR021G1R	0,0215	-0,184
FR022F1L	0,397	0,69
FR022F1R	-0,521	-0,813
FR022G1L	0,94	1,02
FR022G1R	-0,948	-1,04

8.9 Appendix I: Measurements of deviations from simulation 2

	Simulation 2: Measurements (mm)	
Name of measurements	**middle-right-left assembly sequence**	**right-left-middle assembly sequence**
FR010F1L	0,593	0,905
FR010F1R	-0,73	-1,01
FR010G1L	-0,0815	0,235
FR010G1R	0,184	-0,207
FR011F1L	0,41	0,947
FR011F1R	-0,408	-0,977
FR011G1L	-0,136	0,285
FR011G1R	0,29	-0,222
FR016F1L	-1,55	-0,568
FR016F1R	2,1	0,882
FR016G1L	-1,96	-0,415
FR016G1R	2,28	0,423
FR017F1L	-0,105	0,986
FR017F1R	0,558	-0,926
FR017G1L	-0,868	0,553
FR017G1R	1,24	-0,644
FR018F1L	0,749	2,1
FR018F1R	-0,252	-2,21
FR018G1L	-1,06	0,487
FR018G1R	1,04	-0,841
FR019F1L	0,564	1,94
FR019F1R	-0,46	-2,15
FR019G1L	-1,11	-0,46
FR019G1R	1,2	0,451
FR020F1L	0,422	1,29
FR020F1R	-0,468	-1,43
FR020G1L	-0,658	-0,337
FR020G1R	0,82	0,397
FR021F1L	0,807	1,45
FR021F1R	-0,738	-1,4
FR021G1L	0,258	0,486
FR021G1R	-0,0587	-0,402
FR022F1L	0,809	1,32
FR022F1R	-0,97	-1,46
FR022G1L	1,9	2,02
FR022G1R	-1,9	-2,04

8.10 Appendix J: Measurements of forces from simulation 1

	Simulation 1: Measurements (N)	
Name of force measurements	**middle-right-left assembly sequence**	**right-left-middle assembly sequence**
WP_002	0	0,541
WP_004	2,67	0,999
WP_006	0	0
WP_008	0	0
WP_010	10,4	8,92
WP_012	10,5	23,5
WP_014	6,89	17,3
WP_016	4,16	4,66
WP_018	1,87	0
WP_020	0	0
WP_022	7,29	16,1
WP_024	0	0
WP_026	0	0
WP_028	16,5	19,2
WP_030	0	0
WP_032	2,99	0
WP_034	0	0
WP_036	0,819	0,851
WP_038	4,32	1,71
WP_040	0	2,48
WP_042	1,54	1,98

8.11 Appendix K: Measurements of forces from simulation 2

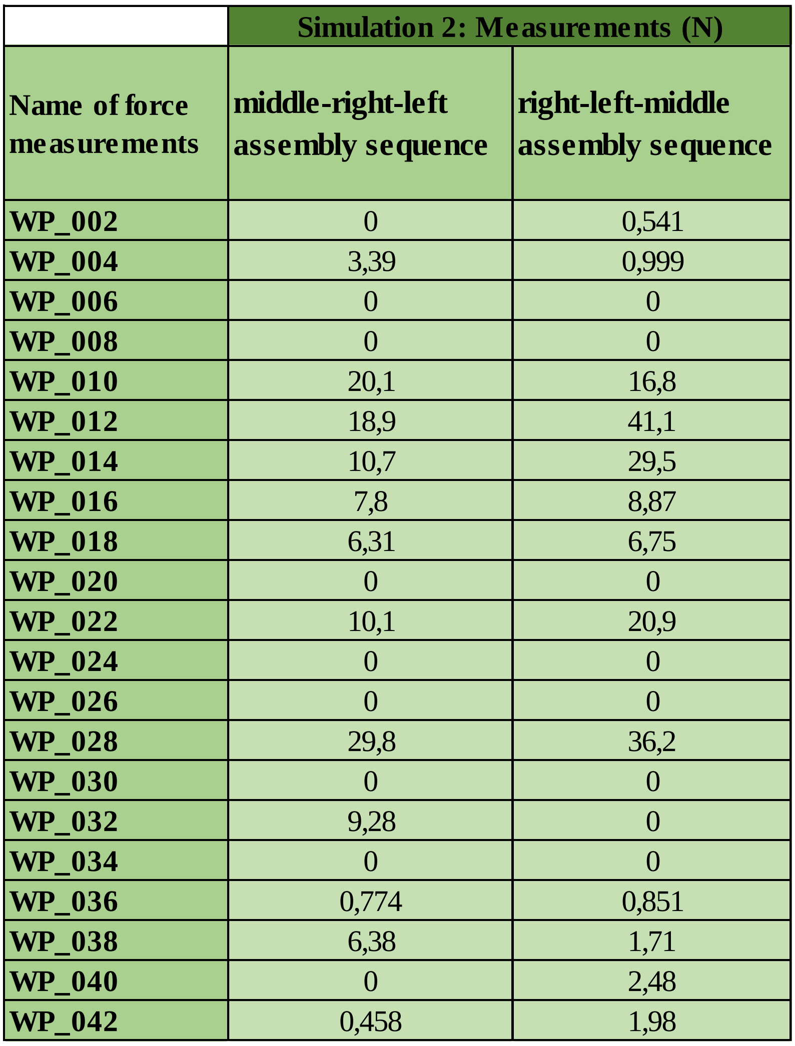

	Simulation 2: Measurements (N)	
Name of force measurements	**middle-right-left assembly sequence**	**right-left-middle assembly sequence**
WP_002	0	0,541
WP_004	3,39	0,999
WP_006	0	0
WP_008	0	0
WP_010	20,1	16,8
WP_012	18,9	41,1
WP_014	10,7	29,5
WP_016	7,8	8,87
WP_018	6,31	6,75
WP_020	0	0
WP_022	10,1	20,9
WP_024	0	0
WP_026	0	0
WP_028	29,8	36,2
WP_030	0	0
WP_032	9,28	0
WP_034	0	0
WP_036	0,774	0,851
WP_038	6,38	1,71
WP_040	0	2,48
WP_042	0,458	1,98